Investigating the Cortical Oscillatory Correlates of Smooth Pursuit Eye Movements: A Magnetoencephalographic Study

Benjamin Thomas Dunkley

Supervisors: K. D. Singh & T. C. A. Freeman

A thesis submitted to Cardiff University for the degree of Doctor of Philosophy.

May 2012

Summary

Models of motion perception propose that eye movement estimates are integrated into middle temporal cortex (MT+) as a mechanism that disambiguates world motion from retinal motion induced by ego movement. Little is known about the relationship between eye movement signals in this area and cortical oscillations, a phenomenon linked to perceptual and motor processing. Magnetoencephalography was used to examine the significance of oscillations in this area during pursuit. Results from Experiment 1 suggest low-frequency suppression in MT+ reflects eye position during sinusoidal tracking. A control study (Experiment 2) examining activity in response to retinal slip suggests this was not due to pursuit error when the stimulus changed direction. Experiment 3 examined oscillations during pursuit at various head-centred eye eccentricities. No difference was found in the magnitude of activity as a function of eye position during pursuit, suggesting modulations in these rhythms was related to another aspect of the eye movement. Experiment 4 found no specific effects of eye velocity on alpha or beta, but there was a consistent effect of eye speed on beta activity. Additionally, there was no such effect found between alpha and eye speed, suggesting some functional distinction in the role of these rhythms in pursuit behaviour. In Chapter 4, two experiments examined cortical changes during pursuit (Experiment 5) and retinal motion adaptation (Experiment 6), and the subsequent motion aftereffect. Beta suppression in MT+ during oculomotor adaptation was a significant predictor of the motion aftereffect duration, perhaps indicating that beta changes index the efficacy with which the visual motion system is able to recalibrate itself in the presence of a stationary stimulus following adaptation. Taken together, these results suggest a role for beta suppression in MT+ during pursuit, which seems to reflect the processing of extraretinal signals for oculomotor control and the estimation of head-centred motion.

Acknowledgements

I would like to say a huge thank you to both of my supervisors, Prof. Krish Singh and Dr. Tom Freeman. They have been more than excellent mentors, and I could not have asked for more encouragement and helpful guidance during my time as a PhD student in Cardiff. Your doors were always open for any questions, queries or general chitchat regarding this project, no matter how unexpected. Thank you both for maintaining my interest in science, I sincerely hope we can collaborate again in the future.

I would also like to thank Dr Suresh Muthukumaraswamy for his assistance in the analysis of the MEG data presented here. If it had not been for his daily 'help hour', I fear this thesis may have taken a lot longer to finish. Cheers dude!

For their friendship and always having the time with which share a beer or two with over the years, whether in Cardiff or elsewhere, I would also like to extend my thanks to my close friends. In no particular order, thanks to Dewi Storer, Tom Gregory, Rachael Cleaver, Chase Gardiner, Tom Bastian, James Taylor, Anthony Walters, Richard Sewell, Peter Kellie, Will Merrett, Faisel Patel, Chris Jones, Richard Grant and Danelle Pettman. You guys kept me grounded over the years, I could not have asked for better mates. To anyone I might have forgotten to mention here, apologies, but you know who you are. Thanks.

Finally, I dedicate this thesis to my family. Without your love and support, none of this would have been possible. I am so grateful for you always having encouraged me to continue studying and choose a career in something that I enjoy. Thank you to Mum, Dad and Lucy, and the new additions to the family, Joel & Lily. I love you all!

Publications

A number of the studies from this thesis have been presented at congress, with some having their abstracts published in scientific journals after undergoing peer review. Additionally, data from Experiment 1 has been compiled and used in a paper, which at the time of submission of this thesis, has been accepted for publication and is currently in press.

Selected conference proceedings:

Pilot data for Experiment 1: Dunkley, B.T., Freeman, T.C.A., Muthukumaraswamy, S.D. & Singh, K.D., (2010). The neuromagnetic correlates of self-initiated smooth pursuit eye movements and finger tracking in the absence of retinal input, *OHBM 2009, San Francisco, USA, NeuroImage*, *Volume 47, Supplement 1*, *July 2009*, *Pages S39-S41*

Experiment 5: Dunkley, B.T., Freeman, T.C.A., Muthukumaraswamy, S.D. & Singh, K.D., (2011). The perceptual and cortical consequences of adaptation to smooth pursuit: An MEG study of the extra-retinal motion aftereffect, *VSS 2011, Journal of Vision, Volume 11, Number 11: 531, 2011*

Journal article:

Experiment 1: Dunkley, B.T., Freeman, T.C.A., Muthukumaraswamy, S.D. & Singh, K.D., (2011). Cortical oscillatory changes in human Middle Temporal Cortex underlying smooth pursuit eye movements, *Human Brain Mapping Journal, doi: 10.1002/hbm.21478*

Contents

List of Figures

Abbreviations

AFC	Alternative forced-choice
BET	Brain Extraction Tool
BOLD	Blood oxygen level dependent
CG	Cingulate gyrus
EEG	Electroencephalography
EOG	Electrooculography
ERMAE	Extraretinal motion aftereffect
FEF	Frontal eye fields
fMRI	Functional magnetic resonance imaging
IPS	Intraparietal sulcus
LGN	Lateral geniculate nucleus
MAE	Motion aftereffect
MEG	Magnetoencephalography
MRI	Magnetic resonance imaging
MT/MT+	Middle temporal cortex
MST	Medial superior temporal cortex
OS	Overlapping spheres
OMAE	Oculomotor motion after effect
PPC	Posterior parietal cortex
SAM	Synthetic aperture magnetometry
SC	Superior colliculus
SEF	Supplementary eye fields
SPM	Statistical parametric map
STS	Superior temporal sulcus
TACS	Transcranial alternating-current stimulation
TMS	Transcranial magnetic stimulation
VOR	Vestibular ocular reflex
V5	Visual area 5

1 Chapter 1 – General Introduction

1.1 Introduction

This thesis details an investigation into the role of cortical oscillatory changes in areas of the visual association cortex and their putative functional role in smooth pursuit eye movements. In the Background section of the General Introduction a concise review of some of the literature undertaken in the study of the smooth pursuit system is given, from a number of different methodological approaches. In particular, evidence from perceptual psychophysical accounts, invasive animal studies and non-invasive neuroimaging research in humans is considered. Particular emphasis will be placed on how the motion processing system in the visual association cortex is thought to play a key role in guiding, and ultimately compensating for problems associated with, pursuit eye movements, as well as some of the current hypotheses on the putative functional roles of cortical oscillations in perception, action and cognition.

Along with an overview of previous literature on the subject, a brief introduction to the methodological techniques that were used in the studies of the experimental chapters of this thesis and a summary of the findings will also be presented. The Experimental Chapters detail the results of several studies looking at the properties of oscillations related to smooth pursuit eye movements, and the final chapter of the thesis discusses the implications of these results within the framework of the existing literature and concludes with the possible functional role these oscillations might play.

1.1.1 Eye movements and associated problems for perception

Having evolved in a mostly stationary world inhabited by numerous, often moving, visual opportunities and threats, the primate brain has developed the necessary neuronal machinery and mechanisms to keep track of moving objects in the world that may ultimately

affect the individual's chances of survival. To do this, the visual system has to analyse retinal image motion, make quick saccadic eye movements to place an object on the fovea where visual acuity is greatest, and then smoothly pursue it with the eyes.

However, the evolutionary adaptation that allows an organism to perceive a stimulus and then guide motor behaviour in a fashion to pursue the target poses two particular problems, one to do with oculomotor control and the other to do with a consequence of action on perception. Firstly, how does the brain analysis target motion and move the eyes to follow the target? To achieve this, the pursuit system needs to be able to compute the retinal image velocity of the target, process this information and transform the retinotopic coordinates of the target's motion into a spatiotopic, or head-centred, coordinate frame. These signals can be used to compute the necessary motor commands to move the eyes and follow the target.

A second problem the brain needs to solve is an associated perceptual consequence of this eye movement. How does the brain disambiguate real motion in the world from that induced by moving the eyes? If the brain were unable to compensate for the retinal motion created by the visual scene when moving the eyes, visual perception would be dominated by a world that moves around during eye movements. Somehow, the brain maintains the perception of a stable environment by disambiguating the resultant retinal motion of the stationary world during eye movements from the real motion of objects moving in space; this is sometimes referred to as maintaining 'spatial stability' or 'space constancy'. Additionally, the brain needs to estimate the velocity of the moving object being tracked through space, even though it is otherwise *stationary* on the retina, as well other moving targets in space that are not being followed. If the brain is unable to solve these associated problems, perception of a stationary world is severely compromised and the animal will likely end up as a predator's free lunch.

The brain is thought to tackle the perceptual problem of maintaining motion invariance associated with eye movements by using a number of compensatory mechanisms. In the particular case of smooth pursuit, one of the models proposed for distinguishing between externally-moving stimuli and self-induced motion is to combine internally generated estimates of the eye movement (known as 'extra-retinal signals', as they are non-retinal in origin) with incoming sensory signals (known as afferent inputs) coding retinal motion (von Holst & Mittelstaedt, 1950). By subtracting the extraretinal component from the retinal signal, it is possible to derive estimates of head-centred motion (in that these signals should cancel each other out, for the most part, resulting in a perceived world that is largely stationary). A brief explanation of the theories on how the brain achieves this is given in the upcoming Literature Review.

Whilst there have been a number of functional imaging studies investigating oculomotor control and a wealth of psychophysical work exploring motion perception during pursuit eye movements, studies utilising techniques that directly measure the neuronal components mediating pursuit and visual stability in humans has been lacking. Therefore, knowledge of the cortical processes underlying this behaviour, and how the brain might implement the necessary physiological strategies to maintain perceptual stability, is impoverished; thus, to complement existing knowledge it is desirable to use a technique that can directly measure neuronal activity during smooth pursuit, as this is of fundamental importance in this area of perceptual neuroscience.

1.2 Background

1.2.1 Behavioural account of smooth pursuit eye movements

Eye movements can be classified based on their underlying mechanisms and specific function, of which there are generally considered two types: gaze stabilising and gaze

shifting. Of the gaze-shifting type, there are principally three sub-classes: saccades (reflexive change of gaze), vergence (disconjugate eye movements where motion is toward the eyes), and smooth pursuit eye movements. Smooth pursuit is a type of intentional tracking eye movement, which is evoked by slowly moving objects of interest in the visual field and aim to maintain a stable image of the stimulus on the retina by matching eye and object velocity. This intentional tracking motion of the eyes is partly-predictive in nature and keeps the target object centred on the fovea, where retinal colour-sensitive photoreceptor cell density is highest, and therefore visual acuity is greatest (the fovea only subtending approximately 1-2º of the visual field) (Carpenter, 1988).

Smooth pursuit is continuous, being performed for the duration of object tracking. Pursuit initiation occurs with a latency of approximately 100-150 msec proceeding target motion (Carl & Gellman, 1987; Kimmig, Biscaldi, Mutter, Doerr, & Fischer, 2002), which is quicker than saccadic eye movements (Yang, Bucci, & Kapoula, 2002). Maintenance of pursuit is achievable up to a maximum velocity of approximately 100º/s (Meyer, Lasker, & Robinson, 1985). Typically, pursuit occurs most effectively (that is, maximum gain and minimal catch-up saccades) for velocities less than 40º/s where the pursuit system can maintain smooth tracking exclusively in the absence of saccades (Leigh & Zee, 2006)

To track an object accurately during motion, the pursuit system needs to analyse the retinal velocity of the target and match this signal through oculomotor control commands sent to the eyes to minimise retinal slip. In other words, information from the retinal image motion processing system (which gives retinal-centred image coordinates) is transformed into a head-centred coordinate frame, transferred to the oculomotor control system, which then generates the eye movement command signals to move the eye muscles and to follow the stimulus (Kimmig et al., 2008).

During the initial phase of pursuit eye movements, any resulting difference in the target and eye position signals (i.e. retinal error of the target caused by the object position being different to the eye position signal) received by the pursuit maintenance system causes the eyes to start to move toward the target. This stage is often known as 'open-loop pursuit', and reflects movement of the eyes based on motion detection signals that were processed when the eyes had not yet begin to move (<100 msec) (Krauzlis & Lisberger, 1994b). Therefore, subsequent pursuit velocity for a time being is not corrected 'online' due to a delay in motion information being able to pass through the visual system (Krauzlis & Lisberger, 1994b) and the resulting eye motion can thought of as 'ballistic' movement (because the motion of the eyes are 'carried by their own momentum' so to speak). The second phase of pursuit is termed 'closed-loop pursuit', and occurs approximately 150 msec after pursuit initiation during which time a corrective saccade can be executed, if needed, to rectify deficiencies in the initial pursuit velocity during the 'open-loop' phase, by which time motion information has had enough time to pass through the visual system.

Furthermore, retinal slip/error during pursuit is then minimised by an 'online correction mechanism' (a negative feedback loop) which executes any necessary catch-up saccades to compensate for slip and place the stimulus back on the fovea (Krauzlis & Lisberger, 1994a). The neural circuitry of pursuit has been studied extensively, but remains the object of debate. The functional neuroanatomy of smooth pursuit and some of the studies into the physiology of perceptual stability will be described in due course.

For the most part, smooth pursuit can usually only accurately be performed in the presence of a visual target (Rashbass, 1961), guided by a system that computes an objects retinal position and velocity (Blohm, Missal, & Lefevre, 2005; Pola & Wyatt, 1980). Nonetheless, it has been shown that pursuit can be performed in the absence of a visual target for a short duration (<300 msec) proceeding the disappearance of a previously visible moving

object, and not just as a result of the momentum of the eyeball (Barnes & Asselman, 1991; Bennett & Barnes, 2003; Joiner & Shelhamer, 2006). It has also been shown that pursuit can be maintained in the absence of a visual target because of the anticipation of a returning object (Kao & Morrow, 1994).

Additionally, it has been shown that the pursuit system may in fact have a limited ability to guide smooth eye movements based on motion information from the tactile and proprioceptive systems in the absence of visual input. However, the gain for pursuit eye movements based on combined tactile and proprioceptive signals for most subjects is low, at around 0.35, although some subjects can perform pursuit with a much higher gain (Berryhill, Chiu, & Hughes, 2006; Gauthier & Hofferer, 1976).

1.2.2 Models of head-centred motion and perceptual stability

As briefly mentioned earlier, one of the inherent problems created by pursuing a target is the consequence of this behaviour on the retinal image and how the visual system maintains the perception of a stable world. During smooth following, the target remains largely stationary on the fovea, but the image of the world will move across the retina at a rate approximately equal and opposite to that of the eye movement. However, we do not perceive a world that moves, but one that is stationary despite the consequence of this motor action. Therefore, the visual system somehow compensates for this visual motion to maintain perceptual stability and there is a wealth on studies into how the motion system processes objects other than to the pursuit target (Champion & Freeman, 2010; Freeman, Champion, & Warren, 2010; Haarmeier, Bunjes, Lindner, Berret, & Thier, 2001; Naji & Freeman, 2004; Schutz, Braun, Kerzel, & Gegenfurtner, 2008; Souman, Hooge, & Wertheim, 2006; Spering & Gegenfurtner, 2006; Turano & Massof, 2001).

Psychophysical studies of smooth pursuit and motion perception during eye movements have been fruitful in positing a number of theories on how head-centred velocity

is estimated. In particular, experiments investigating the integration of retinal and extra-retinal estimates to derive head-centred motion and maintain perceptual stability have provided detailed models about how this is achieved in the brain.

Some of the earliest theories of pursuit compensation and the estimation of target motion propose that the simplest way of achieving perceptual stability is through the combination of velocity estimates for the eyes and retinal motion. In its simplest form, this can be derived by summation of the retinal motion and internally generated eye velocity estimate (based on copies of the oculomotor command, often referred to as an 'efference copy'), which should cancel each other out. This gives an estimate of the resultant motion of the environment (von Holst & Mittelstaedt, 1950). This is often referred to as the 'classical model' and is defined by the equation:

$$h' = R + P$$

where h' is the perception of motion/stimulus velocity, R is the estimate of retinal image velocity and P is the internally generate estimate of eye velocity, perhaps a copy of the efferent oculomotor signal. The efference signal can also be used to generate estimates of the motion of the object being tracked in space, even though it is stationary on the fovea.

The classical model was then further modified in recent times to formalise the errors thought to be inherent in the estimation of the retinal (R) and eye velocity (P) signals. Misrepresentation of the retinal and eye velocity estimates can result in a number of illusions (such as misestimation of background motion, known as the Filehne illusion, and the velocity of the target object/movement of the eyes, known as the Aubert-Fleischl illusion). Gain coefficients were introduced to these estimates to reflect these potential errors (Freeman, 1999; Freeman & Banks, 1998):

$$h' = rR + eP$$

where *r* is the retinal motion signal gain and *e* is the eye velocity signal gain. Whilst the classical model and its modified version provide explanations for how the brain compensates for retinal motion and estimates head-centred velocity, another model posits that the pursuit velocity estimate is derived by the integration of reafferent retinal motion estimates. This is known as the reference signal model (Wertheim, 1981, 1994).

In the reference signal model, it is proposed that information in the retinal motion signal during pursuit can also be used in combination with other signals to estimate head-centred eye velocity. In this model, the purely extraretinal component of the classical model is replaced by a reference signal that combines retinal, extraretinal and vestibular information from which eye velocity and world-centred motion estimates can be derived. The model is defined as:

$$h' = R + f(R,P)$$

where *f* is the reference signal, a function of the retinal and extraretinal estimates.

Generally, the classical model in its simplest form proposed by von Holst & Mittelstaedt (1950) provides a robust description of how head-centred motion is derived, and perceptual stability is ultimately maintained, by combining retinal and extraretinal signals. These abstract representations provide a concrete framework on which to conduct physiological experiments into how these calculations are performed and head-centred motion perception is attained. Whilst there is debate about the exact nature of the signals that provide estimates of motion and how these signals in the models presented here might differ, the definition of the extraretinal and the reference signal given here can be thought of as the same thing within the confines of this thesis and the experiments presented henceforth. Hence, these terms are used interchangeably.

So, what cortical regions are implicated in the control of pursuit and world-centred motion perception, and how might the brain go about performing the calculations necessary to move the eyes and maintain motion invariance?

A patient study provides a profound example of how important extraretinal-based mechanisms in pursuit compensation are, in addition to evidence that motion invariance takes place in visual association cortices. Patient RW would often report feelings of vertigo and nausea during self-induced motion (such as when moving his eyes). By using a combination of psychophysics, neuropsychology and neuroimaging, it was found that patient RW suffered from extensive bilateral extra-striate lesions that lead to a false perception of egocentric motion due to an inability to compensate for self-induced retinal slip when moving the eyes (Haarmeier, Thier, Repnow, & Petersen, 1997). Essentially, any movement of the eyes and the retinal motion induced by this was misinterpreted as motion of the environment; the world was perceived to move in the opposite direction to that of the eyes.

Remarkably, his perception of motion remained intact, as did his ability to pursue a target. This suggested that regions involved in motion processing remained unaffected, as did those for oculomotor control, but that the area that combines the extraretinal signal with the retinal estimates to derive head-centred motion (as in the classical/reference signal models above) was compromised. Neuroimaging data found that this was likely to be in the putative MT+ complex, which the authors concluded was the region primarily responsible for disentangling self-induced and externally-induced visual motion (Haarmeier, et al., 1997).

In the next part of this literature review, evidence for the areas implicated in the oculomotor control of pursuit are described as well as the proposed role for MT+ in the perception of head-centred motion.

1.2.3 Functional neuroanatomy of oculomotor control

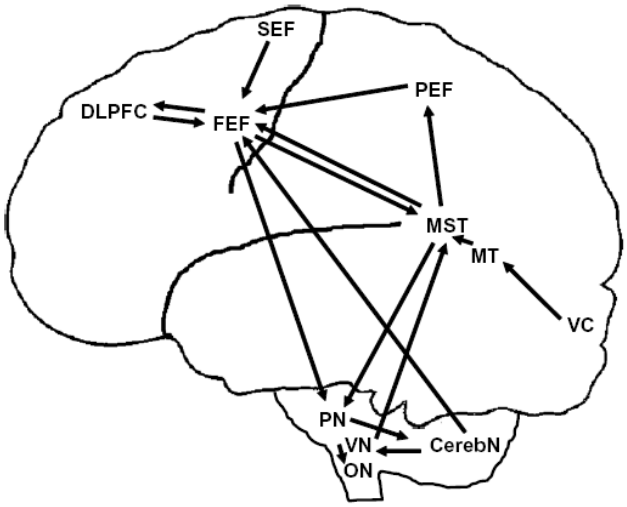

Figure 1. Neuroanatomical areas, functional connectivity and descending control circuits thought to be involved in the control of smooth pursuit eye movements.
CerebN: cerebellum; DLPFC: dorsolateral prefrontal cortex; FEF: frontal eye field; MT: middle temporal area (also known as V5); MST: medial superior temporal area; ON: oculomotor nuclei; PEF: parietal eye field (also sometimes referred to as the intraparietal sulcus IPS or posterior parietal cortex PPC); PN: precerebellar pontine nuclei; SEF: supplementary eye field; VC: visual cortex; VN: vestibular nuclei. Adapted from (Lencer & Trillenberg, 2008).

Figure 1 depicts some of the neuroanatomical areas thought to be involved in smooth pursuit eye movements. The anatomical and functional correlates of pursuit have principally been investigated using invasive neurophysiological studies in animals (Ilg & Thier, 2003; Komatsu & Wurtz, 1988), cognitive neuropsychological evidence from human patients (Haarmeier, et al., 1997; Sharpe, 2008) and functional neuroimaging in healthy subjects (Dukelow et al., 2001; Kimmig, et al., 2008; Konen, Kleiser, Seitz, & Bremmer, 2005; Krauzlis, 2004; Thier & Ilg, 2005). The physiological structures and their functional roles thought to be involved in pursuit have been described in some detail and these will be summarised, before invasive and neuroimaging studies are briefly reviewed.

Evidence suggests a widely distributed set of anatomical regions are involved in smooth pursuit, which, if to be performed correctly, requires functional coupling and coordination between a number of different cortical areas, giving rise to a complicated physiological network which processes and integrates visual motion information and extraretinal eye movement signals.

Information regarding a moving target is first processed at the retina by photoreceptor cells and transmitted along the optic nerve, where it is relayed through the lateral geniculate nucleus (LGN) before arriving at striate cortex (primary visual area V1). V1 primarily responds to low-level visual parameters such as orientation (Hubel & Wiesel, 1977), spatial frequency (Valois, Thorell, & Albrecht, 1985), texture (Heydt, Peterhans, & Duersteler, 1992) and colour (Livingstone & Hubel, 1984), but also motion information, which is then transferred to the middle temporal cortex (otherwise known as MT+, the human homologue of monkey middle temporal, MT, and medial superior temporal cortex, MST) (Maunsell & Essen, 1983a; Maunsell & Newsome, 1987) for further higher-level processing of object motion. This is one of the regions associated with the coordinate transforms required for pursuit initiation and maintenance.

Additionally, it has been shown that posterior parietal cortex (PPC)/intraparietal sulcus (IPS) also plays a role in coordinate transforms and sensorimotor integration (Andersen, Essick, & Siegel, 1985; Maunsell & Essen, 1983a) required for pursuit. In particular, it thought to be one of the locations where transformations of retinotopic visual information into higher-order reference frames takes place, including eye-centred, head-centred and body-centred coordinate frames (Xing, Li, & Andersen, 1995). Additionally, while it was assumed that neurons in PPC coded for image motion based on retinal coordinates, one group recently argued that this site is also responsible for encoding target motion in head-centred coordinates . They propose that this area is also partly responsible for visuo-motor coordinate

transformations used during pursuit movements (Ilg, Schumann, & Thier, 2004), in addition to areas outlined earlier on.

These signals regarding head-centred motion are then thought to be processed by the supplementary eye fields (SEF) (Missal & Heinen, 2001; Tian & Lynch, 1996), cingulate gyrus (CG) (Berman et al., 1999; Konen, et al., 2005) and frontal eye fields (FEF) (Macavoy, Gottlieb, & Bruce, 1991; Ungerleider & Desimone, 1986), with area FEF thought to exert the most control and be involved in selection of a target (Krauzlis, 2005). Once a target is selected, FEF is then thought to send commands for the initiation and maintenance of the pursuit movement to subcortical areas, such as the superior colliculus (SC) (Krauzlis, 2003) and cerebellum (Coltz, Johnson, & Ebner, 2000), which in turn project to optic motor neurons which move the eyes.

As an aside, lesion studies suggest that visual analysis of some types of stimulus motion can bypass information processing centres in early visual cortex and be fed directly to MT+ from the retina via the superior colliculus (SC) (Azzopardi, Fallah, Gross, & Rodman, 2003), which implies two dissociable routes for processing of visual motion signals. Evidence for the dual-route model of motion processing has also been given credence by studies into the phenomenon of blindsight, whereby patients report no conscious awareness of a stimulus, yet manage to correctly discriminate above chance various fundamental features of a visual stimulus (Stoerig & Cowey, 1997) and perform tracking eye movements without the need for conscious perception.

1.2.3.1 Electrophysiological studies on the role of MT+ in pursuit maintenance and motion invariance

Invasive electrophysiological studies in primates have been particularly important in revealing the neuronal basis of pursuit and head-centred motion perception. Single-cell recording in monkey extra-striate cortex (specifically, MT and MST and part of the superior

temporal sulcus, STS) suggests that extraretinal eye movement signals (possibly from corollary discharge or proprioceptive sources) are fed directly to extra-striate visual areas in the dorsal stream to guide the pursuit system and help interpret retinal motion during pursuit eye movements (Komatsu & Wurtz, 1988; Newsome, Wurtz, & Komatsu, 1988).

Additional studies have identified a functional distinction between MT and MST. It was found that neurons in MT respond greatest to retinal image motion, whilst those in MST were clearly coupled to eye movement and modulated by a non-retinal signal, given that these neurons were activated during smooth pursuit whilst in the complete absence of a visual target (Ilg & Thier, 2003). In particular, it was found that the majority (70%) of neurons in MST that showed an extraretinal response seemed to code for eye velocity, with asymmetric spiking profiles revealed when the eyes were tracking in the ipsiversive direction (with respect to the recording site). An exemplary neuron with this characteristic velocity-sensitivity profile can be seen in Figure 2, with an additional activity profile for a position-sensitive neuron also shown.

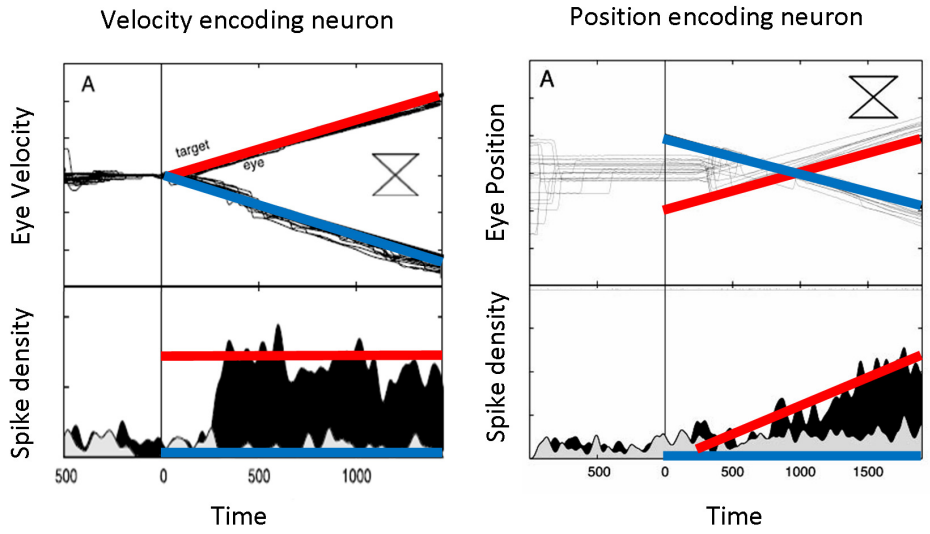

Figure 2. Eye movement traces for pursuit of target and corresponding spike density profiles from neurons in area MST that preferentially code for velocity (left panel) and eye position (right panel).

For the velocity-encoding neuron (left panel), the resultant spike rate density during pursuit in the preferred direction correlates highly with that of the linear eye velocity (as denoted by the red trace). Conversely, when pursuit occurs in the opposite (non-preferred) direction at a

linear velocity, the neuron displays approximately baseline levels of activity (blue trace). Whilst the majority of neurons in MST that show purely eye-movement related responses correlate with eye velocity, a significant minority display eye position sensitivity (right panel). Recording from an exemplary neuron with this response property shows that when the eyes move in the preferred direction, the spike rate activity linearly increases with relative position (red trace), whilst pursuit in the non-preferred direction displays a baseline profile (denoted by the blue trace). Adapted from Ilg & Thier (2003).

Building upon the previous work, Churchland and colleagues recorded activity from neurons in MST whilst modulating eye speed to examine the contribution of extraretinal eye movement signals on neurons in this area under different eye velocities. They found a relationship between firing rate and eye speed that was also direction-selective, but predictions of velocity based on firing rate were only accurate 35% of this time, which led them to the conclusion "that the output of MST may be a poor candidate to drive eye velocity and so may instead regulate another component of pursuit" (Churchland & Lisberger, 2005).

1.2.3.2 Neuroimaging studies on pursuit and perceptual stability

While we can assume the neuroanatomical basis of smooth pursuit eye movements is to some degree homologous between humans and monkeys, inferences at the microscopic level based on invasive electrophysiological recording of neuronal responses related to smooth pursuit might not necessarily be enough to inform us about the neuronal substrates in humans. Additionally, these data do not tell us about the macroscopic network or functional connectivity of larger neuronal populations underlying the pursuit system. For this, it is desirable to utilise non-invasive functional neuroimaging.

Using functional magnetic resonance imaging (fMRI), activation has been shown in lateral occipitotemporal cortex, the homologue of motion sensitive middle temporal (V5/MT+) in monkeys during stationary visual stimulation, retinal motion stimulation and pursuit eye movements (Barton et al., 1996). The response in this area was greatest during pursuit eye movements despite the moving grating condition generating more retinal image

motion. In contrast, activation in V1 was weakest during pursuit compared to image motion, which would suggest extraretinal signals are generated in, or fed directly to, lateral occipitotemporal (extra-striate) areas. However, the authors were only able to speculate on the nature and origin of these signals, suggesting that the signals were an efferent copy (pursuit command) and/or afferent input from the eye muscle system (Barton, et al., 1996).

To further elucidate the functional neuroanatomy underlying pursuit from other types of eye movements (saccades) in humans, one group contrasted pursuit-related activation with that of saccade-related movements and reported activation in FEF, SEF, precuneus and the putative MT+ region, concluding that there are two distinct, but parallel, "cortical systems that subserve pursuit and saccadic eye movements" (Petit & Haxby, 1999). Further studies have revealed distinct subregions of the MT+ complex seen in monkeys, namely the putative MSTl (lateral) and MSTd (dorsal) regions, by using optic flow stimuli limited to the peripheral visual field, and a separate experiment into pursuit eye movements, to isolate areas underlying retinal and extraretinal processing (Dukelow, et al., 2001).

Given that human imaging data would seem to confirm the anatomical findings in the monkey regarding the cortical location of the pursuit system sub-units, recent studies have sought to expand on invasive research and examine the neural networks responsible for encoding eye velocity. Using a similar protocol to one reported in the monkey literature, Nagel and colleagues examined modulation of cerebral activation by varying eye velocity during target tracking and target blanking, and reported positive correlations between the magnitude of the blood oxygen level dependant (BOLD) signal and eye velocity in extra-striate regions. They concluded that MT+ is responsible for smooth pursuit maintenance and perceptual stability during visual feedback, whilst parietal areas are thought to be involved in multisensory integration, task-switching, sensorimotor coordinate transformations (Nagel,

Sprenger, Hohagen, Binkofski, & Lencer, 2008), and the suppression of saccades and the reflexive optokinetic nystagmus (OKN) response (Nagel et al., 2006).

However, one of the limitations of using non-invasive neuroimaging such as fMRI is that these data are only correlational, and causality cannot be implied; activity in these regions might be the result of an unknown intermediary process, undetectable by the present method. Therefore, the role of these regions in pursuit can only be inferred indirectly using these techniques. Consequently, it is desirable to invoke causality if the role of MT+ in head-centred motion perception is to be understood. One of the tools at our disposal for such an investigation is transcranial magnetic stimulation (TMS).

Based on the assumption that MT+ plays a principal role in the maintenance of perceptual stability, Haarmeier and Kammer (2010) used TMS to probe the neuronal underpinnings of this mechanism by stimulating this site during pursuit over a stationary background. It was found that oculomotor behaviour was disrupted as a result of TMS, with the pursuit gain compromised during stimulus tracking and concurrent stimulation, but that perceptual stability remained intact. They proposed that whilst this site is important in maintaining optimal gain during pursuit, its role in motion perception invariance has been overstated. They conclude that this perceptual processing resides in a number of distributed but highly interconnected cortical regions subserving pursuit (Haarmeier & Kammer, 2010).

1.2.4 Delineating intentional versus reflexive extraretinal signals in MT+

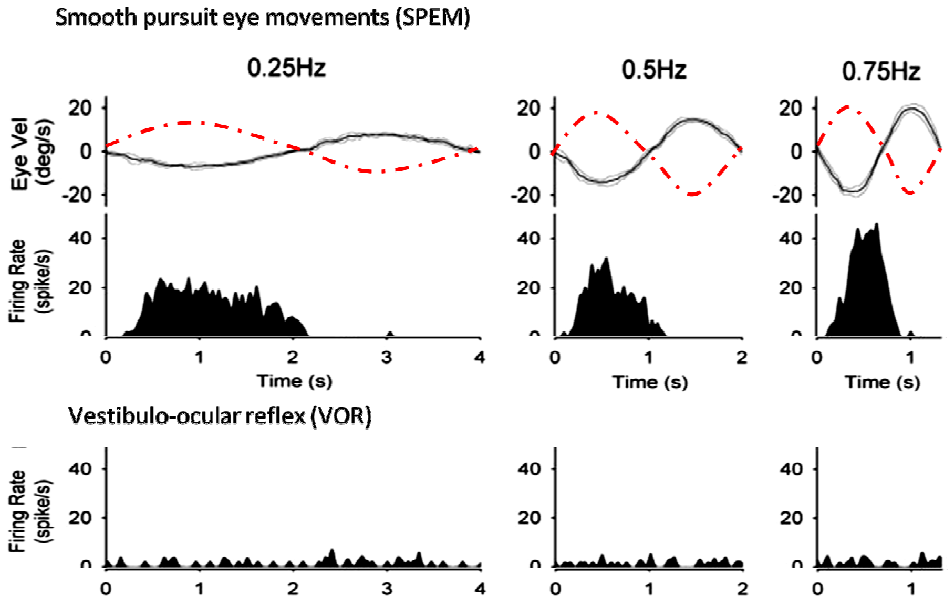

Figure 3. MST responses for eye movements during smooth pursuit compared to those induced by the vestibulo-ocular reflex.
The top panel of graph depicts eye movement data, at three different sinusoidal pursuit frequencies, when maintaining fixation of a target. The solid grey line shows the rotational eye velocity when smoothly following a moving stimulus or that induced by translational movement of the head during the VOR when fixating stationary target. The dashed red line indicates the equal and opposite translational head movements used to induced the VOR eye movement. Below that are activity profiles for a spatiotopic neuron in MST that encodes the velocity of the eyes. The bottom panels show the activity profiles for the same neuron during the VOR when the physical motion of the eyes was identical to that of the pursuit condition, but this time the neuron remains silent. Adapted from (Ono & Mustari, 2006).

A study by Ono & Mustari (2006) attempted to elucidate whether MST processes extraretinal signals that are derived from reflexive (such as proprioceptive feedback/afferent input) or intentional eye commands (such as corollary discharge/efference copy). Shown in Figure 3 are the results from one group using electrophysiology in the monkey, where they compared MST responses during smooth pursuit of a moving target in total darkness with those induced by the vestibulo-ocular reflex (VOR) (Ono & Mustari, 2006).

During intentional smooth pursuit, activity was noted in MST that corresponds to the velocity of the eye movement, shown in the middle row. Conversely, there was no activity

found in the same neurons when eye movements were performed that were identical in their physical motion but generated by the VOR through a translational motion of the head (shown in the bottom panels). This suggests that spatiotopic MST responses resulting from pursuit are transmitted along intentional, rather than reflexive pathways. This led the Ono & Mustari to conclude that only deliberate eye movement signals in MST are involved in the maintenance of space constancy.

Previous psychophysical studies examining oculomotor adaptation and the extraretinal motion aftereffect (MAE) would substantiate the claims that there is a delineation between intentional and reflexive eye movement commands that are processed in MST (Freeman & Sumnall, 2005). The extraretinal MAE is a perceptual consequence of performing repetitive unidirectional smooth pursuit eye movements, where a subsequent test stimulus is perceived to move in the opposite direction to that of the adapting eye movement. This is thought to be because persistent extraretinal eye movement signals sent from the oculomotor control system to MT+ and the sub-complex MST consequently adapt motion-sensitive neurons in this region of cortex. Neurons coding a particular direction of motion are adapted during pursuit and there is a resulting imbalance in the baseline activity of these neurons compared to neurons coding motion in the opposing direction. This imbalance is thought of as a possible explanation for the illusory motion.

Importantly, Freeman & Sumnall (2005) found that pursuit adaptation induced through both intentional and reflexive eye movements produced an extraretinal MAE, but critically noted that when pursuit was deliberate (termed by the authors ‘look nystagmus’), the MAE was found to survive a blank ‘storage’ interval where observers remained in total darkness. However, the MAE resulting from eye movements induced through reflexive optokinetic nystagmus (OKN; ‘stare nystagmus’) was only found to persist when the illusion

was tested immediately following adaptation, but that it did not exist following the blank storage interval (Freeman & Sumnall, 2005).

Evidence for this is shown in Figure 4, which shows storage of an extraretinal motion aftereffect induced by deliberate repetitive pursuit eye movements, but not for reflexive nystagmus, an eye movement that whilst almost identical behaviourally, is actually the result of automatic mechanisms that serve to stabilise a large moving image, rather than a particular moving target. This is compelling evidence for the integration of extraretinal signals into motion processing cortex, but that signals from deliberate and reflexive pursuit eye movements are delineated in this region. In particular, this evidence suggests intentional pursuit eye movements adapt motion-sensitive neurons in MST, resulting in the extraretinal MAE, whilst estimates of eye movements derived from reflexive eye movement behaviour is discounted.

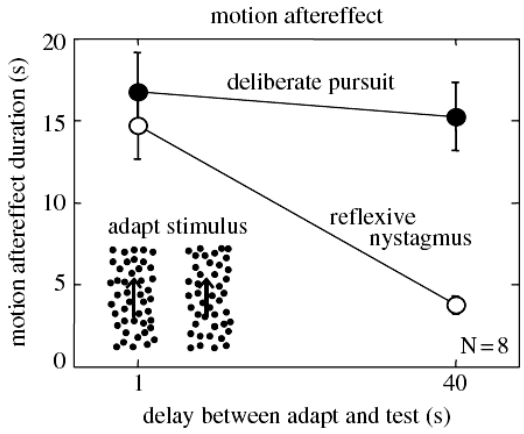

Figure 4. Comparing the motion aftereffect for deliberate versus reflexive pursuit. Following unidirectional smooth pursuit adaptation of neurons in area MST, observers report a perceptual extraretinal MAE, and this illusory motion is only known to be stored following deliberate, rather than reflexive, eye movements. This evidence suggests intentional smooth pursuit signals are integrated into motion processing cortex, MT+. Reproduced with permission from Freeman & Sumnall (2005).

1.2.5 Is there a functional role for cortical oscillations in pursuit eye movements and perceptual stability?

In the previous sections, a number of the studies that have probed the neuronal substrates of the smooth pursuit network were examined, and a description was given of the neurophysiological mechanisms that the brain might use to compensate for pursuit-induced retinal motion, in particular, the use of extraretinal eye movement signals. However, animal studies have for the most part relied on single-unit recording, which may not be a reliable indicator of the neuronal substrates of perception in the brain (Wilke, Logothetis, & Leopold, 2006; Zhang, Logothetis, & Liang, 2009). Furthermore, neurophysiological research has been limited to animals, and non-invasive measures of cortical activity in humans have been for most part limited to fMRI, an indirect correlate of neuronal responses with a relatively poor temporal resolution (compared to single-unit recording and other imaging techniques).

In addition, whilst we can infer how the brain processes extraretinal signals using perceptual and psychophysical methods, without directly measuring neuronal activity in humans, the picture of how the brain integrates and processes these extraretinal components to maintain pursuit and perceptual stability is incomplete.

Therefore, it seems reasonable to complement this previous research with studies into pursuit eye movements using other techniques to study these neurophysiological mechanisms, and, in particular, from the point of view of this thesis, how cortical oscillations might play a role in the underlying execution, control and processing of extraretinal eye movement signals when engaging in smooth pursuit. Whether cortical oscillations play an active role in cognition, sensory-motor processing and perception, or whether they might just be interesting emergent phenomenology because of neuronal activity is a question that has received attention in recent years. A number of theories have been proposed for the putative

perceptual functional role, if any, of these oscillations. Here, a number of those theories that have received particular attention shall be reviewed.

Research from invasive electrophysiological studies measuring changes in local field potentials and non-invasive neuroimaging studies (in particular, EEG and MEG) in humans have found that a wide variety of sensory, motor and cognitive processes appear to be associated with changes in neuronal synchronisation, with supporting evidence that there might be a number of largely-distinct underlying functional frequency bands at play. These cortical oscillators are thought to underpin a number of sensorimotor functions, including visual-feature binding (Singer, 1999), stimulus-specificity (Tallon-Baudry, Bertrand, Delpuech, & Pernier, 1996), spatial attention (Fries, Reynolds, Rorie, & Desimone, 2001; Womelsdorf, Fries, Mitra, & Desimone, 2005) and visuo-motor integration (Andino, Michel, Thut, Landis, & Peralta, 2005), to name but a few.

Furthermore, it has also been shown that changes in oscillatory dynamics present in the LFP signal (gamma, as well as alpha (8-12 Hz) and beta (5-25 Hz) activity) have a high spatiotemporal correlation with underlying cortical activity measured as a function of haemodynamic response (Brookes et al., 2005; Singh, Barnes, Hillebrand, Forde, & Williams, 2002), and spike rate (Mukamel et al., 2005). Together these findings suggest that the spatiotemporal dynamics of cortical synchronisation reflect some underlying neuronal mechanisms that are intrinsically linked to the processing of information in the cortex, and that modulation of these macroscopically recorded oscillations are reliable biomarkers of cortical excitation and inhibition.

1.2.5.1 Gamma in perceptual binding

An interesting feature of neuronal cell assemblies is that they are often seen to engage in task-induced rhythmic oscillatory synchronisation, whereby an increase in power in the gamma (γ) frequency band (30-80 Hz) is observed in the recorded local field potential (LFP),

which reflects an increase in the coherent pattern of on-going brain rhythms. This is often referred to as cortical oscillatory activity, neuronal synchronisation or phase locking. This phenomenon is readily seen when the cortex is engaged in sensory processing, particularly when recording from early visual areas. This led Singer (1999) to propose that gamma activity may be a mechanism by which the brain binds together the features of a scene to maintain perception of a unified visual experience (Singer, 1999), known as the binding hypothesis. However, a number of studies in recent years oppose this view. Some of the latest theories on the role gamma activity will now be discussed.

1.2.5.2 Gamma activity facilitating inter-cell assembly communication

The implicit model of neuronal communication proposes that neurons transmit information encoded by rate integration or degree of synchronisation in the action potential. All anatomically connected post-synaptic neurons combine the different inputs, with the probability of further transmission dependent upon the summation of the electrical activity reaching a pre-determined threshold.

However, this model assumes the distribution, computation and reception of signals is governed by the anatomical structure of these connections; it does not account for the flexible routing of signals throughout the brain required for sensory, motor and cognitive processes it has to perform on a constant basis. To perform such computationally-demanding tasks, the brain requires an inherently flexible and efficient communication mechanism to be implemented on top of the (largely fixed) anatomical array of neurons that comprise the brain (Fries, 2005). This has led to the hypothesis by Fries (2005) that the flexible communication mechanisms required for sensation, cognition and action is executed by oscillatory synchronisation between communicating neuronal groups. This particular hypothesis proposed that gamma activity is a fundamental mode of communication in the brain's neuronal networks.

Effective communication between two neuronal assemblies is thought to depend upon their phase difference, and this has been termed the 'communication-through-coherence' (CTC) hypothesis (Fries, 2005), with active neuronal groups often seen to engage in phase synchronisation in the gamma band. Related to this hypothesis, it has also been suggested that gamma activity is a mode of network activity that allows 'clocking' between neuronal subgroups to occur (Fries, Nikolic, & Singer, 2007).

A recent study that used magnetic resonance spectroscopy (MRS) to measure the concentration of inhibitory neurotransmitters in the human brain sought to provide a link between neurotransmitter and the generation of the gamma rhythm. These findings suggest that gamma activity is the result of inhibitory GABAergic interneurons and their interplay with excitatory pyramidal cells, and that the peak frequency in this band was dependent on the excitatory/inhibition ratio of these interconnected neurons (Muthukumaraswamy, Edden, Jones, Swettenham, & Singh, 2009).

1.2.5.3 Low-frequency oscillatory suppression: what functional role might that play?

Alpha band oscillations were first discovered by Hans Berger using EEG in the 1920s, and are the strongest and most-readily observed electrophysiological signal measured in the awake human brain (Berger, 1929; Lopes da Silva, Vanliero, Schrijer, & Vanleeuw, 1973). Until fairly recently, these prominent oscillations were thought to reflect the resting state of the brain in the absence of any changes in sensory input, or what was once termed the cortical 'idling rhythm' (Pfurtscheller, Stancak, & Neuper, 1996). By this, it was thought that this cortical rhythm reflects the on-going cognitive and perceptual state of the awake human brain when not engaged in the processing any particular task. However, with the advent of high-density EEG/MEG arrays, this view has been challenged in recent years by mounting evidence that alpha oscillations actually play an important functional role in cortical processing.

As briefly mentioned previously, changes in alpha oscillations are also readily observed along with concomitant gamma band changes when subjects are exposed to an external stimulus or task. It has been proposed that their physiological and functional role is in gating information flow between groups of neurons by inhibiting task-irrelevant regions through neuronal synchronisation in the alpha frequency band (Jensen & Mazaheri, 2010). By doing this, the brain is dynamically able to shape the 'functional architecture' of its internal circuitry and direct information flow around the network required for cognitive and perceptual flexibility. The macroscopic alpha oscillatory activity measured using neuroimaging techniques such as EEG/MEG is thought to reflect the 'blocking off' of pathways that direct the flow of information between neuronal nodes (or functional groups of neurons) that are irrelevant to the processing of the current task. A schematic of this is shown in Figure 5.

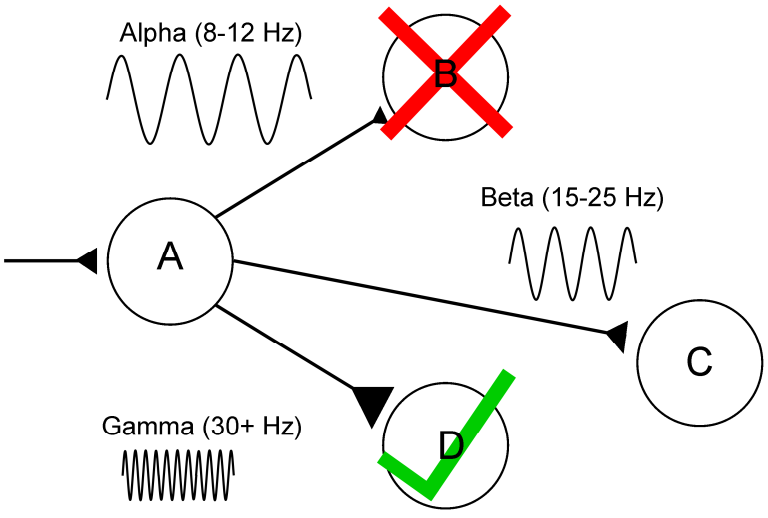

Figure 5. One model for how neurons direct information around the static structural array of the brain proposes that neuronal groups facilitate communication with each other by synchronising at different frequencies.
This in turn modulates the efficacy of information flow between each neuronal group. Functionally, alpha oscillations (8-12 Hz) are thought to reflect the inhibitory gating of information between nodes (Jensen & Mazaheri, 2010), whilst an increase in gamma activity (30+ Hz) is thought to reflect an increase in the coherence between groups and the information processing that is taking place between these nodes. Gamma activity is readily

observed when a sensorimotor change is expected, novel information is being processed or a cognitive task performed. The role of beta oscillations (15-25 Hz) is less clear, although current hypotheses propose that its broad functional role is in the maintenance of the on-going network state in, and between, sensorimotor cortices, and that suppression of this rhythm facilitates processing of a stimulus change, or the expectation of a change (Engel & Fries, 2010; Wilke, et al., 2006; Zhang, et al., 2009). The relative 'strength' of the connection between neuronal groups is represented by the increasing size of the synaptic terminal (denoted by the triangles; this however does not reflect any changes in specific synaptic efficacy, independently of any changes in neuronal synchronisation at different frequency ranges).

This has been explicitly tested by examining whether changes in alpha activity was observed in specific brain regions thought to be engaged when performing a particular perceptual or cognitive task. Numerous studies have used tasks involving the engagement of covert visuo-spatial attentional mechanisms and they are consistent in reporting hemispheric lateralisation of alpha frequency changes; for example, it has been shown that when covert attention is directed to a particular visual hemifield, there is suppression of alpha in the contralateral hemisphere, and conversely alpha increases in the ipsilateral hemisphere (Handel & Jensen, 2009; Rihs, Michel, & Thut, 2007; Worden, Foxe, Wang, & Simpson, 2000; Yamagishia, Callana, Anderson, & Kawatob, 2008). This suggests functional inhibition by way of alpha synchronisation in task-irrelevant areas is required for optimal processing of a task.

Moreover, cortical inhibition as a result of on-going alpha activity is thought to function in a phasic manner (VanRullen & Koch, 2003), with Mazaheri and Jensen (2010) proposing that this results in 'pulsed inhibition' of task processing that coincides with peaks in the alpha duty cycle approximately every 100 msec (Mazaheri & Jensen, 2010). Experimental evidence for this was found when performance on a visual detection task appeared to be modulated in certain phases of the alpha rhythm, with performance greater at some points than others (Busch, Dubois, & VanRullen, 2009).

These studies suggest that alpha oscillations in task-irrelevant regions of the cortex play a functional role in directing information around the cortex; conversely, it could be said that active suppression of this rhythm in regions implicated in processing of task-relevant information is also required for 'shaping functional architecture' (Jensen & Mazaheri, 2010).

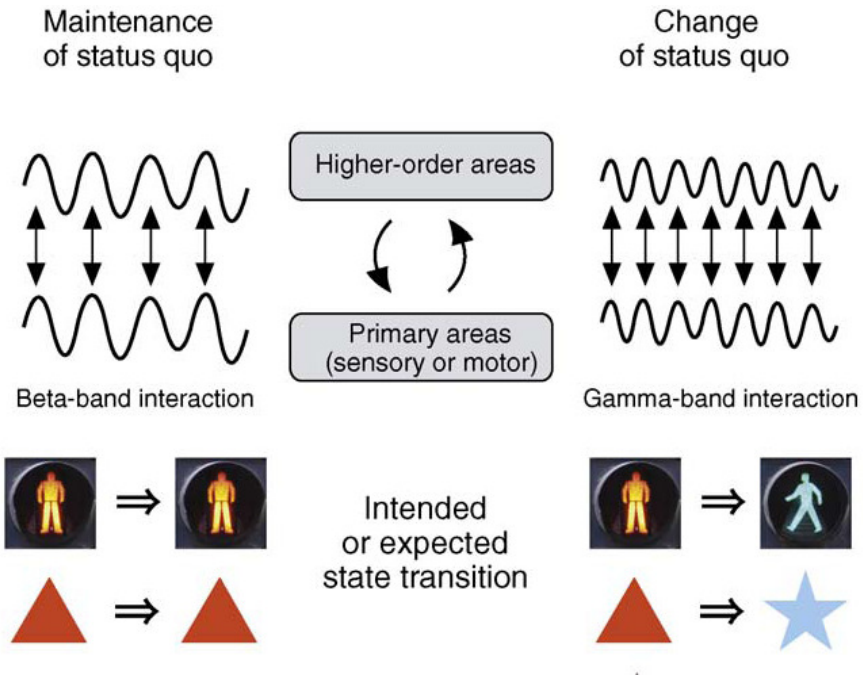

Figure 6. Schematic of the hypothesised functional role of beta-band oscillations in sensorimotor processing.
It has been proposed that beta activity reflects the on-going maintenance of the current sensorimotor state between circuits connecting higher-order and primary areas implicated in the task. When primed for an expectant change in the task, for example the processing of incoming novel information, suppression of these beta band rhythms and a concurrent increase in gamma activity is often readily observed. Adapted from (Engel & Fries, 2010).

In addition to the proposed functional and physiological roles of gamma and alpha oscillations in perceptual and cognitive processing, changes in the beta frequency (15-25 Hz) are also thought to play a mechanistic role in cortical processing, although the function of this activity is less clear-cut. Beta oscillations have been studied extensively in motor and somatosensory cortex within the domain of motor processing and a number of studies have

shown an association between the BOLD signal and rhythmic changes in the beta band (Parkes, Bastiaansen, & Norris, 2006; Ritter, Moosmann, & Villringer, 2009). Decreases in beta power are observed when engaging in execution of movement, with a rebound beta increase when this motor action is concluded (Stancak & Pfurtscheller, 1995; Toma et al., 2000). It was also shown by Gilbertson et al. (2005) that intentional movements are impaired when performed during phases that are temporally coincident with relative enhancement of the on-going beta activity (Gilbertson et al., 2005).

This would suggest that on-going beta oscillations are a reliable biomarker of cortical inhibition, and that suppression of this rhythm is an active process engaged by the brain to facilitate cortical processing, particularly in the processing of motor commands. Therefore, the role of beta oscillations is thought to be similar to that of alpha activity. However, the functional role of beta changes in relatively early stages of visual processing is less well understood, although research suggests low-frequency LFP power changes are more closely related to visual perception than spiking activity (Wilke, et al., 2006).

A recent review put forth the hypothesis that beta-band oscillations exist to maintain an on-going network state in the brain, connecting higher- and primary sensory cortices through neuronal synchronisation (Engel & Fries, 2010). A schematic diagram of this is shown in Figure 6. Termed by the authors as the ‘maintenance of the status quo’, they propose these oscillations serve to facilitate the continuation of the current conditions in any interconnected neural network. Following this there is a subsequent suppression of this rhythm when there is an expected transition to a different state (such as the processing of an impending novel stimulus or change in the task).

Despite this, the authors are cautious to point out that while amplitude modulation of cortical rhythms are considered by many to signify ‘global state changes’ in the brain (Engel & Fries, 2010), any proposed unifying mechanistic roles in changes at a particular frequency

should be interpreted with caution. They posit that is difficult to form a unifying hypothesis on a specific frequency band associated with a particular cognitive or sensory process given the current data.

1.2.5.4 Causal evidence for a functional role of oscillations in perceptual processing

Whilst research into the role of cortical oscillations has for the most part been correlative in nature, a number of studies provide direct casual evidence for the importance of this oscillatory brain activity in sensory and motor processes. For example, it has been shown that by using repetitive TMS in the alpha frequencies over occipital cortex, subsequent performance on perceptual discrimination and detection tasks were significantly impaired, suggesting an intrinsic role for alpha oscillations in visual perception (Thut & Miniussi, 2009).

Furthermore, it has been shown that using subthreshold transcranial alternating-current stimulation (TACS) can entrain cortical activity at the beta rhythm (Pogosyan, Gaynor, Eusebio, & Brown, 2009). Pogosyan and colleagues found that stimulating the motor cortex at 20 Hz in healthy subjects slows the action of voluntary movement, which suggests causality between brain oscillations and the preparation, execution and maintenance of motor behaviour. This shows the importance of beta oscillations, and ultimately their suppression, in the act of sensory-motor integration.

Therefore, previous research suggests that changes in oscillatory dynamics represent some underlying cortical activity and that specific sensory-motor processes seem to be mediated by such changes in neuronal oscillations. To understand the role of MT+ in oculomotor control and the processing of extraretinal eye movement signals, the induced neuromagnetic correlates of smooth pursuit needs to be investigated. One way to do this is to use non-invasive neuroimaging. In the specific case of this thesis, MEG was used to explore the rhythmic changes generated in the cortex related to extraretinal eye movement signals and

the possible functional roles they might play in encoding aspects of the eye movement in motion processing regions.

1.3 Methodology

In this part of the General Introduction, a brief overview is first given of the theoretical foundations of the methodological approaches employed throughout the experimental sections of this thesis. Then, specific details about the recruitment procedures employed, the apparatus used, and some of the data acquisition and analysis parameters that remained constant throughout the studies presented in this thesis are described. Any case-specific acquisition configurations or analysis techniques are described in the relevant chapters.

1.3.1 Recording cortical activity non-invasively

1.3.1.1 Magnetoencephalography

Magnetoencephalography (MEG) is a non-invasive functional neuroimaging technique that provides us with a comprehensive spatiotemporal description of neuronal activity. It does this by measuring neuromagnetic fields produced by the mass action of spatially co-aligned apical dendrites of pyramidal neurons in the brain which are oriented along a similar axis (Vrba & Robinson, 2001). Electrical currents are produced by the summation of post-synaptic potentials, the movement of positively-charged ions across the cell membrane in the dendrites of the neurons, and it is this electrical current that produces an associated magnetic field perpendicular to the direction of ion current (Singh, 2006). The MEG system uses a fixed-array of extremely sensitive magnetometers, known as superconducting quantum interference devices (SQUIDs), to detect magnetic field changes at the level of the scalp. The array of magnetometers is arranged in a similar fashion to that of the shape of the head.

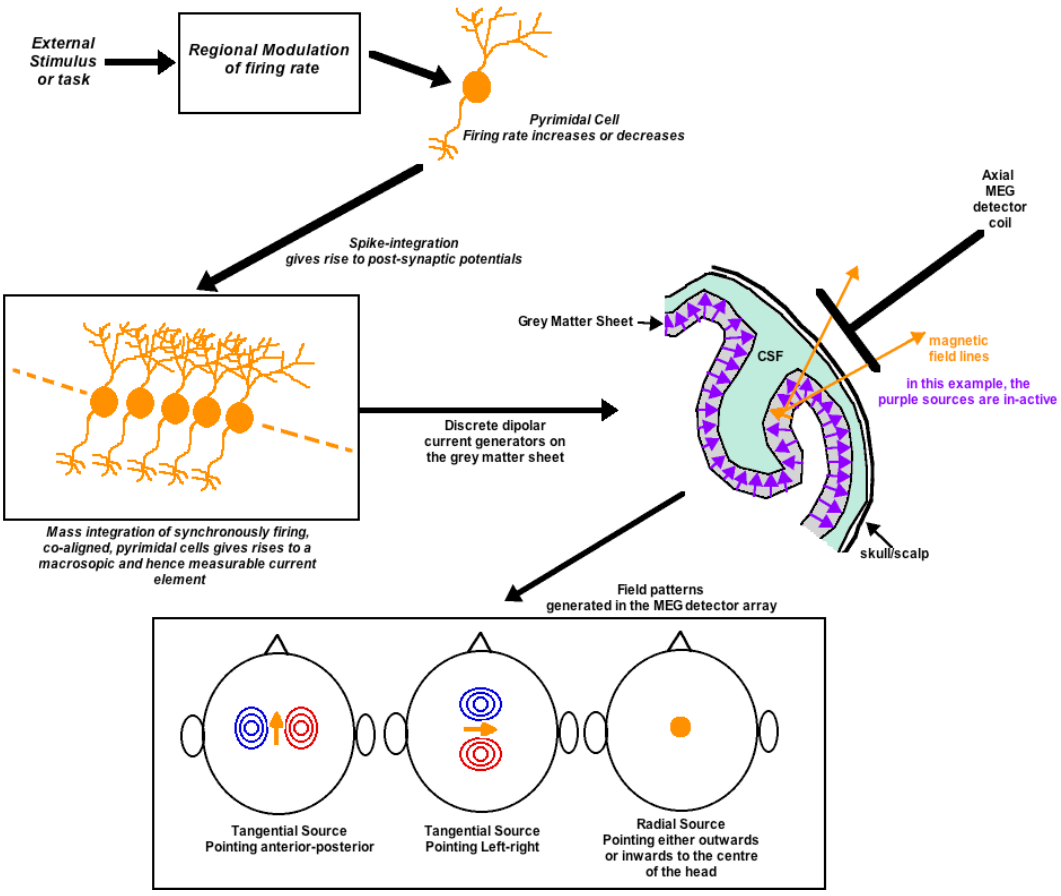

Figure 7. Schematic diagram showing how MEG detects the neuromagnetic changes generated in the cortex as a result of task-induced activity in co-aligned pyramidal cells in the cortical sheet.
Action potentials are brief spikes in activity and are likely not detected due their temporally uncorrelated nature, in addition to axons not being spatially co-aligned. Reproduced from (Singh, 2006).

MEG is closely related to electroencephalography (EEG) but benefits from being able to record the magnetic flux originating from primary currents in the cortex. MEG is considered a relatively more robust technique than EEG for measuring and estimating the source of neuronal processes in the brain because magnetic fields pass unimpeded through the otherwise electrically resistive skull, meninges and scalp, which is tissue that interferes with the electrical currents originating in the cortex measured using EEG (Baillet, Mosher, &

Leahy, 2001). Furthermore, MEG benefits from a comparative immunity to electrophysiological noise (such as eye blinks and muscle twitches).

1.3.1.2 SAM source estimation

Despite the excellent temporal resolution afforded by MEG, a fundamental limitation of the technique is that of the ill-posed inverse problem. This means that the exact source of cortical activity can never be truly be inferred from the activity recorded by an external MEG (or EEG) sensor array, as there is insufficient information to construct a unique solution for the distribution of brain electrical sources that are generating the externally measured field. However, using a number of a priori assumptions about conductivity profiles, brain shape/location and the nature of dipolar sources, with the implementation of sophisticated localisation techniques it is possible to estimate the most likely source distribution given a number of specific constraints that are imposed.

One particular source estimation technique, known as 'beamforming', has seen a substantial increase in use in recent years. A variant of this method called Synthetic Aperture Magnetometry (SAM) is now widely used for analysis of MEG data, and this particular method is employed in this thesis (Vrba & Robinson, 2001). SAM is based on algorithms implemented in fixed-array radar technology, in which sensors (in this case, the magnetometers) are weighted in the offline analysis in such as a fashion as to scan each portion of the brain (which is divided into volumetric pixels, or voxels) and estimate the contribution of that particular cortical location to the measured signals. Once these estimates are computed, beamforming algorithms can be used to weight each of the sensors in a suitable fashion to act as a 'spatial filter' and optimise sensitivity to neuromagnetic changes in a particular voxel location.

MEG data is then projected through the spatial filter to provide a time series of current density at this location and this allows accurate estimation with millisecond precision

of the source strength at the region of interest (Singh, et al., 2002), with the output known as a 'virtual electrode' (Barnes & Hillebrand, 2003). Pseudo t-values for oscillatory changes in cortical dynamics (such as task-induced changes in oscillatory power) are obtained by comparing the defined spectral power content in the baseline/passive phase of a trial to the active/task phase, and then normalising the differential power estimates by dividing by an estimate of the MEG sensor-space noise, projected through the beamformer weights (Hillebrand, Singh, Holliday, Furlong, & Barnes, 2005; Vrba & Robinson, 2001). By doing this, it is possible to assess induced (time-, but not phase-locked) oscillatory activity in populations of neurons situated in a particular region of the brain.

1.3.1.3 Induced responses

As described in the Background section of this chapter, there has been much debate over the functional significance of induced oscillatory responses in the cortex and the putative role they might play in perception, action and cognition. A description is given here of the general analytical approach on how to extract evoked and induced oscillatory changes from time series data collected over the course of an experiment

Evoked responses in the brain are both time- and phase-locked to the onset of a task or stimulation. This means that the underlying latency of the response on any given trial appears at approximately the same time (in that there is often very little 'jitter' in the signal) and of the same phase (in that the deflection of the response if in the same direction). Therefore, analysis of evoked responses can be achieved by simply averaging the signal in the time-domain to increase the signal-to-ratio of the specific time-locked response of interest.

However, using a similar approach to the analysis of evoked and induced changes in oscillatory power would result in the cancellation of any effect. This is because spectral power changes in the signal are time-locked to the onset of a task, but the underlying phase of

the oscillatory change on any given trial is essentially random. Averaging these non-phase-locked components in the time-domain will cancel out any effect as the phase of the induced response can be different each trial, whilst the latency of the oscillatory change is the same. This means that induced oscillatory responses manifest themselves as changes in the frequency power content of the signal at a time that is similar on every trial, but the phase of the response can be different. Therefore, if the same approach to analysis of evoked responses is used when looking for induced activity by time-domain averaging of the epochs, any frequency-specific neuronal activity related to the task is lost. Consequently, this requires a different analytical approach in which task-induced oscillatory modulations are quantified by analysing the data in the frequency-domain.

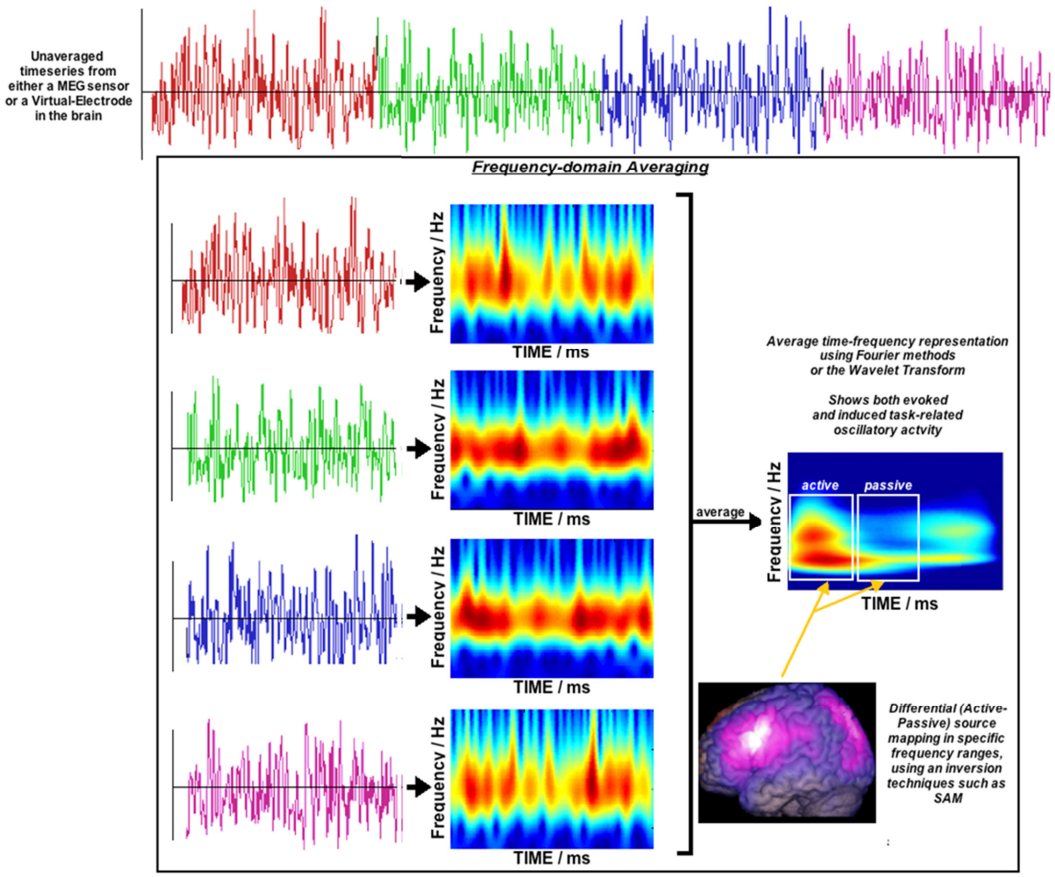

Figure 8. Frequency-domain averaging of MEG time-series data to allows evoked and induced oscillatory changes related to task processing to be extracted from the signal.

The multi-coloured time series data at the top of the figure depicts an example of MEG data (from either a sensor or virtual electrode recording) over an experimental run. These data are then epoched into individual trials, on which a time-frequency analysis is then performed, revealing the spectral power content of any particular epoch over time. This time-frequency content is then averaged, showing the mean frequency power changes related to the task. Adapted from (Singh, 2006).

Figure 8 shows how this analysis might be conducted. At the top of the figure is an example of some time series data over the course of an experimental run, which in this case, might be from a sensor in the MEG array or extracted from a virtual electrode within the brain. The time series is then epoched (perhaps divided into individual trials, as depicted by the four coloured traces on the left hand side of the bounded box). These trials are then averaged separately in the frequency domain to extract the changes in spectral power over time, which can be seen in spectrograms in the centre of the box. These spectral plots are then averaged together to reveal both the evoked and induced task-related oscillatory power changes during the experiment, which is shown by the final spectral plot on the right hand side of the box.

1.3.1.4 Functional Magnetic Resonance Imaging

Functional magnetic resonance imaging is a popular neuroimaging technique for use in the investigation of the functional regions of the brain involved when performing sensory, motor and cognitive processing. Since its introduction in the early 1990's (Bandettini, Wong, Hinks, Tikofsky, & Hyde, 1992; Kwong et al., 1992; Ogawa, Lee, Kay, & Tank, 1990; Ogawa et al., 1992), it has proven instrumental in delineating distinct functional regions of the cortex whilst being (relatively) non-invasive, allowing researchers to understand how the brain works in healthy human participants without the need to introduce tracers or subjecting participants to radiation.

Whilst the temporal resolution of the technique is inferior to that of EEG/MEG, it has a high spatial resolution, making it an effective complementary method to MEG for the imaging of functional brain states. The fMRI technique relies on using the endogenous contrast associated with haemodynamic changes in the cortex during neuronal activity. One particular implementation of this technique most in use today is called the Blood Oxygen Level Dependence (BOLD) effect (Ogawa, Lee, Nayak, & Glynn, 1990), which utilises the difference in the magnetic properties of oxygenated and deoxygenated blood, and how these magnetic gradients change in the blood vessels of the brain during neuronal activity. This particular method of assessing cortical function is employed in the fMRI part of Experiment 1, Chapter 2.

1.3.2 Participants

All participants used in the following studies were recruited internally or from the Cardiff University Human Participant Panel database using the Experiment Management System, having given prior informed consent and agreeing to receive monetary compensation or course credits for participation in the experiment. All participants had normal or correct-to-normal visual acuity and no history of neurological disorders. All experimental procedures were approved by the Cardiff University School of Psychology Ethics Committee.

1.3.3 Apparatus, data acquisition protocols and analysis parameters

In all the experiments, participants wore customised goggles fitted with cross-polarized filters. This was to ensure that any scattered background light in the laboratory was attenuated, thereby minimising activation related to pursuit-induced retinal image motion of any visible landmarks peripheral to the projector screen. During the setup of any experimental run, participants were asked whilst wearing the goggles to report whether the

only visible object was the stimulus. If not, successive layers of cross-polarized filter were added to the goggles until the only perceived object was the stimulus.

In each experiment, electrooculographic (EOG) recordings were taken to characterise eye movements during MEG data collection. During eye movements, the retina induces an electrical current in the surrounding tissue, and this propagates to the skin, which in turn is recorded as a change in the potential difference (voltage) between pairs of electrodes, from which it is possible to infer the position of the eyeball within the socket. Skin preparation was performed using alcohol wipes and electrolyte gel was applied to these areas to minimise electrical resistance between the skin and electrode. Pairs of electrodes were placed above and below the eye to record vertical displacement, and to the lateral corner of each eye to record horizontal displacement.

The impedance of each electrode was then measured to ensure satisfactory conductance of the EOG signal. Skin preparation was performed again and the electrodes were re-applied if the electrical resistance was found to be above a pre-defined threshold of 5 kΩ. Whilst the temporal resolution of this technique (which is dependent upon sampling rate, but nevertheless in the order of milliseconds) is superior to that of infrared eye tracking, the spatial resolution remains comparatively poor and is more susceptible to electrophysiological noise, e.g. muscle artefacts. However, with the eyes occluded by near-opaque goggles during the experiment, this is the only appropriate technique to use. A pre-run calibration routine was always performed where participants were required to saccade to and fixate a number of stationary targets at various positions on the projector screen.

During the MEG experiments, visual stimuli were generated on a GeForce graphics card (NVidia Corporation) and back-projected (Sanyo XP41 LCD) onto a screen at 60 Hz (size 34 x 24.7 cm, total visual angle 25.6 x 19.2 degrees, resolution of 1024 x 768) at a distance of 71 cm. The visual stimuli and experimental protocols were programmed in Pascal

(Delphi 7, Borland Software Corporation) using an OpenGL software library for graphics hardware.

MEG data was recorded using a 275 channel whole-head system (CTF Systems Inc., a subsidiary of VSM MedTech Ltd.) in a magnetically shielded room at a sample rate of 600 Hz using an axial gradiometer configuration, with the primary sensors analysed as synthetic third-order gradiometers. During data acquisition, head position and motion was monitored using three fiduciary markers placed on the nasion and 1 cm anteriorly from both the left and right tragi. Each participant's MEG data was then co-registered with their anatomical data based on the position of these easily identifiable anatomical landmarks from the MR scan. These points were verified using high-resolution digital photographs taken during fiducial placement.

SAM images were constructed on a 5 mm^3 grid throughout the brain for each participant. Oscillatory power changes between the passive and active periods in each experiment for all epochs were mapped for broadband alpha (5-15 Hz), beta (15-25 Hz) and gamma (30-70 Hz) frequency ranges. Specific details about the duration of the active and passive periods are detailed within the Methods section of each chapter.

Peak coordinates for activation in the specified frequency band in the SAM images were visualised using mri3dX (Singh, 2009) and chosen on the basis of their locality within the region of interest (ROI) for each particular study. Peak locations were identified using an automatic algorithm that first breaks the SAM image into discrete clusters using a moderate pseudo-t threshold of 0.5. Multiple peaks identified within a radius of 5 mm are considered to represent a single peak. These coordinates were used to compute suitable weights for virtual electrode generation on an individual basis and used in all subsequent analyses (performed using Matlab). Additional computation of time-frequency spectrograms were performed at peak voxel locations based on the Hilbert transform, using frequency ranges 0.1 to 90 Hz in

0.5 Hz steps and 8 Hz frequency smoothing. The percentage change in oscillatory power during the experimentally defined active period was then baselined against the passive period.

1.4 Focus and summary of the thesis

1.4.1 Aims of the thesis

Given that functional neuroimaging studies in healthy humans of the smooth pursuit system have been for the most part been limited in scope to using fMRI, the objective of this thesis was to expand on previous findings and utilise MEG to explore the changes in cortical oscillations associated with smooth pursuit eye movements. In particular, the aim of this work was to examine how rhythmic changes in neuronal activity in motion processing cortex might subserve aspects of oculomotor control and the integration of extraretinal eye movement signals during pursuit, a mechanism that might ultimately be used in perceptual stability. Following on from this, a number of general questions guide the experiments presented hereafter:

- Do pursuit eye movement induce cortical oscillatory changes in MT+?
- If so, are they integral in the maintenance of pursuit and perceptual stability or just interesting emergent phenomenology of cortical processing?
- Furthermore, are aspects of the eye movement encoded in the MEG signature originating from this region of the cortex?
- Finally, are there any distinct functional roles that different frequency bands might play in this behaviour?

1.4.2 Rationale behind the studies

Whilst the spatial resolution of fMRI remains superior to MEG, using MEG has allowed researchers to resolve, with a temporal resolution in the order of milliseconds, both

the spatial extent and magnitude of neuronal oscillations associated with sensorimotor processing, something which is not possible using fMRI alone. Additionally, whilst EEG might be considered an appropriate alternative technique to use when studying oscillatory activity underlying perception and motor control, this technique is severely affected by the rejection of artefactual data induced in the electronic signal during eye movements.

Furthermore, localising the high-frequency oscillatory components (gamma activity) originating in neocortex is not always possible using EEG, due to the largely-unknown conductivity profile of the skull, meninges and scalp which essentially act as a low-pass filter (Fuchs, Wagner, & Kastner, 2007). Therefore, using MEG allows measurement of neuromagnetic changes which remain unaffected by the mediating tissue between cortex and magnetometers, and these can be localised in the cortex using sophisticated beamforming algorithms (which as well as providing an estimate of source localisation also acts to enhance signal-to-noise by its action as a spatial filter). Analysis of this data in the frequency domain also allows the cortical oscillatory dynamics underlying cortical processing to be investigated. By using MEG, it is possible to mitigate the disadvantages associated with both fMRI (poor temporal resolution) and EEG (retinally-induced artefacts in the data related to eye movements and a limited ability to image gamma activity).

Consequently, MEG provides a robust means to study these phenomena related to smooth pursuit eye movements, providing a comprehensive spatiotemporal map of cortical oscillatory changes underlying pursuit, and in particular, the functional role, if any, that neuronal oscillations in the MT+ region might play in the processing of extraretinal eye movement signals. In all the experiments presented within this thesis, the observers head was stationary throughout the procedure, therefore all eye movement data is presented within a head-centred coordinate frame.

1.4.3 Summary of the findings

Experiment 1 probed the cortical representation of smooth pursuit using fMRI and MEG. Using fMRI, the regions implicated in the processing of visual motion stimuli and oculomotor control of pursuit were resolved. This activity was then compared with the MEG correlates of activity in identical paradigms. Of special focus was how the activity revealed in both domains compared in their spatial localisation in extra-striate cortex, thought to be MT+, and how oscillatory changes in this region during pursuit, retinal motion and a combination of the two compared. Consistent activity was found in MT+ associated with smooth pursuit eye movements in the dark in both modalities. An additional result initially provides evidence that changes in alpha-beta activity in this area reflect an eye position signal during pursuit, which suggests this area carries extraretinal eye movement signals. It is proposed that these signals are likely to be used when deriving estimates of real motion in the world when tracking a moving target and in the maintenance of perceptual stability.

Experiment 2 was a control study for the eye-position signal observed in Experiment 1. It seemed possible that the hemifield-dependent eye position response could have been an artefactual result and driven by retinal motion processing due to slip of the stimulus when the eyes were at the maximum contralateral position during the eye movement. Thus, the modulation of the alpha and beta responses in Experiment 1 that showed eye position-dependence were compared with those induced by retinal slip of a target during fixation. Whilst the characteristics of the response were similar for both eye position and transient retinal motion processing, retinal motion induced alpha and beta activity with a significant latency in the maximal response, beyond that which might have been observed if the apparent eye position-dependency effect was due to retinal slip. The timing differences in these responses suggest that the pattern of activity observed in Experiment 1 was due to either eye position or some other fundamental aspect of the eye movement, and not retinal error.

Experiment 3 was designed to test the interpretation of the hemifield-dependent eye position signal found in Experiment 1. In Experiment 3, the excursive pursuit paradigm, observers pursued a moving sinusoid at various head-centred eccentricities. By contrasting the alpha and beta amplitude envelopes when performing pursuit at various head-centre eccentricities, it would be possible to infer from the relative shape of the envelopes whether the eye position finding of Experiment 1 was due to head-centred eye position or some other aspect of the eye movement. The findings suggest that modulation of the alpha and beta rhythm was due to some other aspect of the eye movement, with no evidence of a head-centred eye position signal in MT+.

Given the results from Experiment 3, it seemed plausible that the alpha and beta activity could reflect a velocity-encoding signal that lags the motion of the eyes. In Experiment 4, the modulation of the alpha and beta activity as a function of linear increases in eye velocity was investigated. In addition, it was examined whether there is any eye movement direction-bias in the response properties of those neurons in MT+ that display pursuit-related activity. Whilst there appeared to be no clear or specific dependency of this response on velocity and the direction of the motion of the eyes, there was a significant effect of eye speed on the magnitude of the beta suppression, with increasing eye speed generally resulting in a decrease in beta amplitude. Furthermore, there was no clear effect of eye speed on alpha power. This dissociation suggests some functional distinction in the role of the alpha and beta rhythm in oculomotor control and the processing of extraretinal signals in MT+.

Experiment 5 and 6 examined the neuronal substrates of oculomotor and retinal motion adaptation (respectively), and the perceptual consequences of these actions. Motion adaptation is known to induce an illusion known as the motion after-effect. Experiment 5 aimed to elucidate whether changes in cortical oscillations in some of the principal cortical regions that subserve pursuit mediate aspects of the extraretinal MAE. In particular, this

study aimed to see whether objective neuronal measures, such as the duration of alpha and beta suppression, correlate with the subjective percept of illusory motion. Whilst this was not possible to conduct this analysis due to noisy estimates of signal changes, it was however found that beta activity in motion-processing cortex during adaptation was a significant predictor of the MAE duration. In Experiment 6, there appeared to be no clear relationship between the low-frequency suppression in MT+ induced during motion adaptation, but there was tentative evidence that alpha and beta suppression persists during illusory motion when there is no real motion. This perhaps suggests this activity mediates aspects of the MAE.

In the final chapter of this thesis, the General Discussion, an interpretation of the data presented is given within the framework of existing knowledge, the limitations of these studies are considered and the potential future directions of related research is proposed.

2 Chapter 2 – A study of MT+ activity in response to smooth pursuit eye movements and retinal motion processing

2.1 Abstract

Extra-striate regions are thought to receive non-retinal signals from the pursuit system to compensate for retinal motion and maintain perceptual stability during smooth pursuit eye movements. In Experiment 1, MEG and fMRI was used to study the cortical representation of smooth pursuit eye movements in extra-striate visual areas under 3 conditions: 'pursuit' of a small target, 'retinal-motion' of a large background and 'pursuit + retinal motion' combined. All stimuli moved sinusoidally. MEG source reconstruction was performed using SAM. 5-25 Hz ('broadband alpha-band') suppression was observed over bilateral extra-striate cortex (consistent with MT+) during all conditions. An fMRI study using the same experimental protocols confirmed an MT+ localisation of this extra-striate response. The alpha-beta envelope power in MT+ in the 'pursuit' condition showed what appeared to be an hemifield-dependent eye-position signal, such that the global minimum in the alpha-beta suppression recorded in extra-striate cortex was greatest when the eyes were at maximum contralateral eccentricity in the pursuit cycle. The 'retinal-motion' condition produced sustained alpha-beta power decreases for the duration of stimulus motion, with very little modulation of the alpha-beta rhythm during an average pursuit cycle. The 'pursuit + retinal motion' condition revealed a double-dip 'W' shaped alpha-beta envelope profile such that the global minimum in power corresponded to eye gaze position directed toward the contralateral visual hemifield during pursuit, with a secondary local minimum in power contiguous with eye gaze toward the ipsilateral hemifield. It seemed possible that the modulation of the alpha-beta signal in the 'pursuit' condition could have been due to retinal slip of the target when the eyes were at maximum amplitude of the pursuit cycle. Therefore, a second experiment was designed as a

control. In Experiment 2, the temporal dynamics of the alpha and beta response to transient retinal motion was characterised, approximating the motion that would have occurred during retinal slip of followed target when the eyes changed direction. The results here revealed a similar shape in the profile of the alpha and beta envelopes induced by motion, but the timing differences in the peak response suggest that the eye-position dependency effect found in Experiment 1 was not due to retinal error. These results taken together suggest that MT+ receives retinal as well as extraretinal signals from the pursuit system as part of the process that enables the visual system to compensate for the retinal motion during eye movement. It is proposed that the suppression of the alpha-beta rhythm reflects either the integration of an eye position-dependent signal or one that lags the velocity of the sinusoidally moving target.

2.2 Introduction

As previously described in the General Introduction chapter, smooth pursuit eye movements exist to maintain a stable image of a moving target on the fovea. To achieve this, the pursuit system needs to be able to compute the retinal image velocity of the target, process this information and transform the retinotopic coordinates of the target's motion into a spatiotopic, or head-centred, coordinate frame (Krauzlis & Lisberger, 1994a). These signals can then be used to compute the necessary motor commands to move the eyes and follow the target (Kimmig, et al., 2002; Krauzlis, 2004). At the same time, the visual system must somehow compensate for the retinal motion associated with objects other than the pursuit target (Champion & Freeman, 2010; Freeman, et al., 2010; Haarmeier, et al., 2001; Naji & Freeman, 2004; Schutz, et al., 2008; Souman, et al., 2006; Spering & Gegenfurtner, 2006; Turano & Massof, 2001).

Both oculomotor control and the perception of motion during eye movements are subserved by a variety of cortical processes that integrate retinal motion signals with motor commands. The functional neuroanatomy and perceptual bases of these systems has been studied extensively, using invasive electrophysiological recording (Ilg & Thier, 2003; Komatsu & Wurtz, 1988; Newsome, et al., 1988) and non-invasive functional neuroimaging (Dukelow, et al., 2001; Nagel, et al., 2008; Petit & Haxby, 1999). These techniques have revealed a functional network that subserves pursuit eye movements distributed across numerous cortical sites, and the principal regions involved have been studied in detail. In particular, human neuroimaging studies have mapped the spatial extent of the circuitry involved, and have found reliable activation in V1, middle temporal cortex (MT+), posterior parietal cortex (PPC)/intraparietal sulcus (IPS), the precuneus, the frontal eye fields (FEF), supplementary eye fields (SEF), and the cingulate gyrus during smooth pursuit eye movements (Kimmig, et al., 2008; Konen, et al., 2005; Thier & Ilg, 2005). The role of MT+

during pursuit has been of special interest as this area is thought to play a principal role in the estimation of object motion on the basis of eye movement signals and the integration of these signals in compensating for retinal motion induced by pursuing a target in a largely stationary world (Haarmeier, et al., 2001; Ilg, et al., 2004; Komatsu & Wurtz, 1988; Nagel, et al., 2008; Newsome, et al., 1988; Petit & Haxby, 1999).

Despite the numerous neuroimaging studies of pursuit-related extraretinal activation of the motion processing area MT+ and its sub-region, the medial superior temporal cortex (MST), to the best of our knowledge these have mostly been limited in scope to using fMRI, with one exception (Tikhonov, Haarmeier, Thier, Braun, & Lutzenberger, 2004). In this study, MEG dipole analysis was used to localise neuromagnetic responses in the 'late' stages of the visual processing hierarchy related to the perception of self-induced motion during eye movements. However, to the extent of our knowledge, there exists no literature on the cortical oscillations that might mediate such processes. Therefore, the experiments in this chapter hope to expand on previous knowledge and investigate the role of cortical oscillations in MT+ in smooth pursuit eye movements.

In Experiment 1, MEG and fMRI was used to probe the cortical correlates of smooth pursuit eye movements, retinal motion processing and a combination of the two. Particular emphasise is directed to the role of MT+ responses in relation to these tasks. Experiment 2 was devised as a complementary control experiment as a result of observations made from Experiment 1.

2.3 Experiment 1 – A fMRI and MEG study of smooth pursuit eye movements and retinal motion processing

2.3.1 Overview

Whilst the relatively high spatial resolution of fMRI has been key in delineating the MT+ complex into a number of functionally distinct sub-regions, all thought to play different but related roles in sensory-motor processing, recent neuroimaging studies have shown that cortical oscillations mediate a number of cognitive and perceptual processes, in particular those within the visual domain (Edden, Muthukumaraswamy, Freeman, & Singh, 2009; Hadjipapas, Adjamian, Swettenham, Holliday, & Barnes, 2007; Muthukumaraswamy & Singh, 2008; Tallon-Baudry, et al., 1996). However, to the extent of our knowledge, there is only one study using MEG on perceptual stability (Tikhonov, et al., 2004), and none on the role of cortical oscillations implicated in smooth pursuit. Therefore, it is important that the role of neuronal synchrony underlying pursuit is examined if we are to understand how the brain processes oculomotor commands and integrates extraretinal eye movement signals into motion processing areas in visual association cortex. With this in mind, MEG was used to expand on previous findings to explore the changes in cortical oscillations associated with smooth pursuit.

Based on the results from neuroimaging in healthy human subjects, together with the invasive electrophysiological studies on primates, it was hypothesised that extra-striate regions (specifically, areas located in the dorsal visual stream, including MT+) should exhibit pronounced oscillatory power changes related to smooth pursuit. In particular, it was predicted that alpha-band (5-15 Hz) and beta-band (15-25 Hz) power decreases and gamma-band (>30 Hz) increases, both correlates of cortical activation (Brookes, et al., 2005; Muthukumaraswamy & Singh, 2008; Singh, et al., 2002), would be present in these regions. Evidence of this might suggest that these dynamic cortical rhythms are part of a putative

mechanism in the maintenance of smooth pursuit and perceptual stability through integration of non-retinal signals into motion processing cortex.

Three conditions were investigated, similar to a previous study using fMRI (Kimmig, et al., 2008), to investigate the cortical substrates of pursuit and motion processing. The 'pursuit' condition involved smooth pursuit of a moving target and therefore isolated oculomotor control processes and concomitant extraretinal eye movement signals. The 'retinal-motion' condition used a large moving background and stationary fixation point and so isolated retinal motion signals in the absence of eye movement. The 'pursuit + retinal' condition combined the first two by investigating oscillatory changes related to smooth pursuit over a stationary background. By comparing and contrasting the oscillatory dynamics of MT+ in these conditions, some of the neuronal mechanisms that underpin smooth pursuit and how retinal and extraretinal motion signals are processed in this area would be elucidated.

Although the focus of this study was to measure and characterise cortical oscillatory modulations using MEG, there is always a concern regarding the accuracy of source-localisation, especially given the non-unique EEG/MEG inverse problem. Therefore, an additional fMRI experiment was performed using modified versions of the three conditions described above to help confirm the accuracy of our MEG source localisations. This also enabled the test of a subsidiary hypothesis – namely whether increases in fMRI-BOLD activation are co-localised with amplitude reductions in the alpha/beta bands and a concomitant increase in gamma oscillation power.

2.3.2 Method

2.3.2.1 Participants

Seven healthy participants completed both the MEG and fMRI parts of the experiment, with a further eight participants completing either the MEG or fMRI experiment (four for each modality), giving a cohort of eleven participants for each part of the study in total (MEG – 6 females, mean age 23.4 years; fMRI – 4 females, mean age 24.2 years).

2.3.2.2 Design and procedure

The experiment consisted of three conditions (see Figure 9, below, for a schematic): 'Pursuit', 'Retinal motion' and 'Pursuit + retinal motion'. In all three conditions, ambient background light was attenuated using customised goggles fitted with cross-polarized filters to minimise activation related to pursuit-induced retinal image motion of any visible landmarks peripheral to the projector screen. The spatial extent of any remaining light on the screen itself was minimised using opaque occluders placed horizontally above and below the oscillating dot. As a check, participants were asked to report whether they could see any objects other than those shown on the screen. If not, successive layers of cross-polarized filter were added to the goggles until the only perceived object in the 'pursuit' condition was the faint target dot.

The 'pursuit' condition consisted of smooth pursuit eye movement to a faint, low-contrast, monochromatic dot in the dark that moved sinusoidally in the horizontal plane (amplitude ±5º, frequency 0.5 Hz). The second 'retinal motion' condition required participants to fixate a static central point while viewing a large field random dot-pattern that moved sinusoidally with the same amplitude and frequency used in the 'pursuit' condition. The third 'pursuit + retinal motion' condition combined the first two – participants pursued a dot that moved sinusoidally over a stationary random-dot background. This condition

therefore resulted in stimulation related to both the pursuit eye movement and the background retinal motion. Condition order was pseudo-randomised and counter-balanced between participants.

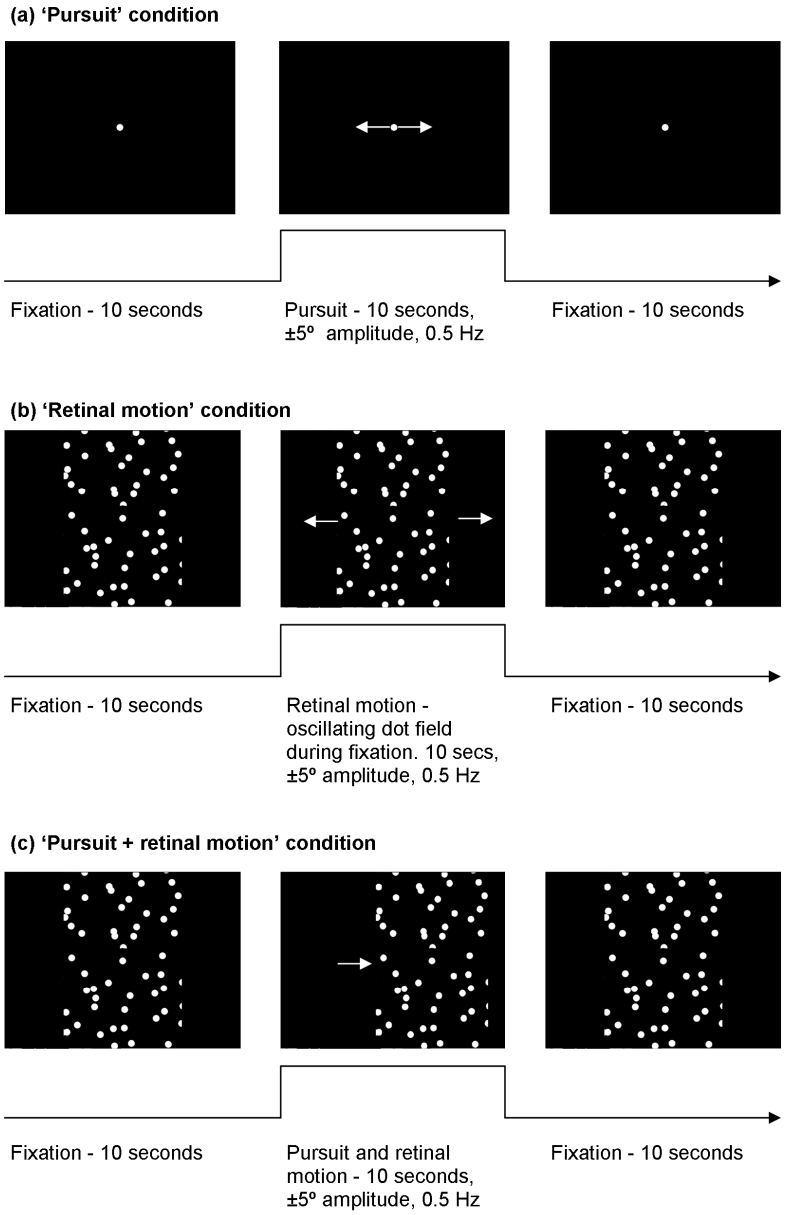

Figure 9. Schematic of experimental protocol for MEG experiment. fMRI parameters are detailed within the text.

(a) A single stationary low-contrast, monochromatic dot is presented as a fixation point for the 10 second passive/rest phase. The dot then oscillates back and forth sinusoidally in the horizontal plane for 10 seconds at ±5º at a frequency of 0.5 Hz, followed by another passive period consisting of 10 seconds fixation. This is repeated for 30 trials. (b) 'Retinal motion'

condition. A central dot is fixated for 10 seconds (rest), followed by 10 seconds of an oscillating background consisting of a random dot field. (c) Pursuit and retinal motion condition. Fixation is maintained for 10 seconds, followed by pursuit over a stationary random dot field (only the window aperture over the random dot field follows the path of pursuit).

As part of the exclusion criteria, individual trial EOG data was visually inspected for saccadic eye movements during pursuit-related conditions and, if found, that trial was subsequently omitted from further analysis. For the 'pursuit' condition, this resulted in an average exclusion rate of 6.36 trials per run (21.2%), and for the 'pursuit + retinal' condition this was 5.36 trials per run (17.9%). None of the participant's final averaged MEG data was excluded from the later analysis (n=11).

The MEG experiment used a boxcar design, with 30 x 20 second epochs each consisting of a 10s passive period (baseline/resting brain state) immediately followed by a 10s active period (of pursuit, retinal motion, or pursuit + retinal motion). Each series ran for approximately ten minutes in total. In the fMRI experiment, the three conditions were repeated but with 20 epochs, lasting 30 seconds each (15 seconds passive fixation followed by a 15 second active period). For all conditions, participants were instructed to attend to the central fixation point at all times, following it when the dot moved and keeping their eyes stationary when it did not.

For the fMRI part of the study, data was acquired on a 3T GE scanner with an 8-channel receive-only head radio-frequency (RF) coil, using a gradient echo planar imaging (EPI) sequence taking 37 axial slices at 2 mm isotropic voxel resolution covering the occipital, parietal and a significant portion of temporal cortex, at 128x128 matrix size, Field-Of-View 256x256 mm, echo time 35 msec, 90º flip angle and a repetition time (TR) of 3s. For each participant, a 3D FSPGR scan with 1 mm isotropic voxel resolution was also obtained, to which functional data from both the MEG and fMRI studies could be co-

registered. A single-volume whole-brain EPI scan, which matched the functional volume in orientation and position but had 75 slices to increase head coverage was also acquired, in order to aid co-registration between the anatomical scan and the functional volumes.

2.3.2.3 Data analysis

For the MEG part of the experiment, the percentage change in oscillatory power during the active period was baselined against the 0-10 second passive period.

fMRI data analysis was conducted using the FSL software library using a number of pre-processing steps, including motion correction using MCFLIRT (Jenkinson, Bannister, Brady, & Smith, 2002), brain extraction/non brain removal using BET (Smith, 2002) and spatial smoothing using a Gaussian kernel of FWHM 5mm. A GLM model was used to model a 15s on/15 s off boxcar for the stimulus, after convolution with a standard haemodynamic response function to account for haemodynamic effects. Functional data was initially registered to a whole-brain EPI scan and then to a high-resolution FSPGR scan. Statistical thresholding for cortical activation was implemented using cluster-based thresholding, corrected for the whole brain volume, at $p = 0.05$.

2.3.3 Results

2.3.3.1 Behavioural data

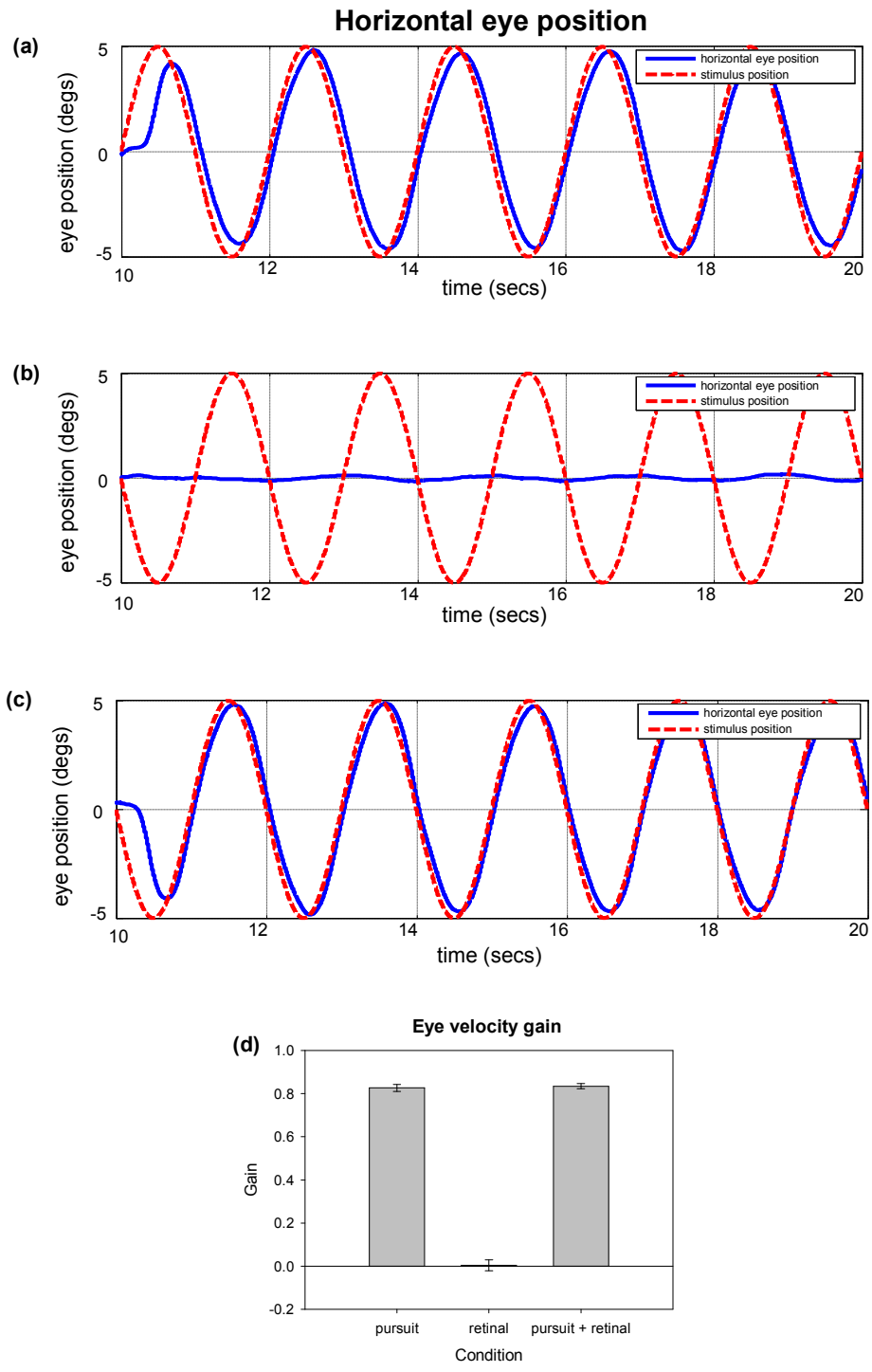

Figure 10. Group-averaged eye movement data for the MEG experiment.

(a) Group-averaged horizontal eye movement during the active period, with the blue traces denoting eye position and the dashed red traces denoting stimulus position during 'pursuit' (condition 1), (b) 'retinal motion' (condition 2) and (c) 'pursuit + retinal' (condition 3). (d) Mean eye velocity gain for all conditions.

Figure 10 shows group-averaged eye velocity gain in all three conditions during the MEG experiment. The blue traces denote the eye position during each experiment, and the red traces show the stimulus position. Eye-velocity gain was calculated as the ratio of pursuit eye velocity to stimulus velocity. Individual trial EOG data was visually inspected for saccadic eye movements during pursuit-related conditions and, if found, that trial was subsequently omitted from further analysis. Therefore, we can be confident that imaging data recorded was pursuit- and/or retinal motion-related, rather than the result of saccadic eye movements.

EOG recording revealed that participants were able to track the target stimulus close to unity (a ratio of eye/stimulus velocity close to 1) when instructed to pursue it as smoothly as possible for both the 'Pursuit' condition and the 'Pursuit + retinal motion' condition. Moreover, a paired t-test revealed no significant difference in the eye velocity gain for these two conditions ($t(10) = -0.482$, $p = 0.641$; see Figure 10d). Additionally, participants were able to maintain fixation during the 'retinal' motion condition.

2.3.3.2 fMRI data

2.3.3.2.1 The cortical representation of pursuit eye movements

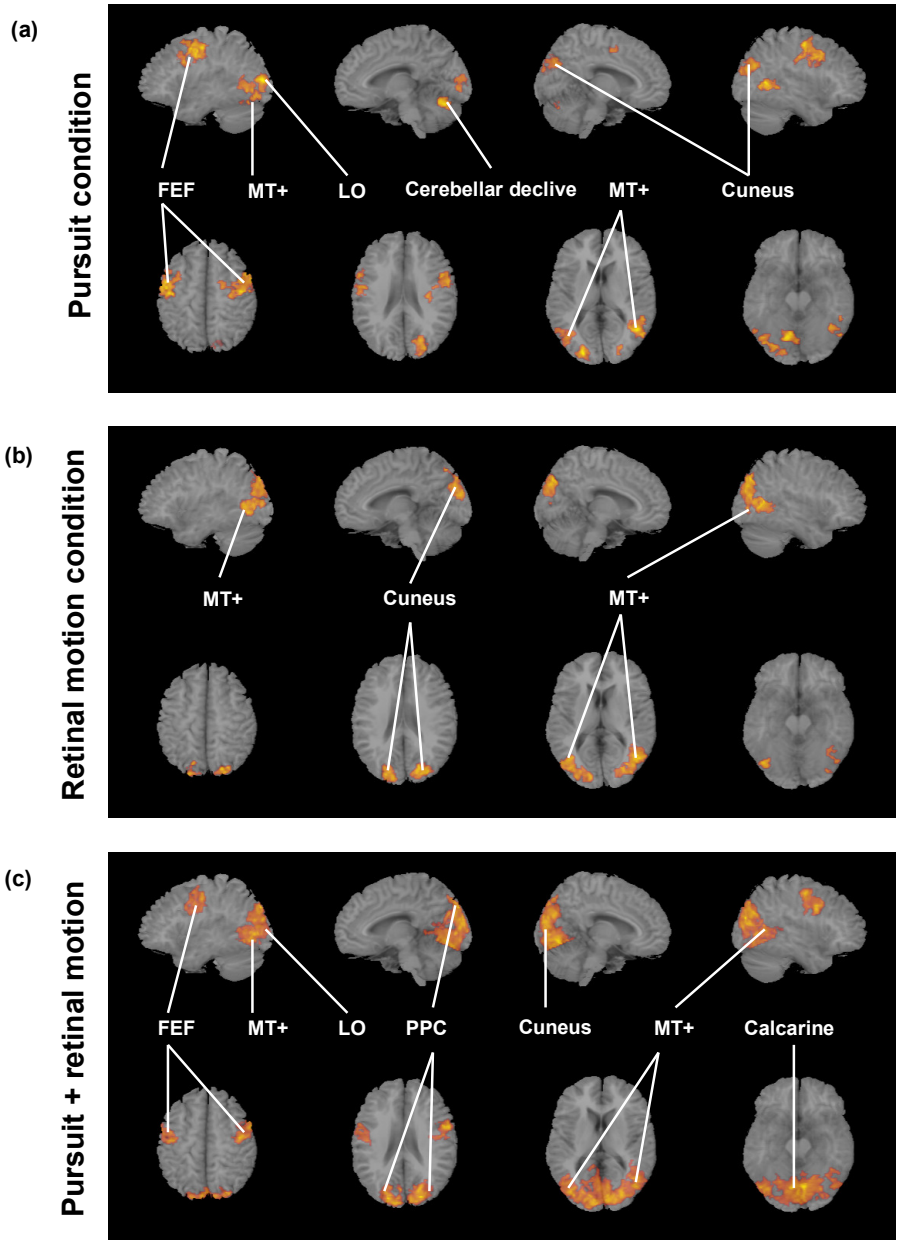

Figure 11. Group-based cortical activation (active period vs. passive period) in the fMRI experiment.
(a) For the 'pursuit' condition, (b) 'retinal motion' condition and (c) 'pursuit + retinal motion' condition, overlaid on a template brain for sagittal and axial orientations. Cluster-based thresholding set at $p < 0.05$ ($n = 11$).

Figure 11 shows the group-based BOLD activation maps for the three conditions in the fMRI experiment. For the 'pursuit' condition (a, top plate, pursuit versus rest), significant increases in activity (using cluster-based thresholding at $p < 0.05$) were found in MT+, FEF, SEF, LOC, the cuneus, precuneus and the cerebellar declive. Surprisingly, no significant activity was observed in parietal regions. During visual stimulation (b, middle plate, 'retinal motion' condition), activity was observed in MT+, cuneus, precuneus and parietal regions. Finally, in the 'pursuit + retinal' condition (c, bottom plate, pursuit over a stationary background versus rest) significant increases in activity were found in MT+, FEF, SEF, LOC, PPC, cuneus, the precuneus and V1. For a summary of significant regions of BOLD activity during all three conditions, see Table 1 (below).

Table 1. Location of significant BOLD activity for all three conditions.

Anatomical area	Pursuit				Retinal motion				Pursuit + retinal			
	Voxel coords.			z-score	Voxel coord.			z-score	Voxel coords.			z-score
	x	y	z		x	y	z		x	y	z	
Inferior Frontal Gyrus L	-57	11	33	3.4								
Inferior Frontal Gyrus R									53	5	35	4.46
Precentral Gyrus L	-51	-7	47	4.2					-41	-13	49	4.16
Precentral Gyrus R	45	-11	55	4.12					43	-9	55	4.46
Middle Frontal Gyrus L												
Middle Frontal Gyrus R	49	9	37	3.74								
Cuneus L					-13	-93	21	3.57	-21	-89	37	4.86
Cuneus R	27	-85	23	3.57					23	-87	23	5.23
Precuneus L					-23	-89	41	4.03	-5	-85	43	3.98
Precuneus R					21	-81	41	4.04	25	-81	43	4.33
Middle Temporal Gyrus L	-45	-79	3	3.09	-45	-73	-3	3.77	-39	-81	1	4.42
Middle Temporal Gyrus R	47	-61	7	4.36	47	-63	11	4.45	47	-61	7	3.97
Middle Occipital Gyrus L	-23	-93	9	4.46					-9	-91	11	4.36
Middle Occipital Gyrus R					39	-85	3	3.5	45	-73	1	4.1
Lingual Gyrus L									-7	-75	-9	4.57
Lingual Gyrus R									7	-75	-7	5.23
Cerebellar declive L	-17	-71	-21	4.08								
Superior parietal lobule L					-17	-73	53	3.47				

Anatomical location and voxel cluster coordinates (based on the Talairach and Tournoux atlas) of peak activity (active versus the passive fixation condition) as a result of the group-based analysis in all three conditions. Significant cluster-based activation thresholded for Z-scores at $p < 0.05$.

2.3.3.2.2 Comparing extraretinal and visuo-oculomotor activation in visual association cortex

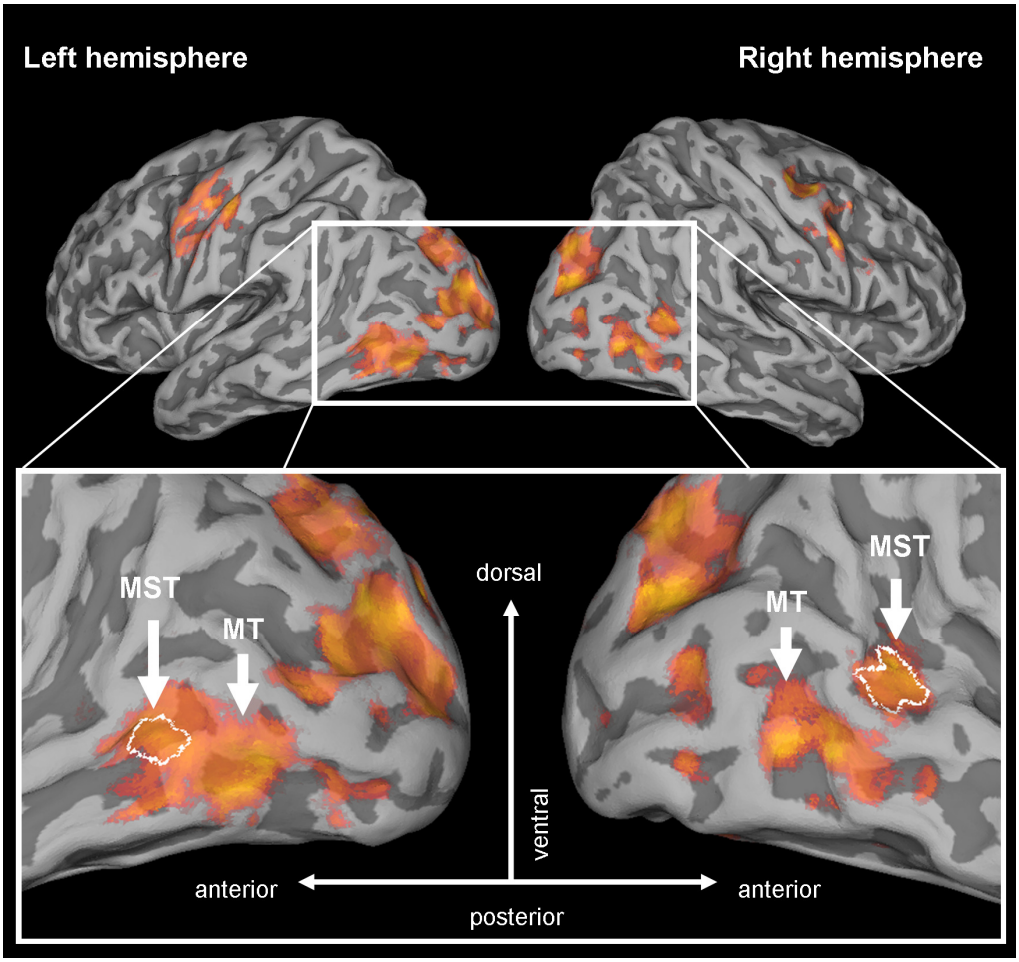

Figure 12. Cortical BOLD response for the 'pursuit + retinal' condition overlaid on an inflated template brain (yellow/orange/red colour map defines increases in BOLD for the 'pursuit + retinal' condition).
A magnified view of comparative occipital BOLD activity for the 'pursuit + retinal' condition is indicated by the orange colour map, with the white outline, labelled MST, delineating regions that are active during pursuit in the 'pursuit' only condition. This shows that the MT+ subregion MST carries extraretinal signals during pursuit eye movements.

Figure 12 shows a more detailed examination of activity induced in extra-striate regions. The figure shows that the 'pursuit + retinal motion' condition revealed significant activity over a distributed region of extra-striate cortex (where BOLD increases are depicted

by the orange colour map). Comparing this with activity in the 'pursuit' condition (depicted by the small white bounded box in the magnified view, labelled MST), BOLD increases were seen in a comparatively smaller region of the cortex than was active during the 'pursuit + retinal motion' condition. BOLD increases were noted in the fundus of the ascending limb of inferior temporal sulcus/middle temporal cortex, anteriorly located to MT region (which is likely to be the putative spatiotopic sub-division MST of the homologue MT+ complex).

2.3.3.2.3 Comparing the oscillatory and BOLD response in visual cortex

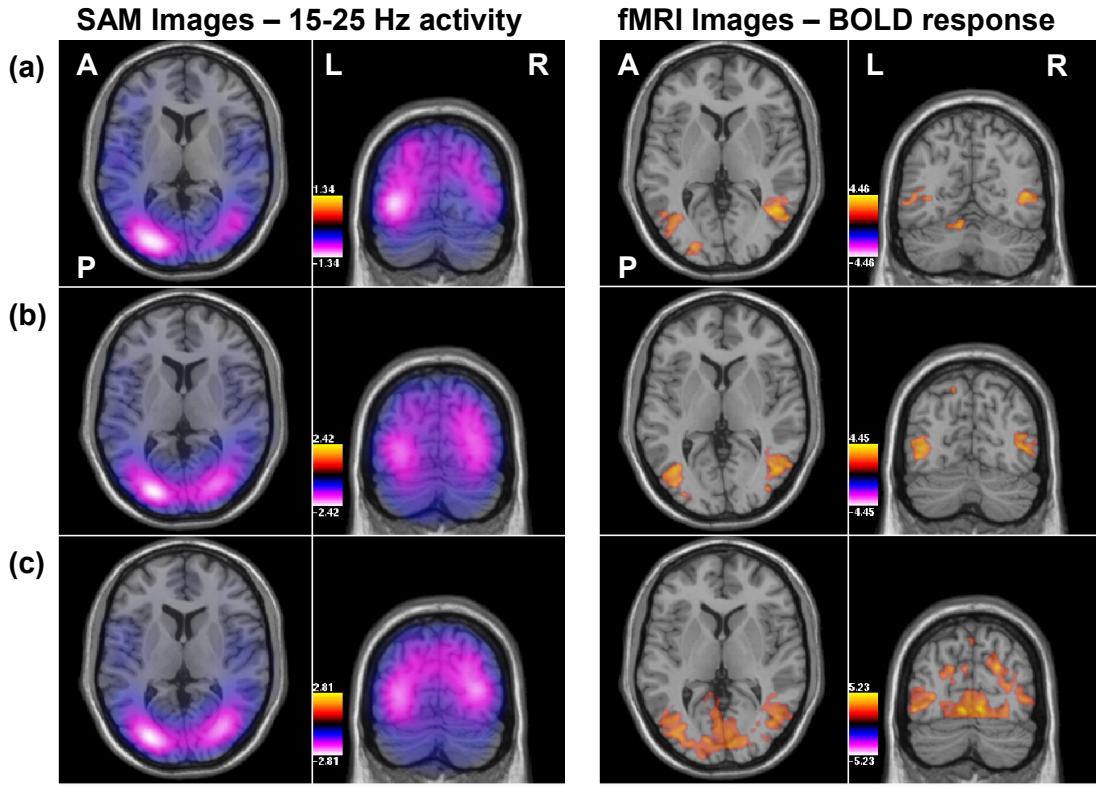

Figure 13. Group results from MEG and fMRI in all three conditions.
(a) MEG data, left panel: Group-averaged SAM images in the 15-25 Hz band during pursuit, overlaid on a template brain. Beta suppression occurs in bilateral extra-striate cortex consistent with putative MT+. Cool colour map indicates negative power changes with colour bar showing pseudo-T values. fMRI data, right panel: Group fMRI data showing significantly activated clusters ($p < 0.05$) during pursuit, with warm colours indicating increasing BOLD amplitude. Note the similar spatial locations of the beta suppression in the MEG data and the BOLD effect in the fMRI data. (b) Group SAM images (15-25 Hz) during 'retinal motion' and fMRI data. (c) Group SAM images for 'pursuit + retinal motion' and fMRI data.

Figure 13a, left panel, shows group-average (n=11) source power estimates reconstructed using SAM for the MEG data in the beta range (15-25 Hz) during pursuit, overlaid on a template brain. The peak power changes for pursuit were localised to bilateral extra-striate cortex, consistent with MT+. In comparison, fMRI results (Figure 13a, right panel) revealed clusters in similar regions, showing bilateral extra-striate cortical activity for the pursuit-related response, consistent with previously reported Talairach coordinates for MT+ (Dumoulin et al., 2000). The spatial separation between the peak voxel location in the BOLD cluster and the location of the beta suppression estimated using SAM was small, given that the long side of a SAM voxel is 8.7 mm and the mean distance was 8.9 mm (Figure 13a, right hemisphere). Therefore, the spatial difference between the peak activity measured using these two modalities was approximately the long side of a SAM voxel, and given the inherent non-uniqueness of the MEG inverse problem and the possibility of minor co-registration errors when fitting functional data to structural scans, this can be considered an acceptable co-localisation of pursuit-related activity and an important cross-modal validation of the task.

For the 'retinal motion' condition, SAM (Figure 13b, left panel) revealed bilateral beta suppression in MT+, that again shows a spatial pattern of activation consistent with the fMRI data. MEG data of pursuit over a stationary background ('pursuit + retinal' condition, Figure 13b, left panel) showed a similar spatial coincidence of beta suppression as the 'pursuit' condition, with peaks in power decreases for the 15-25 Hz response identified in bilateral extra-striate cortex. The fMRI results corroborated this pattern of activation, along with additional peaks identified in early visual cortex (Figure 13c, right panel).

Alpha SAM images revealed activity in similar regions to the beta frequency in some but not all participants. Therefore, the region-of-interest (ROI), MT+, was localised on the results of the beta images for all three conditions. Additionally, no consistent responses in the gamma band were found in any of the tasks.

2.3.3.3 Time-frequency analysis

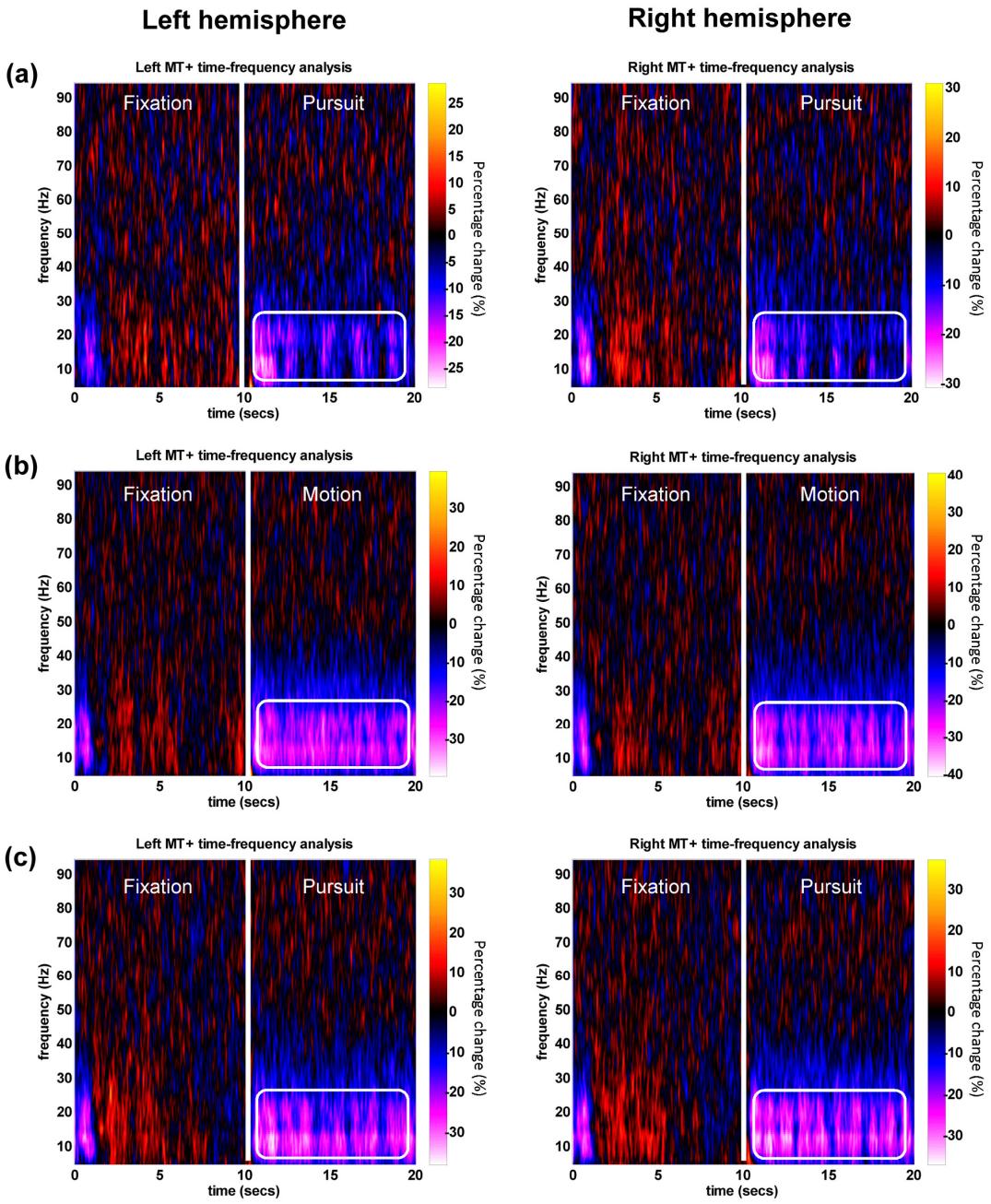

Figure 14. Grand-averaged time-frequency spectrograms.
(a) During 'pursuit' for the extra-striate virtual sensor location in both left and right hemispheres, showing broad-band alpha-beta activity decreases for the duration of pursuit. (b) Spectrograms for the 'retinal motion' and (c) 'pursuit + retinal' conditions.

To assess the spectral characteristics of the neuromagnetic response in the 'pursuit' condition, a ROI analysis was conducted on an individual basis for peaks identified in the SAM beamformer reconstructions that were consistent with the MT+ complex in extra-striate cortex. Virtual sensors were constructed at these peak locations and a time-frequency analysis performed. The individual spectral analyses were then averaged to give a group-mean spectrogram for both left and right hemispheres. Figure 14a shows the results from the 'pursuit' condition in both the left and right hemispheres. The results revealed a broad-band alpha-beta (5-25 Hz) activity decrease (as % change from baseline) for the duration of stimulus tracking in both left and right hemisphere, with a steep initial perturbation in the peak alpha-beta power change of approximately -25% following eye movement initiation. This alpha-beta power decrease appeared to be modulated in a time-varying fashion for the duration of the pursuit period.

A time-frequency analysis of peak voxels in extra-striate cortex during the 'retinal motion' condition showed sustained bilateral 5-25 Hz oscillatory power decreases in the region of approximately 25% for the duration of retinal motion (Figure 14b, left & right panel), in contrast to the suppression of the alpha-beta rhythm seen during 'pursuit', which appears to vary over time. Inspection of the oscillatory response for voxels in extra-striate cortex during the 'pursuit + retinal motion' condition revealed similar looking patterns of activity to the 'retinal motion' condition, albeit with a possible evidence of some task-induced modulation of the alpha-beta rhythm (Figure 14c).

2.3.3.4 Alpha-beta envelope response

2.3.3.4.1 'Pursuit' condition

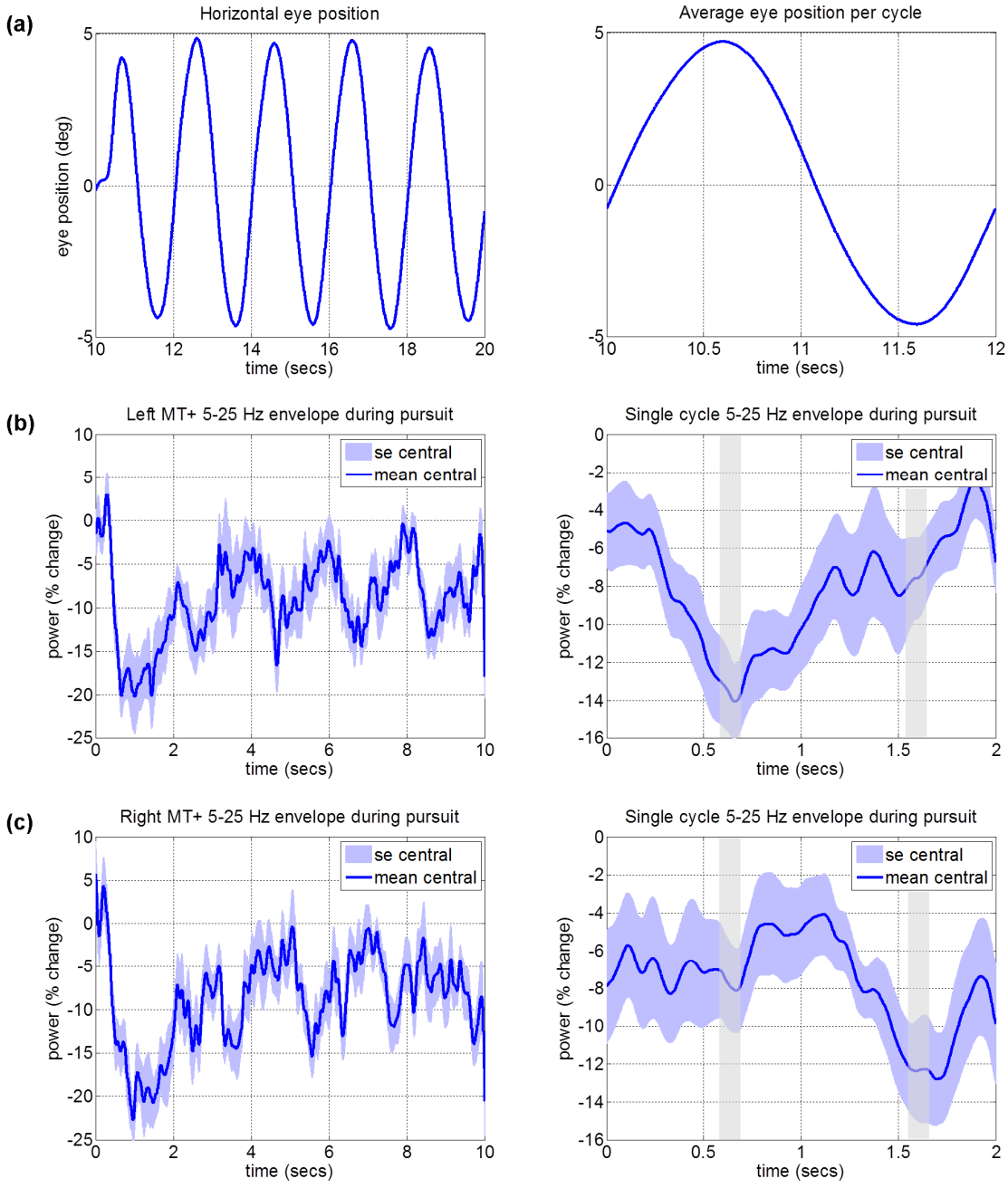

Figure 15. Comparing the eye position and the alpha-beta amplitude envelope in the 'pursuit' condition

(a) Group average horizontal eye position data for the duration of object tracking, and the mean eye position during a single pursuit cycle. (b) Group-averaged 5-25 Hz amplitude

envelope during pursuit from the left hemisphere MT+ voxel, with the average amplitude envelope during a single pursuit cycle. Maximum suppression of the rhythm appears to correspond to pursuit position when the eye gaze was at maximum eccentricity in the contralateral visual hemifield. The vertical grey bars denote the window over which the mean alpha-beta power was quantified when the eyes were at maximum amplitude of the pursuit cycle. (c) Same as (b), except 5-25 Hz envelope power from right hemisphere MT+ voxel.

To investigate the modulation of the 5-25 Hz response evident in the spectrogram of the 'pursuit' condition, the amplitude envelope in this frequency band was extracted from each of the bilateral extra-striate virtual sensors and compared to the eye position during smooth pursuit. Figure 15a, left panel, shows the group-average eye position during the pursuit period and a single pursuit cycle, right panel, during the 'pursuit' condition. Figure 15b shows the group-averaged envelope power in the 5-25 Hz frequency band (as percentage change from baseline) during the active pursuit period from the peak voxel location in extra-striate cortex in the left hemisphere, left panel. The average 5-25 Hz envelope during a single pursuit cycle is shown in the right panel. The oscillatory power changes during the initial 2s of the pursuit cycle were omitted from the average power change calculation to exclude the influence of any retinal-motion or saccadic eye movement related activity during pursuit initiation; therefore, we can be confident this average cycle data is almost-exclusively the result of pursuit maintenance when eye velocity gain was close to unity. Figure 15c shows the extracted beta envelope power from the peak voxel in the right hemisphere.

Comparing the 5-25 Hz envelope power from bilateral virtual sensors during the average pursuit cycle (shown in Figure 15b & c, right panel), it would appear that there is an asymmetry in alpha-beta oscillatory power that reflects a hemifield-dependent eye position signal from MT+. In other words, the maximum suppression (global minimum) of the 5-25 Hz rhythm coincided with the position of the eyes when they were at maximum eccentricity in the contralateral visual hemifield (that is, to the hemisphere from which the virtual sensor is recorded). It appears that these dynamic oscillatory changes of low-frequency brain

rhythms in MT+ reflect eye position when pursuing a target in the contralateral visual hemifield. Thus, when recording from left hemisphere MT+, a maximum power decrease of approximately 13% in the alpha-beta envelope was seen when the eyes were at maximum eccentricity in the right visual hemifield, and conversely, when recording from right hemisphere MT+, an oscillatory power decrease of approximately 12% occurred when the eyes were at maximum eccentricity in the left visual hemifield.

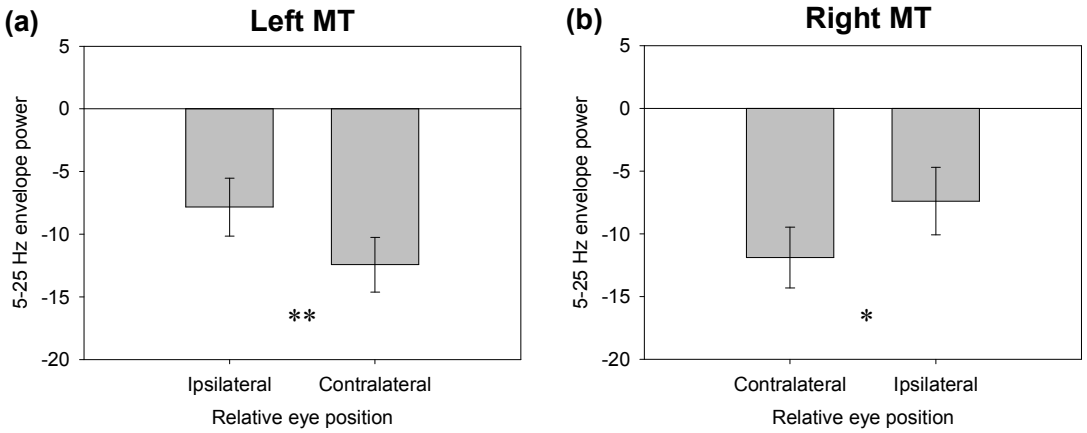

Figure 16. Alpha-beta (5-25 Hz) amplitude changes (% from baseline) for maximum opposing eye positions during sinusoidal pursuit.
(a) Group-averaged broadband alpha-beta amplitude changes from left MT+ during smooth pursuit, quantified over a 100 msec window when eyes were at maximum amplitude, relative to virtual electrode location. (b) Same as before, for right MT+. ** $p < 0.01$, * $p < 0.05$.

To test this apparent hemifield-dependent eye position effect, the average alpha-beta power was quantified over a 100 msec window when the eyes were at maximum opposing eccentricities (maximum amplitude in the pursuit cycle) from each hemisphere and a paired t-test was performed. This revealed a significant difference in the alpha-beta power for ipsi- vs. contralateral eye positions from left MT+ ($t(10) = 4.67$, $p < 0.001$; Figure 16a) and right MT+ ($t(10) = 2.86$, $p < 0.018$; Figure 16b).

2.3.3.4.2 'Retinal motion' condition

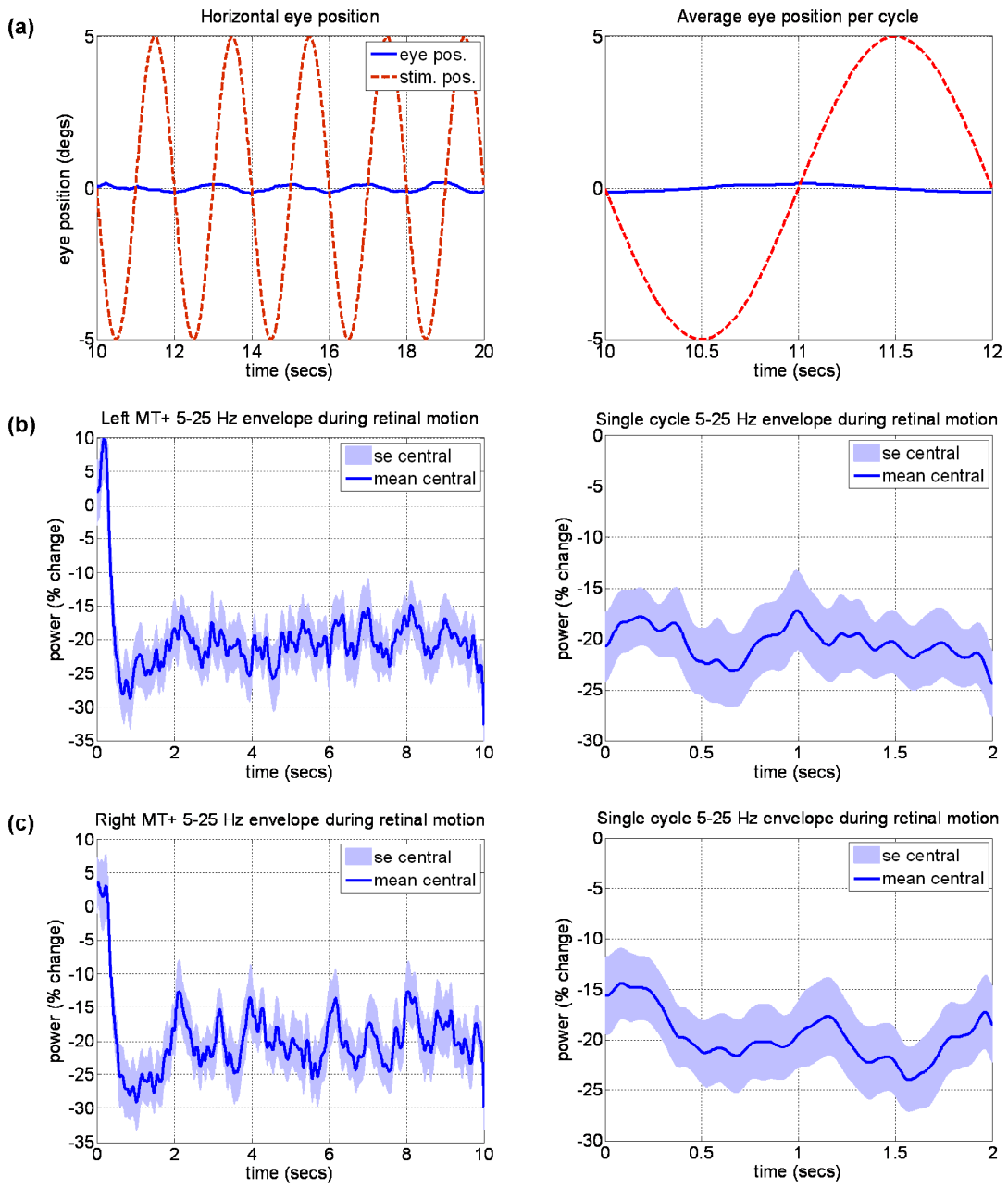

Figure 17. Alpha-beta amplitude envelope analysis for the 'retinal motion' condition. (a) Stimulus position (moving dot-field pattern, denoted by the red trace) during retinal motion and eye position (blue trace), and the average eye position during a stimulus movement cycle (b) Group-averaged 5-25 Hz amplitude envelope change during retinal motion from the left hemisphere MT+ voxel (left panel), with the average alpha-beta amplitude during a stimulus cycle. Alpha-beta rhythm suppression appears largely sustained

for the duration of stimulus motion. (c) Same as (b), except 5-25 Hz envelope power from right hemisphere MT+ voxel.

Figure 17 shows the extracted 5-25 Hz amplitude envelope for the 'retinal motion' condition in comparison to stimulus motion. Unlike the 'pursuit' condition, both hemispheres showed a largely sustained suppression for the duration of stimulus motion, with a decrease in power of approximately 20% for a single cycle, as opposed to displaying an envelope profile that is asymmetric in nature. This effect was especially prominent in the left MT+ virtual sensor recording.

2.3.3.4.3 'Pursuit+ retinal motion' condition

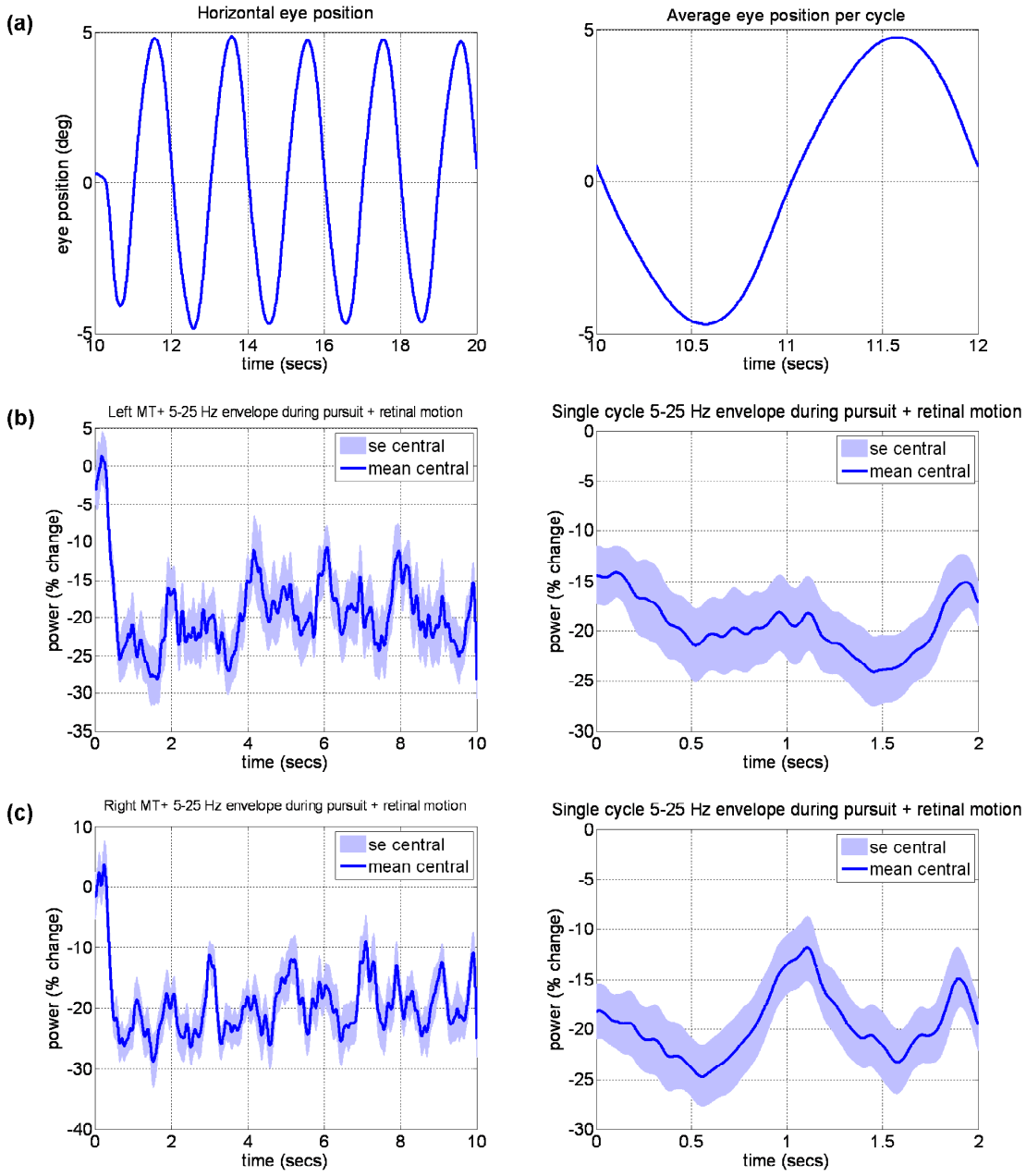

Figure 18. Alpha-beta amplitude envelope analysis for the 'pursuit + retinal' condition
(a) Eye position during pursuit (left panel) and the average eye position during a single cycle. (b) Group-averaged 5-25 Hz amplitude envelope during pursuit over a stationary background from the left hemisphere MT+ voxel (left panel), and the average alpha-beta amplitude during a during a pursuit cycle (right panel). The peak alpha-beta activity decrease occurs with maximum eye eccentricity in the contralateral visual hemifield, with a second peak decrease appearing to reflect eye position in the ipsilateral hemifield during pursuit (c) Same as (b), except 5-25 Hz amplitude envelope from right hemisphere MT+ voxel.

For the 'pursuit + retinal motion' condition, it might be expected that the alpha-beta envelope profiles would be similar to the summation of the oscillatory amplitude envelopes found in the 'pursuit' and 'retinal-motion only' condition. However, as Figure 18 shows, this was only approximately the case. Thus, as Figure 18a & b, right panels depicts, the average alpha-beta amplitude envelope during an eye movement cycle showed a partially asymmetric profile, resembling a double-dip 'W' shape. Maximum suppression of the alpha-beta rhythm corresponded to eye position at maximum eccentricity in the contralateral visual hemifield, with a second, smaller, local minimum in the magnitude of alpha-beta activity when the eyes were at maximum eccentricity in the ipsilateral visual hemifield. This evidence of a smaller, local decrease in power that corresponded to ipsilateral eye position eccentricity was not evident in the 'pursuit' condition.

2.3.4 Conclusion

Using fMRI and MEG recording in human subjects, the cortical correlates of smooth pursuit eye movements was investigated. Attention was focused on the spectral characteristics of the neuromagnetic response during activation of the visual pursuit and retinal motion systems, with a particular emphasis on the mechanisms underlying sensory processing involved with the integration of extra-retinal eye movement signals in MT+. This was achieved by comparing three conditions: a 'pursuit' condition that used an oscillating target stimulus and custom-made cross-polarised goggles that eliminated any unwanted retinal motion peripheral to the projector screen; a 'retinal motion' condition in which a background stimulus moved in the absence of eye movements; and a 'pursuit + retinal' motion condition that combined the first two. Consistent BOLD increases and alpha-beta frequency band (5-25 Hz) power decreases that showed a marked spatial invariance in its cortical location were found, with SAM demonstrating a source location in extra-striate cortex consistent with MT+ throughout all three conditions. In line with previous research, this spatial concordance suggests that BOLD activity is related to concomitant changes in beta oscillatory power (Singh, et al., 2002).

In the two conditions containing pursuit eye movements, modulation of neuronal oscillations that appeared to be related to the processing of extra-retinal motion signals was found. In particular, activity in MT+ was observed that covaries with eye position in the contralateral visual hemifield when engaging in pursuit eye movements ('pursuit' condition). Whilst brain rhythms in other cortical structures known to mediate oculomotor control (e.g. the frontal eye fields) were not explored here, it is tentatively proposed that this alpha-beta response represents an increase in neuronal activity and the processing of signals sent from the oculomotor control system to motion-processing areas, which code for eye position

during pursuit. This, in turn, might be one of a number of mechanisms used in the maintenance of perceptual stability.

There are, however, a number of limitations in this present study. First, whilst head position was recorded both before and after each run as a diagnostic tool to ensure head movement was minimal and an accurate source reconstruction could be estimated, continuous recordings of head position were not made. Therefore, it is possible that modulation of the oscillatory response could in fact be due to correlated head movements during stimulus tracking. Whilst this might be possible, this is unlikely as the eye velocity gain values for the pursuit eye movement conditions were approaching unity and far above that which might have been expected had participants been tracking the stimulus with gaze changes involving head rotation. Additionally, whilst it could be argued that head and gaze control are regulated by similar mechanisms, previous research would suggest that relatively small amplitude eye movements like those used here can be dissociated and uncoupled in the brain from head movements, and controlled independently (Collins & Barnes, 1999).

Finally, despite efforts to minimise retinal image motion during tracking movements by using the customised goggles, it was not possible to exclude the contribution of retinal slip of the target stimulus to the oscillatory changes that were measured. Inspection of eye position during maximum deceleration of the target stimulus showed a decrease in pursuit gain (eye/object velocity mismatch), with the eye movement lagging slightly behind the stimulus when the eyes were changing direction at the maximum amplitude of the pursuit cycle. This "error" in tracking will generate a retinal motion signal that might induce an oscillatory change in the MEG signal, with previous research showing that transient changes in translational motion can induce activity in MT+ (Martinez-Trujillo, Cheyne, Gaetz, Simine, & Tsotsos, 2007). Therefore, changes in the alpha-beta that appear contiguous with eye position could be due to this retinal artefact, and not due to oculomotor control, or

extraretinal signals. Any contribution of this retinal slip to changes in cortical activity is likely to be relatively small, however, a cautious approach to the interpretation of these results must be made due to this potential confound. Due to this, a complementary control experiment was devised looking at the temporal characteristics of the alpha and beta responses due to transient retinal motion. In this next study, Experiment 2, stimulus motion was viewed during fixation that would approximate the retinal slip observed when pursuing a target non-optimally. This experiment comprises the next part of this chapter.

2.4 Experiment 2 – Emulating retinal slip: MT+ responses to transient retinal motion

2.4.1 Overview

In Experiment 1, results from the 'pursuit' condition showed that maximum alpha-beta suppression was temporally congruent with maximum pursuit amplitude, suggesting changes in this signal were dependent on contralateral eye position during pursuit. However, this effect also co-occurred with a change in direction of the eye movement and the greatest amount of retinal slip. It could be possible that modulation of the alpha-beta profiles seen in the 'pursuit' condition was due to transient retinal motion (target slip) as a result of non-optimal tracking at the extrema of the pursuit cycle.

Therefore, a control experiment was designed to examine the temporal characteristics and magnitude of the alpha and beta response in MT+ induced during a small amount of transient retinal motion. The retinal motion that might have been observed in the previous study when the pursuit target slipped on the retina was approximated and the resultant alpha and beta response to this stimulation was compared with that seen in the 'pursuit' condition of Experiment 1. It was predicted that this would provide a clearer picture as to whether the pursuit-related amplitude modulation of the alpha-beta rhythm seen in the previous

experiment was the result of minor but consistent retinal motion stimulation due to non-optimal pursuit eye movements (retinal slip of the target dot).

2.4.2 Method

2.4.2.1 Participants

Eleven healthy participants (five female, mean age = 24 years) with normal or corrected-to-normal visual acuity completed Experiment 2. All participants were naïve as to the purpose of the experiment and consented to participate in return for course credits or monetary recompense.

2.4.2.2 Design and procedure

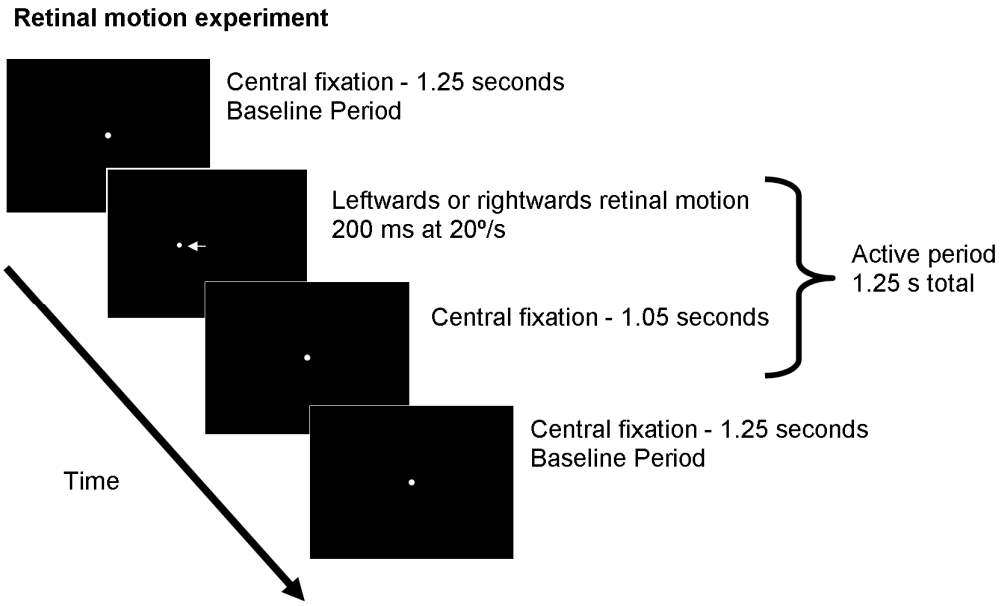

Figure 19. A schematic diagram of the transient retinal motion experiment.
Participants view a stationary fixation point that induces a small amount of retinal motion stimulation by making transient movements in the left- or rightwards direction. The resultant retinal motion would approximate the retinal slip induced by non-optimal pursuit when tracking a stimulus at the extrema of a sinusoidal pursuit cycle (as seen in the 'pursuit' condition in Experiment 2).

Figure 19 shows the basic design of Experiment 2. Participants fixate a stationary central dot displayed for 1.25 seconds (baseline period). This was then followed by a small movement of the stimulus, either to the left or to the right (45 trials of each, referenced as the active period), at 20º/s for 200 msec. This transient retinal motion was designed to approximate the turnover time of the stimulus at the edges of the pursuit cycle in the previous experiment and the resultant retinal slip that might have been induced when pursuing an oscillating stimulus non-optimally. This is evident in the eye movement data in the 'pursuit' condition of Experiment 1, when the stimulus was at maximum amplitude, stimulus acceleration was greatest and the eyes were changing direction. This was then followed by 1.05 s of central fixation. Taken together with the 200 msec of retinal motion, this was used as the 'active' period in the SAM source reconstruction contrasts. Condition order was pseudo-randomised to mitigate any potential expectancy effects. Visual inspection of the EOG data showed that all participants were able to maintain satisfactory fixation during the experimental session, and subsequently all participants data was used in the final MEG analysis (n=11).

2.4.2.3 Data analysis

For Experiment 2, the percentage change in amplitude for the active period (200 msec of transient motion plus 1050 msec central fixation) was baselined against the passive period (1.25 seconds of central fixation).

2.4.3 Results

2.4.3.1 Eye movement data

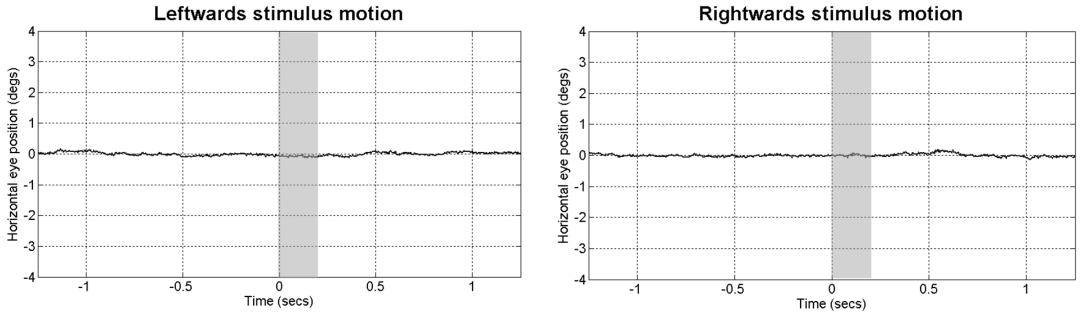

Figure 20. Group averaged eye movement data for leftwards (left panel) and rightwards stimulus motion.
Group averaged eye movement data. Observers were able to maintain fixation for the duration of duration of the trial. Grey boxes denote the duration of stimulus motion in either the left- or rightward direction in each condition.

Figure 20 shows the group-averaged (n=11) horizontal eye movement traces for both the leftwards (left panel) and rightwards (right panel) stimulus motion conditions. Participants were able to maintain fixation for the duration of the trial, and there is no evidence of any eye movement induced by the stimulus motion (which lasted 200 msec and is denoted by the transparent grey boxes centred on the 0 second time point).

2.4.3.2 SAM source analysis

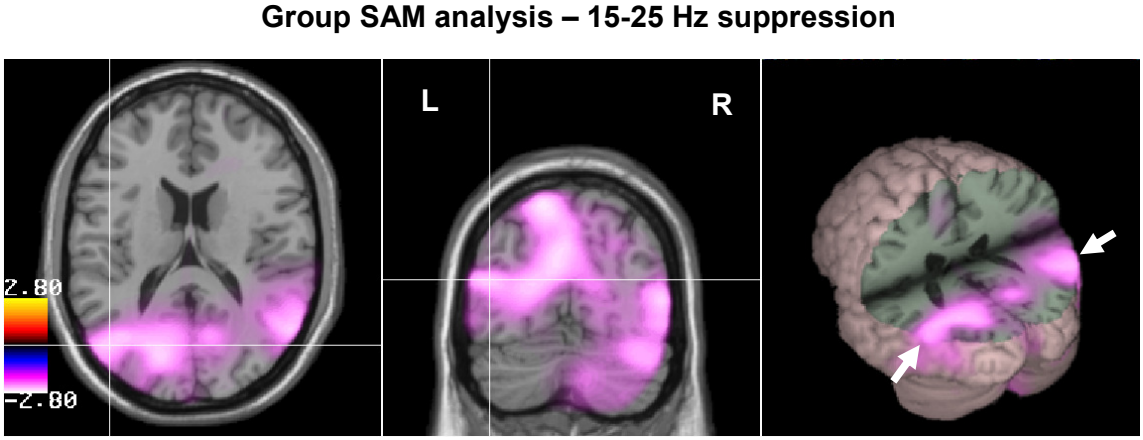

Figure 21. Group mean SAM images for the 15-25 Hz oscillatory response for the rightwards motion condition (transient retinal motion versus baseline central fixation), overlaid on a template brain.
Cold-colour map indicates motion-induced oscillatory power decreases, with the greatest peaks localised to bilateral extra-striate regions. Additional peaks were also found in parietal regions, although these were not investigated further.

Figure 21 shows the group mean (n=11) SAM analysis for the 15-25 Hz response for the rightwards motion condition. This revealed consistent bilateral extra-striate suppression of beta activity during transient retinal motion in all participants. Additionally, parietal areas and the cuneus showed evidence of beta rhythm power decreases. Similar patterns of activity were also found for leftwards retinal motion. Alpha peaks were for the most part spatially coincident with the beta peaks and there were no consistent gamma (30-70 Hz) responses evident in any individual or Group SAM images. These peak locations in the beta rhythm were used to compute weights for virtual electrode recordings, on which a time-frequency analysis was performed.

2.4.3.3 Temporal dynamics of the amplitude envelope response

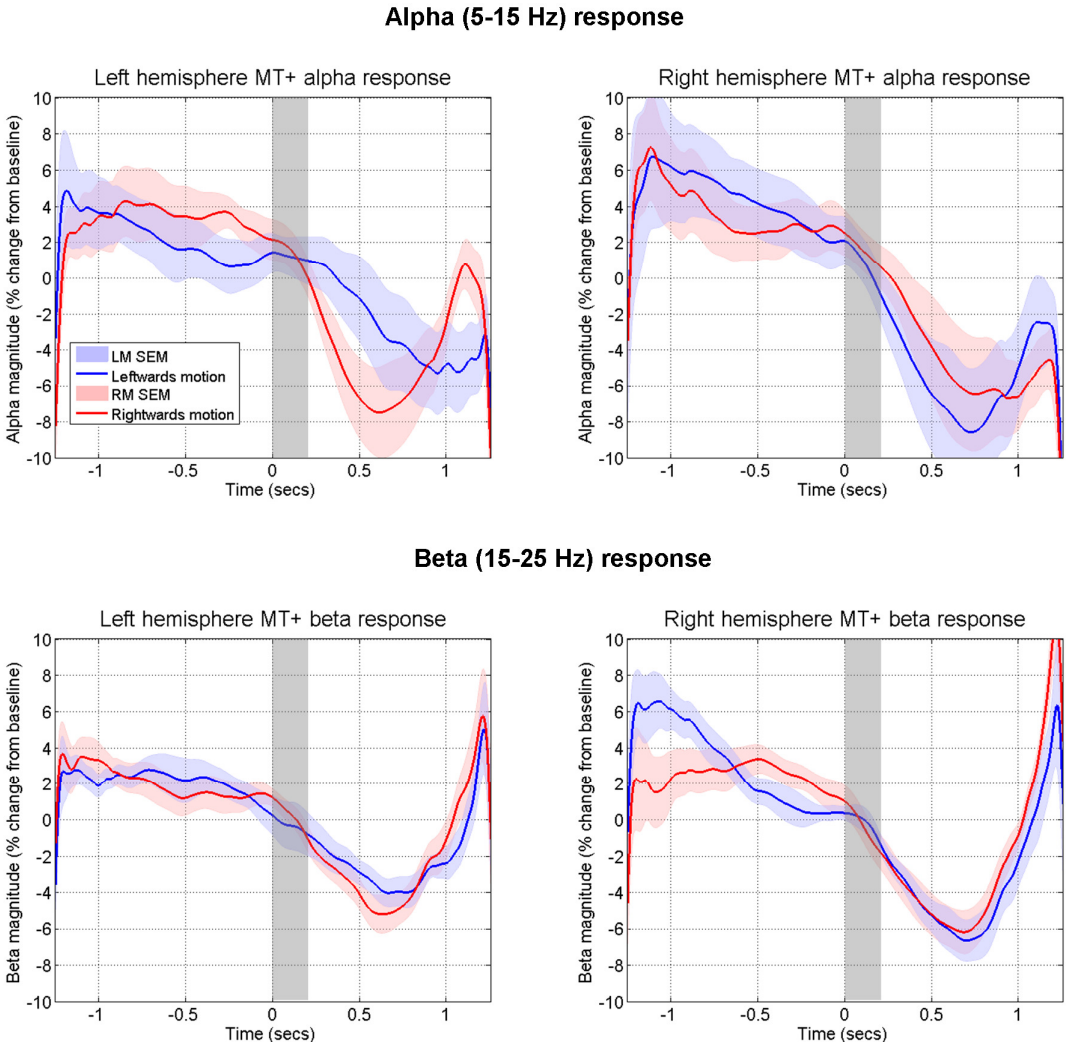

Figure 22. Comparing the temporal characteristics of the alpha and beta amplitude envelope response profiles from bilateral MT+ regions during both left- and rightwards transient retinal motion.
The top two panels show the alpha response from both and right hemispheres during transient retinal motion. Blue traces indicate the mean amplitude envelope for leftwards motion, whilst red traces denote rightwards motion. The lower two panels show the beta response. The grey transparent box (from 0-200 msec) shows the period of transient retinal motion stimulation.

Figure 22 shows the alpha and beta response in both left and right MT+ induced by transient retinal motion. For the alpha response in left MT+ (top left panel), there is a peak power decrease of ~8% for rightwards motion as depicted by the red trace (contraversive target motion), compared to a power decrease of ~5% for leftwards motion (ipsiversive

motion depicted by the blue trace). The latency of the response is approximately 600 msec and 800 msec respectively. This relationship was largely maintained when recording from the opposite hemisphere, which can be seen in the top right panel.

For the beta response (depicted in the lower panels), there appears to be largely identical changes in the amplitude envelope, irrespective of the stimulus motion direction (ipsi- versus contraversive direction). For the beta response in left MT+ (lower left panel) there is a maximum power decrease of ~5% for both rightwards (red trace) and leftwards (blue trace) target motion. For right MT+ (lower right panel) there is a power decrease of ~6% for both leftwards and rightwards motion. The beta suppression rises steadily and the peak of the response manifests itself with a latency of around 600 msec following the initiation of the transient retinal motion in all cases, before returning to baseline levels of relative beta power at around 1200 msec. Therefore, the beta response peaks 400 msec after the cessation of stimulus motion, and only returns to baseline levels almost 1000 msec after the target has stopped moving.

In compliance with the EOG recordings, it appears these effects are due to retinal motion processing and not eye movements. However, there appears to be an increase in the oscillatory amplitude envelope during the baseline period. This may in part be analogous to a rebound and subsequent overshoot of synchronisation following task processing.

2.4.4 Conclusion

In Experiment 2, the temporal dynamics of the alpha and beta response to transient retinal motion was investigated. The purpose of this experiment was to use a stimulus with identical features to that used in the previous pursuit condition and approximate the retinal slip that would been observed when pursuing a target non-optimally. It was found that this translational motion induced low-frequency suppression in the putative MT+ region, as evident in the SAM source localisation. A time-frequency analysis of the alpha response in this area to showed a small bias towards contraversive target motion, with the greatest peak in the 5-15 Hz amplitude envelope displaying a latency of ~600 msec. A slightly smaller peak in the alpha envelope change for ipsiversive motion was found with is lagging behind the contraversive motion by ~200 msec (~800 msec following the onset of stimulus motion). For the beta response, there appears to be no such direction-selective bias, with both contra- and ipsiversive transient stimulus motion inducing largely identical responses from MT+. However, there still appeared to be a significant latency in the response following target motion, with the greatest decrease in this beta amplitude envelope lagging the onset of movement by ~600 msec.

Although the shape of the envelope profiles shown in this experiment appear to match that of the 'pursuit' condition in Experiment 1, the timing/latency of the maximal response in this experiment lagged the onset of target motion by up to 600 msec. Had the effect in the previous experiment been due to retinal error, the motion-related suppression of the alpha-beta response would have been expected to arise about 600 msec after the eyes were at maximum amplitude; in other words, approximately the same time as the point at which the eyes were at maximum velocity during the pursuit cycle. As this was not the case, the result presented here suggests the alpha-beta effect found in Experiment 1 during the 'pursuit' condition was not due to slip of the target.

2.5 Discussion

Preliminary results from the MEG data in Experiment 1 seem to suggest that there could be a hemifield-dependent eye position signal generated during smooth eye movements in the 'pursuit' condition of Experiment 1. However, this finding requires exploration before it is possible to decisively conclude that this is the case; for example, it is not known whether this signal represents an absolute (as in craniotopic) or relative (in terms of a predictive pursuit cycle) position signal. Animal data suggests that there are neurons with a head-centred eye position-sensitivity in MST, but when compared to those that display response characteristics that are coincident with changes in eye velocity, they are in the clear minority (Ilg & Thier, 2003). It might have been expected that the contribution of the more common velocity-sensitive neurons would dominate changes in the MEG signature, so it is not clear why the activity of the disproportionately small percentage of craniotopic neurons might manifest as a 5-25 Hz oscillatory change.

It is worth pointing out, however, that our use of sinusoidal modulation means that it is not possible to disentangle the relative contribution of velocity- and position-sensitive signals from the MEG signature. This is because any hypothetical position signal is a phase-lagged version of the velocity signal, and due to this experimental design, it was not possible to acquire an independent measure of whether amplitude changes in these oscillations are delayed with respect to changes in the underlying neural activity within MT+. However, in Experiment 2, the temporal characteristics of the alpha and beta responses were examined, and it was found that the maximal response lagged behind retinal motion, which suggests suppression of oscillations in MT+ is delayed with respect to ongoing activity. Additionally, these results suggest the alpha-beta change in Experiment 1 was not due to retinal slip.

In Chapter 3, two experiments are reported that were designed to test the apparent eye position-dependency of the alpha and beta response, and whether modulation of this

activity is due to velocity-sensitive neurons. In Experiment 3, pursuit was conducted at various eccentricities, to see if alpha and beta activity reflects head-centred eye position. Experiment 4 used an alternative temporal design, comprising a pseudo-step-ramp protocol where eye velocity was parametrically varied. Together these experiments were designed to establish a more categorical link between low frequency suppression and either eye velocity or position.

As for the task-related suppression of oscillations in the brain, and the question of whether they play an active role in processing or are simply an interesting emergent property of activity, recent literature suggests they play an important functional role. For example, it has been shown that entrainment of cortical rhythms using transcranial alternating current stimulation at the beta frequency over the motor cortex inhibits motor function (Pogosyan, et al., 2009), and clinical studies of Parkinsonian patients displaying symptoms of bradykinesia show abnormal and enhanced beta oscillations (Kuh et al., 2008). Taken together, these data imply a functional role of low-frequency rhythms in inhibition of task-irrelevant information (or 'gating by inhibition'), and conversely, their suppression in regions that process task-relevant information (Jensen & Mazaheri, 2010).

In addition, is seems reasonable to assume that pursuit-related modulation of oscillations in the MT+ region might also reflect the engagement of further superordinate processes that have not been controlled for in Experiment 1. These might include an increased load in visuo-spatial attention, known to be integral in the maintenance of deliberate pursuit eye movements (Lovejoy, Fowler, & Krauzlis, 2009), as well as facilitating neuronal response characteristics and oscillatory power changes in this area (Yamagishia, et al., 2008). Whilst the exact nature of the oscillatory modulations displayed in this area during pursuit and its underlying role in perceptual-motor processing remains unclear at this point, these questions guide forthcoming experiments presented in this thesis.

3 Chapter 3 – Pursuit-related modulation of low-frequency oscillations in MT+: Eye position or eye velocity-dependent?

3.1 Abstract

Results from Experiment 1 suggest that changes in the alpha-beta (5-25 Hz) range in human MT+ during pursuit eye movements codes for eye position in the contralateral visual hemifield based on head-centred coordinates. This indicates that this region plays a role in oculomotor control and/or the integration of extraretinal signals as part of a process that maintains motion invariance during the eye movement. However, it is possible that this result could be due a velocity signal that lags the movement of the eyes, rather than head-centred eye position-dependence. Therefore, an explicit test was devised to see whether these changes in cortical rhythms reflect true eye position sensitivity by examining the alpha and beta amplitude envelope profiles at various pursuit eccentricities (Experiment 3). If the alpha-beta suppression does reflect a head-centred eye position code, a difference in amplitude for the envelope profiles might be expected when pursing a target in different portions of space. If, however, the alpha-beta envelopes are the same regardless of the eye position when engaged in pursuit, this would suggest this signals reflects some other aspect of the eye movement. An alternative possibility is that the alpha-beta suppression witnessed during the pursuit cycle in Experiment 1could have resulted from a velocity signal that lags behind the movement of the eyes. With this in mind, a further experiment was designed to investigate the relationship between alpha and beta activity when pursuing a target at different velocities (Experiment 4). For Experiment 3, it was hypothesised that pursuit modulation of the alpha and beta amplitude originating from MT+ would be significantly different for eye movements at different eccentricities (portions of head-centred space) if these oscillations do in fact reflect a hemifield-dependent eye position signal. Participants pursued a sinusoidal target in the dark

at various eccentricities based on a craniotopic reference frame. Results revealed largely identical patterns of modulation in the alpha and beta amplitude envelopes irrespective of the eccentricity at which pursuit was performed. In Experiment 4, it was hypothesised that there would be an effect of eye velocity (specifically, for motion in the ipsiversive direction) on alpha and/or beta activity. Participants tracked a linearly moving target at different velocities in a pseudo-step ramp fashion. Results show no evidence of any velocity-specific effects on either alpha or beta activity. However, there was a significant effect of eye speed on the magnitude of the beta suppression, with increasing eye speeds inducing increased beta suppression. There was no such effect of eye speed on alpha activity. These results taken together would suggest that oscillatory changes related to pursuit in MT+ probably reflects activity from a number of different sources encoding various aspects of the eye movement, including responses from both eye position- and velocity-dependent pursuit neurons.

3.2 Experiment 3 – Alpha and beta activity in response to excursive pursuit

3.2.1 Overview

In Chapter 2, Experiment 1, oscillatory changes related to the processing of eye movement signals and retinal motion in human MT+ was explored using MEG. It was speculated that responses in the alpha-beta frequency band reflect a head-centred eye position code, with a further control experiment ruling out the possibly of this effect being due to retinal slip. However, it did seem possible that this effect could be due a velocity signal that lags the movement of the eyes.

At the neuronal level, the vast majority of those neurons that display a purely pursuit-related response in this area (i.e. those that do not show a response to retinal motion) have been shown to code for eye velocity during pursuit, whilst only a small minority actually display any kind of head-centred eye position sensitivity (Ilg & Thier, 2003). The findings reported in Experiment 1 are surprising, as suppression of the 5-25 Hz response (a correlate of increased cortical activity) might have been expected to covary with eye velocity instead of position, in line with previous animal (Churchland & Lisberger, 2005) and neuroimaging studies (Nagel, et al., 2008; Nagel, et al., 2006). However, given the paradigm used and the data given, it was not possible to explain this discrepancy. The experiments presented in this chapter were devised as a way to differentiate between the two possibilities that oscillatory changes in MT+ during pursuit represented either an eye position- or velocity-code.

The main aim for this experiment was to explicitly test whether the alpha-beta suppression observed during pursuit is the result of a true hemifield-dependent, eye position-related signal. This was done by utilising the exact stimulus parameters as before and simply varying the eccentricity (relative excursive pursuit position based on a craniotopic reference

frame) at which the pursuit cycle was performed. This allowed predictions to be made about the amplitude envelope profiles that might be observed if this signal is related to eye position.

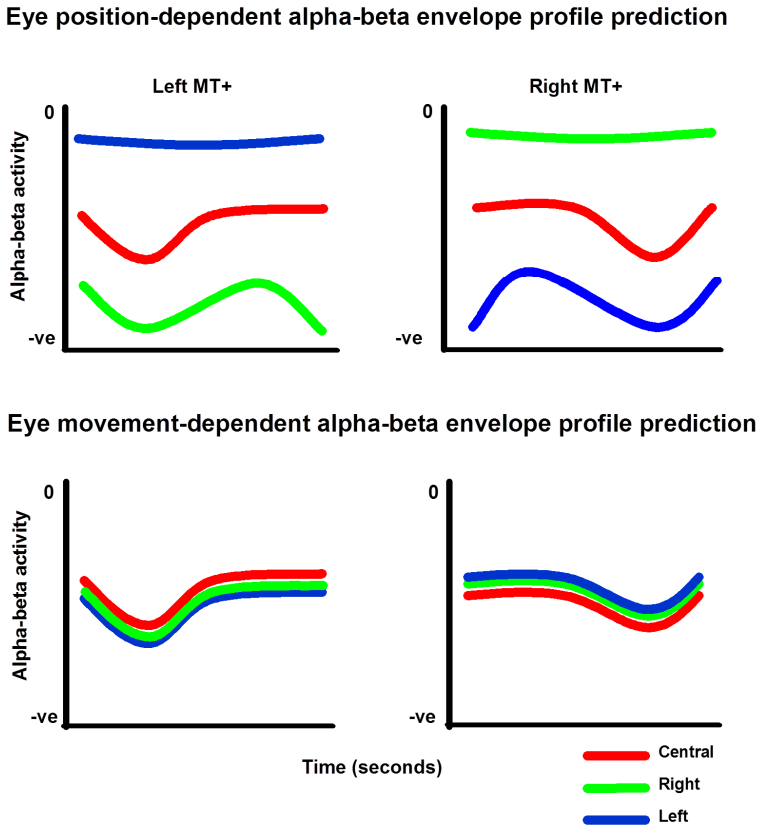

Figure 23. Predictions for possible alpha-beta (5-25 Hz) amplitude response profiles from putative MT+ during pursuit in different portions of space.
Shown here are pursuit-related oscillatory changes when tracking a sinusoid stimulus motion that might reflect either a hemifield-dependent eye position signal originating from MT+ (top two panels), or a measure dependent on some other aspect of the eye movement (in this case a lagged eye velocity signal, bottom two panels).

It was predicted that if this signal is the result of neuronal activity coding for the position of the eyes during pursuit, then we might expect to see distinct amplitude envelope profiles for alpha and beta activity dependent on the eccentricity of the pursuit cycle. For example, as shown in Figure 23, top panels, when engaging in a pursuit cycle in the contralateral hemifield (with respect to the recording site), relatively *greater* suppression (a relative decrease in oscillatory amplitude) of the activity in MT+ might be expected. Equally,

less suppression of these brain rhythms might be expected when pursuing a target in the ipsilateral visual hemifield when recording from the same cortical location. Conversely, if the changes in the amplitude envelopes are the same irrespective of the pursuit cycle eccentricity (shown as similar shapes in the amplitude envelopes, which can be seen in the bottom panels of Figure 23) then it can be assumed that these macroscopic signals actually reflect some other aspect of the pursuit eye movement, such as velocity.

3.2.2 Methods

3.2.2.1 Participants

Eighteen healthy participants (thirteen females, mean age = 23 years) completed Experiment 3. All participants were naïve as to the purpose of the experiment.

3.2.2.2 Design and procedure

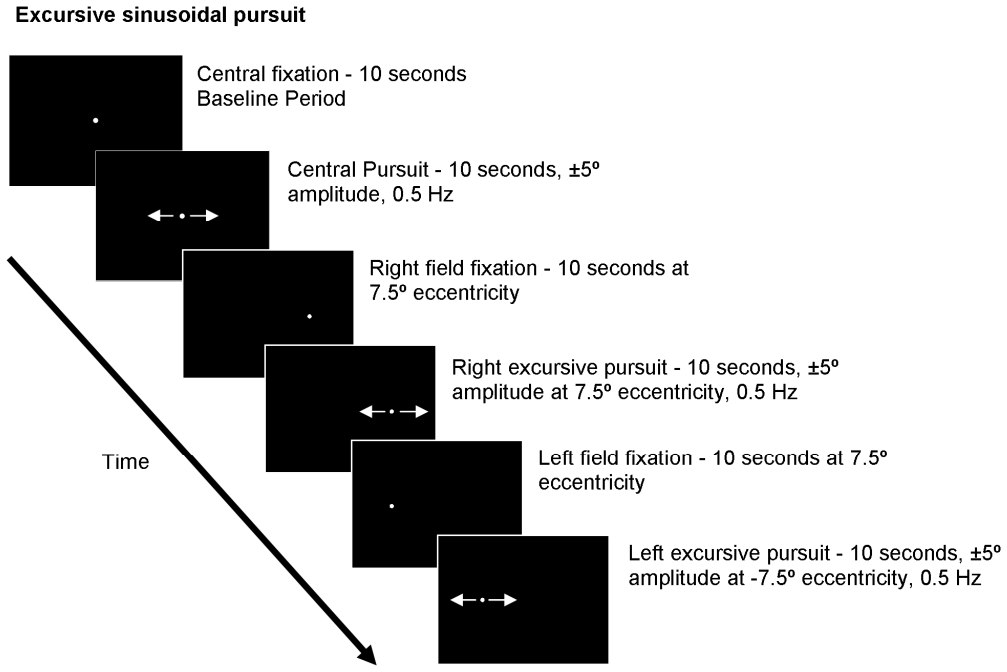

Figure 24. A schematic diagram of the experimental protocol for the excursive pursuit eye movement paradigm.

Sinusoidal smooth pursuit eye movements were performed at various horizontal eccentricities in different portions of head-centred space, including the central, right and left hemifield, in the sequence shown.

Figure 24 shows the experimental protocol for Experiment 3. The experiment consisted of 3 conditions. In the first condition, 'central pursuit', participants were required to make sinusoidal horizontal pursuit eye movements by tracking a faint dot in the central portion of the screen (0.5 Hz frequency, amplitude ±5º). In the second 'right pursuit' condition, participants made horizontal pursuit eye movements that took place completely in the right hemifield; that is, in a spatiotopic (head-centred) coordinate frame, starting at 7.5º eccentricity, with an amplitude of ±5º and a frequency of 0.5 Hz (otherwise identical to condition 1, 'central pursuit'). In the third condition, 'left pursuit' participants engaged in sinusoidal pursuit with amplitude of ±5º and a frequency of 0.5 Hz, except this time the pursuit cycle starts at -7.5º eccentricity.

Figure 25 (below) depicts a schematic of the eye movement conditions, and the portion of head-centred space in which the pursuit cycles were made. Below that is a representative example of eye position for all three conditions. This is provided to clarify the description of the experimental protocol given above. Visual inspection of the individual EOG recordings showed that all observers (n=18) were able to accurately and smoothly pursue the target stimulus, resulting in no participants being excluded from the final MEG data analysis.

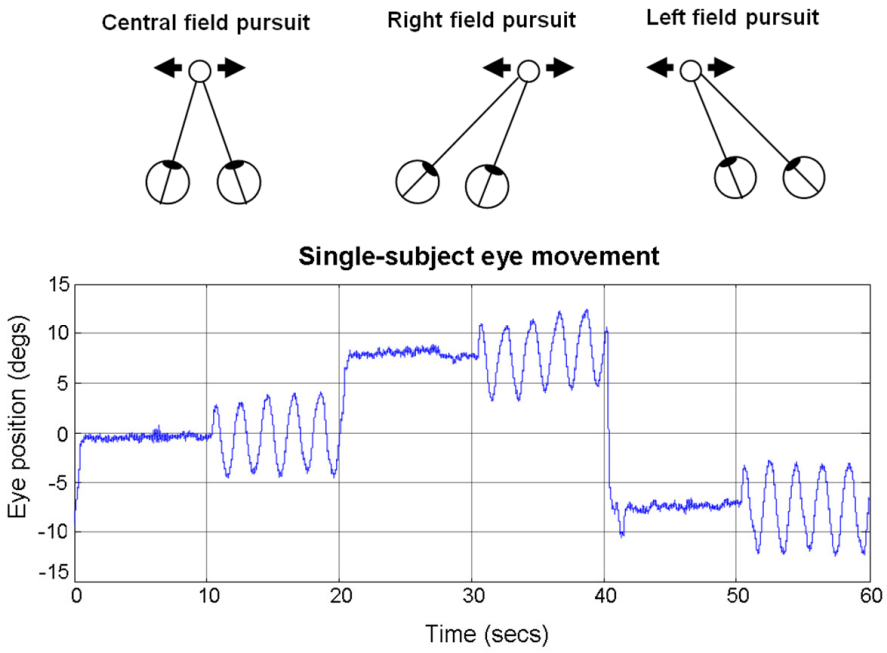

Figure 25. A schematic diagram of the 3 sinusoidal pursuit eye movement conditions (top) for Experiment 3, along with representative single subject eye movement data across all trials (bottom).
The top panel of the figure shows a schematic representation of the relative portions of head-centred space in which three conditions of sinusoidal pursuit eye movements occurred. Below that is an example of a single subject's eye movement data averaged over all trials.

The experiment comprised of a traditional boxcar design, with 15 x 60 second epochs consisting of a 10s central fixation baseline period immediately followed by the 10s 'Central pursuit' condition (active period), then a 10s right fixation period, 10s 'right pursuit' condition, 10s left field fixation and finally 10s of 'left pursuit', taking approximately 15 minutes per run in total.

3.2.2.3 Data analysis

For Experiment 3, the percentage change in oscillatory amplitude during the active period (central pursuit) was baselined against the 0-10 second passive period (central fixation).

3.2.3 Results

3.2.3.1 Eye movement data

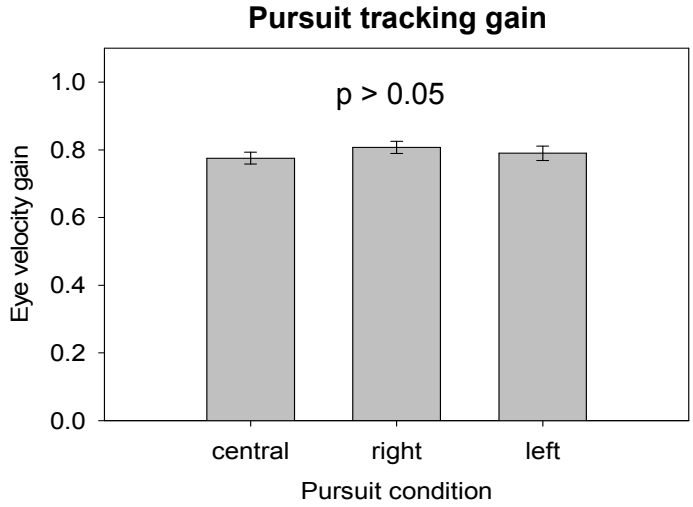

Figure 26. Eye movement velocity gain for the excursive pursuit experiment.
Group-averaged eye velocity gain values for all three pursuit conditions, with no significant main effect of gain between the different pursuit eccentricities.

Figure 26 shows the group mean (n=18) eye velocity gain when pursuing the stimulus, in all three conditions. Visual inspection of the EOG traces revealed that observers were able to track the moving stimulus fairly accurately with a gain close to unity, and this was confirmed by a mean eye gain that was calculated to be approaching 0.8 for all of the conditions at the various eccentricities. Subsequently, as detailed in the *Methods* section, no participants were omitted from the final MEG analysis. As with Experiment 1, any trials that were found to be severely contaminated with saccadic eye movements or blinks were removed from any further imaging analysis, which resulted in an average trial exclusion rate of 13.3% per participant per session. Crucially, a Repeated Measures ANOVA revealed no significant difference between the eye velocity gain for the 3 pursuit conditions ($F(2,17) = 1.722$, $p > 0.05$).

3.2.3.2 SAM source analysis

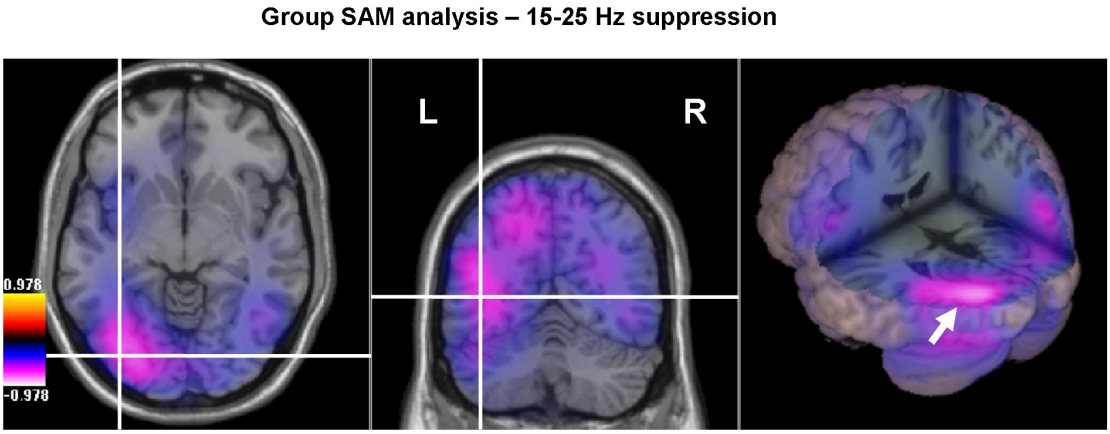

Figure 27. Group mean SAM images for the 15-25 Hz oscillatory response during the central pursuit task versus the baseline central fixation condition, overlaid on a template brain.
Cold-colour map indicates task-induced oscillatory power decreases, with the greatest peaks localised to bilateral extra-striate regions, with a dominant peak in the left hemisphere.

Figure 27 shows the group mean (n=18) SAM analysis for 15-25 Hz activity. This revealed consistent bilateral extra-striate suppression of the beta oscillatory response for the 'central pursuit' versus baseline central fixation condition in all participants. As this frequency band displayed the most consistent peaks localised to putative MT+, these coordinates were used to compute the weights required for the virtual sensors and the subsequent time-frequency analysis. Additionally, areas of the PPC, FEF and cuneus showed evidence of beta rhythm power decreases. The group average beta response with a peak in left association cortex shown in Figure 27 is indicative of the individual source localisation results. Furthermore, alpha oscillatory changes for central pursuit eye movements were, for the most part, spatially coincident with the beta response shown above; that is, located in association cortex consistent with MT+, PPC, FEF and cuneus. However, the beamformer reconstruction of the beta rhythm proved to be more consistent in its estimation of MT+.

Finally, there were no consistent gamma (30-70 Hz) responses evident in any individual or Group SAM images.

3.2.3.3 Time-frequency analysis

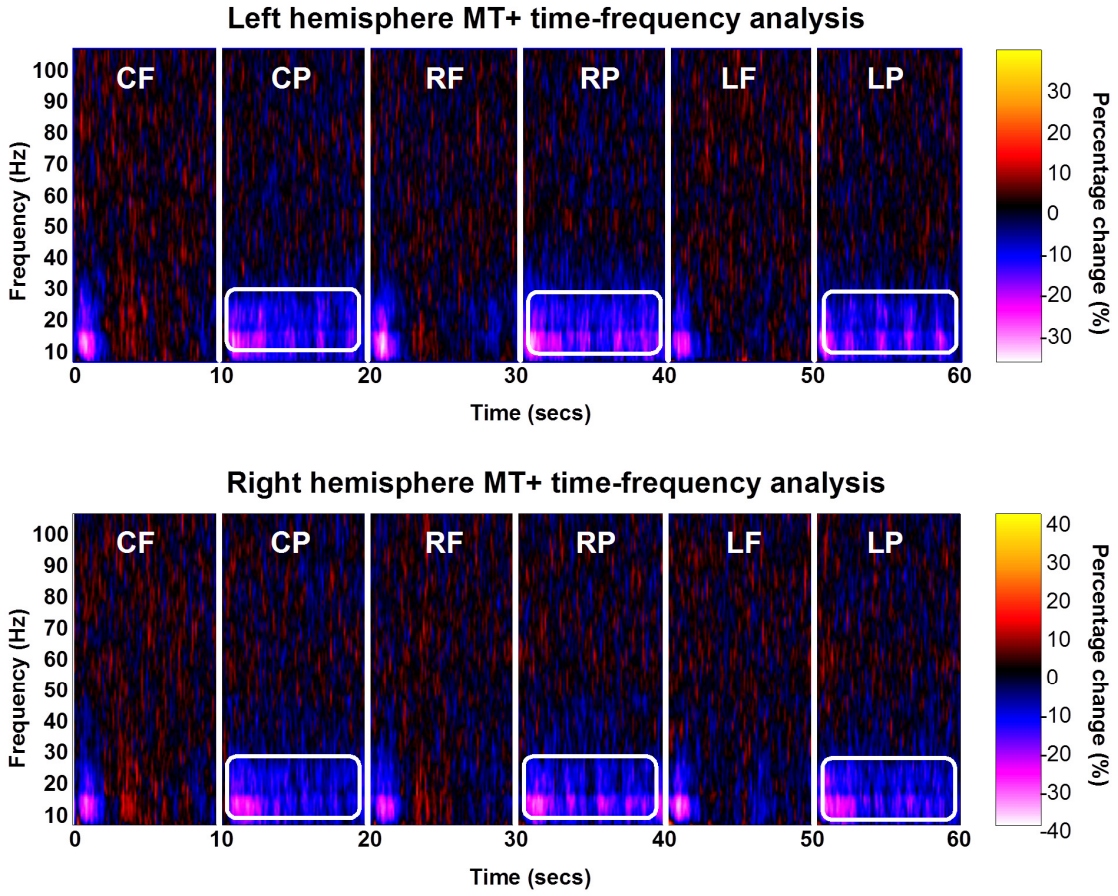

Figure 28. Grand averaged time-frequency spectrograms for peak voxel locations in MT+ from both the left and right hemisphere as defined by the 15-25 Hz SAM analysis. Low-frequency suppression (5-25 Hz power decreases, delineated by the white-bounded box) is observed for all three pursuit conditions as denoted by the cold-colour map (indicating percentage change from baseline). CF: Central fixation; CP: Central pursuit; RF: Right fixation; RP: Right pursuit; LF: Left fixation; LP: Left pursuit.

Figure 28 shows the group-averaged (n=18) spectral analysis from left and right MT+ during eye movement for all three pursuit eccentricities. The top panel depicts results for the left hemisphere and the bottom row panel is for the right hemisphere. Each of the panels begins with the central fixation baseline window (denoted by CF). This is then followed by

the 'central pursuit' condition (CP), right fixation (RF), 'right pursuit' condition (RP), left fixation (LF) and finally 'left pursuit' (LP). The time-frequency analysis from left MT+ revealed sustained, low frequency (5-25 Hz) power decreases for the duration of tracking for all three conditions. A similar response profile alpha-beta changes is also observed in right MT+, with sustained suppression for the duration of all three conditions. There is no evidence in the spectrograms of any discernable difference in the alpha or beta response as a function of pursuit cycle eccentricity.

Additionally, there appears to be demarcation in the oscillatory power changes of the 5-25 Hz frequency band (denoted by the white bounded box in the spectrograms), showing sustained power decreases during pursuit eye movements in MT+. One, in the range of the 'classical' alpha band (5-15 Hz), which displays a relative power decrease of approximately 20-30%; and another showing sustained suppression in the higher 'classical' beta frequency band (15-25 Hz), with power decreases in the region of 10-20% for the duration of pursuit. The pattern of these responses is similar to those found in Experiment 1, being modulated in a time varying fashion. This effect appears more prominent in the left MT+ voxel.

To more accurately assess the spectral characteristics of these responses, and to see whether there is any difference in the pursuit-related modulation of this activity at the three pursuit eccentricities, the amplitude change for alpha (5-15 Hz) and beta (15-25 Hz) was extracted from the time-frequency data. This was then compared across conditions during the sinusoidal pursuit cycle.

3.2.3.4 Oscillatory amplitude envelope analysis

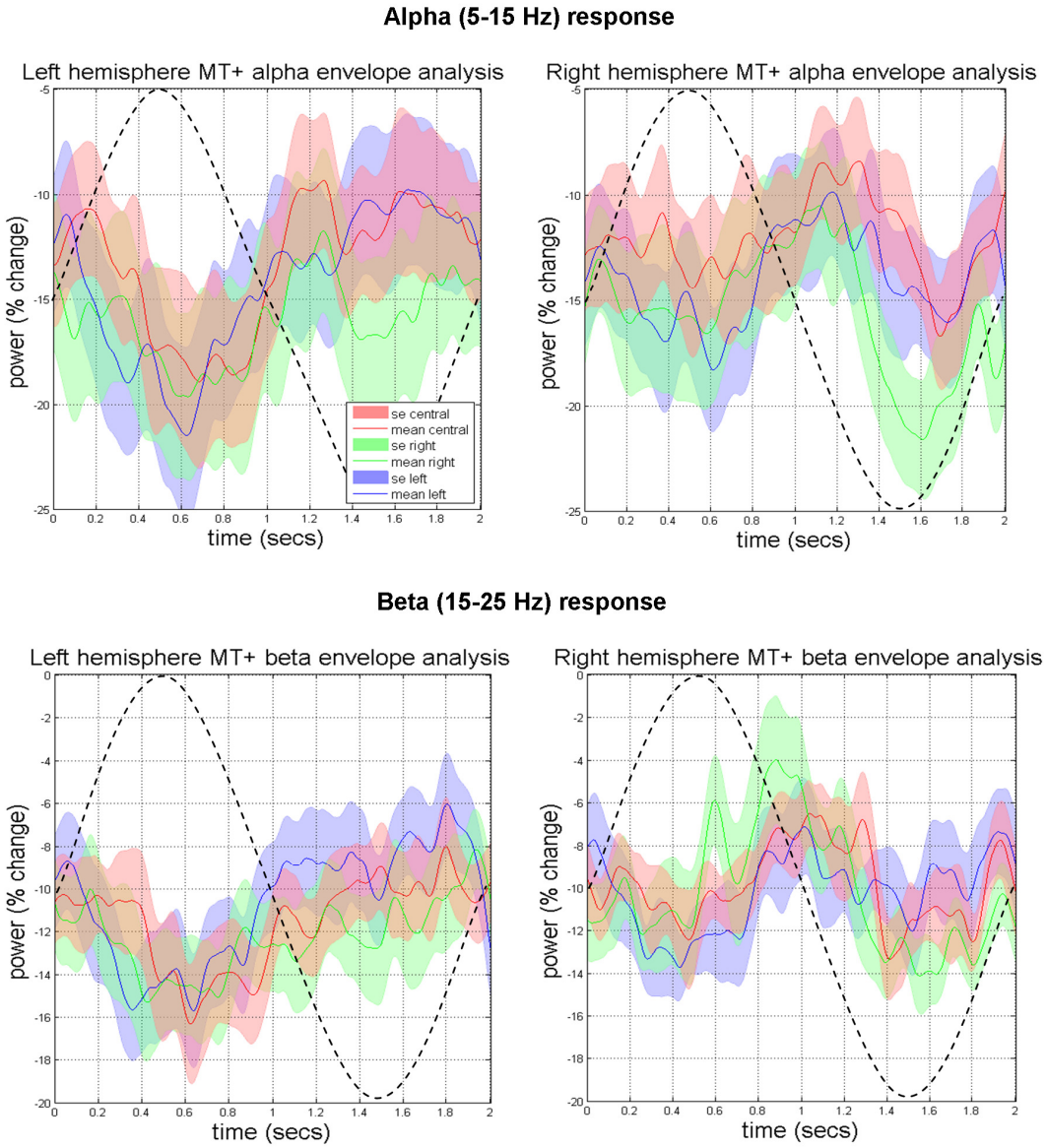

Figure 29. Group-averaged amplitude envelope analysis for alpha (top panels) and beta (bottom panels) frequency bands.
A representative sinusoidal pursuit cycle is denoted by the dashed grey line (irrespective of the absolute eye position). The 'central pursuit' condition is depicted by the red trace, 'right pursuit' condition in green, and the 'left pursuit' condition in blue, with shaded standard error bars. The percentage amplitude changes are relative to the baseline central fixation period.

Figure 29 shows the group-averaged (n=18) amplitude envelopes in the alpha (top panels) and beta bands (bottom panels) relative to the baseline central fixation condition, in

both left and right MT+ during a pursuit cycle. This modulation can be compared to the 'average' eye position during each cycle, irrespective of the eccentricity, as shown by the dashed grey line. For both alpha and beta responses, there is no difference in amplitude between conditions over the course of a pursuit cycle, irrespective of whether the eyes were tracking in the central-, left- or right portion of head-centred space. The modulation of low-frequency oscillations in MT+ observed during Experiment 1 is therefore most likely the result of eye velocity, with no evidence here of ipsi- or contralateral eye position-dependence (relative to the MT+ recording site).

As in Experiment 1, however, there does appear to be a consistent modulation of the alpha and beta amplitude envelope within the pursuit cycle. In the left MT+ recording site, alpha and beta suppression increases and seems to covary with eye position in the contraversive phase of the pursuit cycle. In other words, when the eyes are moving away from the left recording site (irrespective of their absolute position in space), a decrease in the amplitude envelope is observed, with a shape similar to that seen in the results in Chapter 2, Experiment 1. For right MT+ however, the shape resembles more of a symmetrical 'W' shape, with two minima in the alpha and beta power corresponding to the maximum amplitude of the eyes during the pursuit cycle. The maximum alpha-beta suppression in right MT+ does not appear to show any eye position or movement direction bias.

Therefore, it is possible these amplitude envelope response profiles could reflect a process that reflects eye speed or velocity (albeit one that actually lags the eye movement).

3.2.4 Conclusion

Experiment 3 was designed to test whether the induced oscillatory response in MT+ during pursuit eye movements reflects the activation of neurons sensitive to eye position and whether this signal is dependent on the hemifield in which pursuit is engaged.

This was a follow-up experiment to initial findings that seemed to suggest low-frequency suppression in this region (specifically, the 5-25 Hz response) during pursuit reflected a hemifield-dependent eye position signal (Experiment 1). By instructing participants to pursue a sinusoidally oscillating dot at various eccentricities (based on a head-centred coordinate frame), the hypothesis that pursuit conducted completely in the contralateral hemifield (that is, relative to the site of virtual electrode recording) would induce significantly greater low-frequency suppression in MT+ was put to the test. Furthermore, it was hypothesised that pursuit in the ipsilateral hemifield would induce significantly less alpha-beta suppression relative to pursuit in the central region.

It was predicted that differential amplitude envelope profiles in the alpha and beta bands during a pursuit cycle at various eccentricities would suggest that the oscillatory changes evident in the MEG signal emanating from this region of cortex would be due the activation of neurons coding for a hemifield-dependent eye position signal. Conversely, it was also predicted that if the alpha-beta amplitude envelopes were indistinguishable from one another, irrespective of the pursuit eccentricity, would suggest this signal is the result of some other eye movement-dependent measure (possibly a velocity or speed-based signal).

Analysis of the alpha and beta amplitude envelopes during excursive pursuit showed no evidence of a differential response related to eye position. Activity for both alpha and beta bands were found to be virtually identical, regardless of the region of space in which pursuit was conducted. This would suggest that the oculomotor control and extraretinal eye movement signals recorded from MT+ reflect the activity of neurons that actually code for

some other aspect of smooth pursuit. Therefore, it could be speculated upon that the peaks in alpha-beta suppression that appeared to correlate with eye position in the contralateral hemifield during pursuit in Experiment 1 is due a lagged velocity signal. This proposal forms the basis of the next experiment in this chapter, where a pseudo step-ramp design was implemented to investigate the dependence of this activity on eye velocity.

3.3 Experiment 4 – Alpha and beta activity in response to eye velocity modulation

3.3.1 Overview

Given the results of Experiment 3, it seems that the findings in Experiment 1 showing changes in alpha-beta activity that covaries with eye position is not due to a strict hemifield-dependence. It was speculated this effect might be a phase-shifted measure of maximum eye velocity. In other words, the peak suppression of this response is one that lags behind the underlying neural activity that reflects eye velocity. Therefore, an experimental design was implemented to test whether oscillatory changes in this area were related to eye velocity. Participants had to track a linearly moving stimulus at parametrically varied velocities in a pseudo-step ramp fashion. This design allowed assessment of whether the magnitude of oscillatory suppression reflects changes in eye velocity. Additionally, it has been shown in both the animal and human literature that the majority of pursuit-related neurons in MT+ have a directional bias for eye movements in the ipsiversive direction (Dukelow, et al., 2001; Ono & Mustari, 2006). Therefore, we sought to expand on this and examine whether there is any evidence of a directional bias in the alpha and beta response for different pursuit directions in humans.

Whilst there has been, to our knowledge, only a handful of neuroimaging papers on pursuit velocity modulation of activity in MT+, Nagel et al. (2008) reported a main effect of velocity, with an increasing BOLD effect observed for increasing stimulus velocity (Nagel, et

al., 2008; Nagel, et al., 2006). However, this is a misrepresentation, as they tested *speed*-related modulation of activity, ignoring the direction of pursuit and collapsing across velocity vectors to end up with a speed scalar. Therefore, whilst they report a novel finding for an eye velocity-dependent modulation of the BOLD signal in human MT+, they did in fact only report a main effect of eye speed. Additionally, they lacked a test that might detect the presence of extraretinal signals in MT+ that reflects the activity of neurons with a preferred directionality of pursuit (of which the animal literature suggests would be the majority of neurons in MST sensitive to pursuit; (Ilg & Thier, 2003; Ono & Mustari, 2006)). In addition to supplementing these findings, the principal rationale and motivation behind Experiment 4 was to expand on the findings presented in this thesis thus far and elucidate any putative functional roles for alpha and beta activity in MT+ during pursuit eye movements.

Given that there has been shown to be a significant link between spike-rate, the BOLD effect and suppression in low-frequency oscillations (Mukamel, et al., 2005), and animal data that suggests a velocity-dependence of pursuit-sensitive neurons in MT+ (Ono & Mustari, 2006), it was hypothesised that increasing alpha and beta suppression in unilateral MT+ with increasing ipsiversive pursuit velocity (that is, relative to the recording site) would be found. Conversely, it was predicted that for contraversive pursuit (away from the recording site), a monotonic relationship between alpha and beta suppression and increasing eye velocity would be found (in other words, a 'gated' alpha and beta response that is suppressed relative to baseline but no greater for increasing eye velocities).

3.3.2 Method

3.3.2.1 Participants

Twenty healthy naïve participants with normal or correct-to-normal visual acuity completed the experiment (12 females, mean age = 22.3 years).

3.3.2.2 Design and procedure

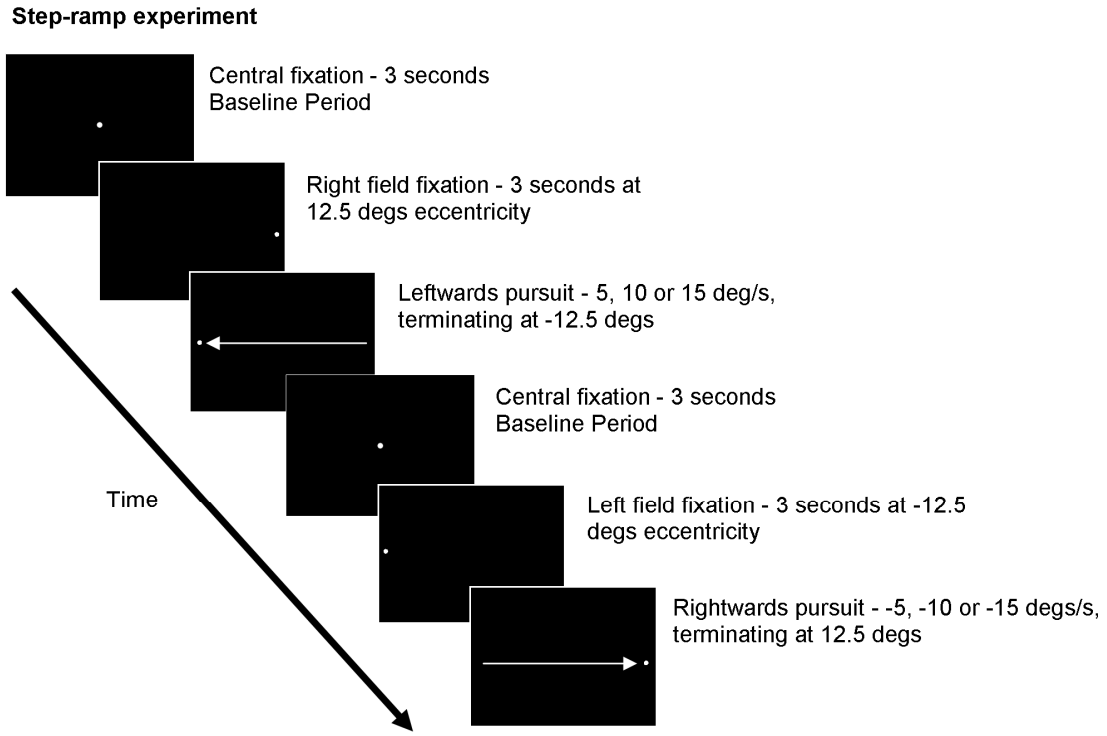

Figure 30. Schematic diagram of the experimental protocol for the velocity modulation experiment.
Participants fixate a central stimulus for 3 seconds (baseline condition), followed by either a fixation to the left or right at -12.5º or 12.5º respectively. Then follows an active tracking period where the participants pursue the target stimulus at one of three speeds (5, 10 or 15º/s) in either direction, given six total velocities/conditions.

Figure 30 depicts the experimental protocol for this experiment. Participants begin by fixating a central point (baseline period, 3 seconds), which was followed by the appearance of a target in the right hemifield at 12.5º eccentricity, for 3 seconds, which observers fixated. The target stimulus then moved leftwards at either -5, -10 or -15º/s for 25º of visual angle. This period is then immediately followed by another central fixation (3s), which in turn is followed by a left field fixation (amplitude -12.5º, gaze held for 3s). A period of rightwards smooth pursuit at 5, 10 or 15º/s for 25º then follows. Thus, there were six conditions in total, each comprising one of three speeds in both directions along the horizontal meridian, with 15

trials of each velocity. Condition presentation was pseudo-randomised and counter-balanced within the whole run.

3.3.2.3 Data analysis

For Experiment 4, the SAM images were constructed for each pursuit velocity condition versus the central fixation baseline period. The percentage change in the amplitude envelope for the active period (pursuit condition) was baselined against the passive period. Alpha and beta power for all later analyses was sampled over a 1 second time window during the central portion of the pursuit phase. By sampling the oscillatory amplitude changes partway through the linear pursuit phase, this meant that eye velocity was most likely to be uniform and close to unity. Therefore, any pursuit-related modulation in oscillatory amplitude would have predominantly been related to velocity-sensitive neurons, and not the result of any responses related to initial pursuit execution, retinal slip during target acceleration or saccadic eye movements.

3.3.3 Results

3.3.3.1 Eye movement data

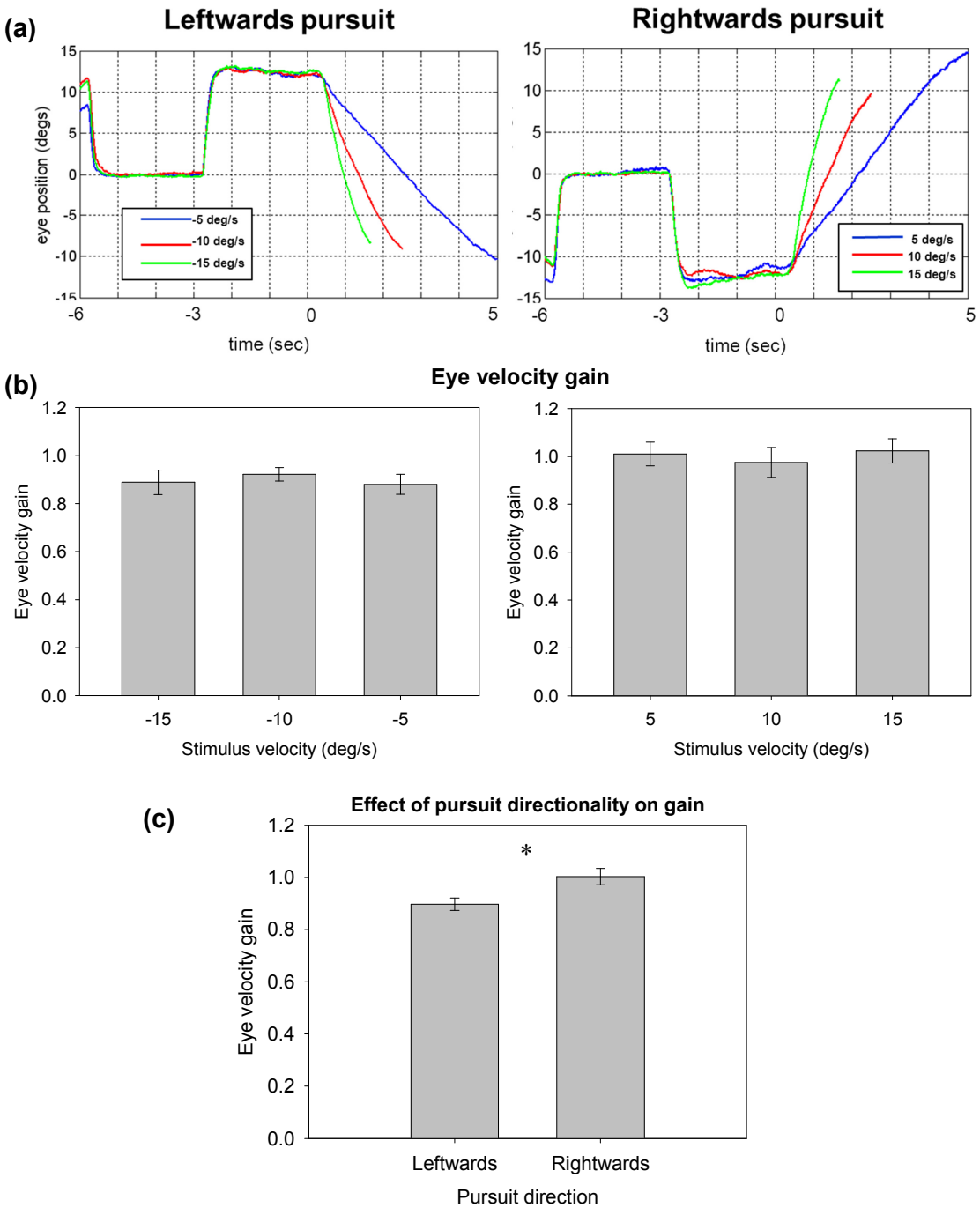

Figure 31. Group averaged eye movement data for the velocity modulation experiment. (a) Group-averaged horizontal eye position traces for pursuit eye movements in both the leftwards (left panel) and rightwards (right panel) direction. (b) Group mean eye velocity gain

for leftwards (left panel) and rightwards (right panel) pursuit eye movement velocity conditions. Gain was calculated over the central 1 second window midway through the pursuit eye movement, with ±1 standard error bars (c) Group mean eye velocity gain, collapsed across all velocity conditions, for both the left and rightwards direction, with ±1 standard error bars (* $p < 0.05$).

Figure 31 shows the group-averaged (n = 19) horizontal eye position trace for pursuit eye movements when tracking the stimulus in both the left- and rightwards directions and the mean eye velocity gain for each condition (quantified over the middle 1 second window during tracking of the stimulus). Participants with mean gain values not falling within the predefined gain values of 0.8 to 1.2 across all conditions were excluded from further behavioural and imaging analysis. By thresholding the gain of pursuit to within these limits, the neuromagnetic activity recorded during this time was predominantly the result of extraretinal eye movement signals and therefore was not severely contaminated by strong retinal motion due to slip of the target dot or saccadic eye movements. This resulted in the exclusion of one participant whose average gain value was 0.78 (therefore 19 participant's data was used in the imaging analysis).

Two separate One Way ANOVA tests were conducted on eye velocity gains for leftwards and rightwards pursuit direction. There was no significant difference in velocity for leftwards pursuit ($F(2,36) = 0.30$, $p > 0.05$) or rightwards pursuit ($F(2,36) = 0.20$, $p > 0.05$). However, when mean eye velocity gain was collapsed across conditions to give a mean measure of pursuit gain based on directionality, there was a statistically significant difference in the mean eye velocity gain for left- ($M = 0.90$, $SD = 0.18$) versus rightwards ($M = 1.00$, $SD = 0.23$) pursuit (paired t-test, $t(56) = -2.62$, $p < 0.05$). This shows an asymmetry in pursuit efficiency, with observers more often able to track the stimulus closer to unity in the rightwards direction.

3.3.3.2 SAM source reconstruction

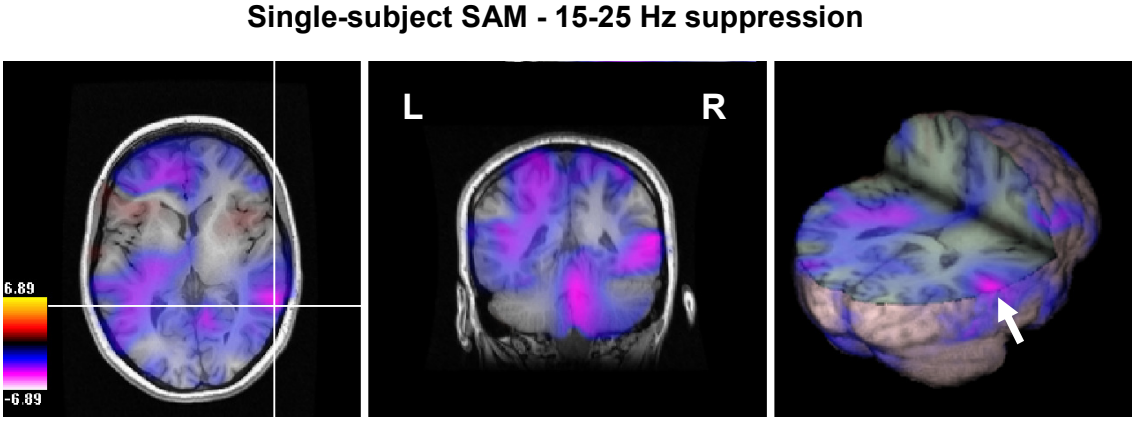

Figure 32. Representative single-subject SAM analysis for the 15-25 Hz oscillatory response during leftwards pursuit eye movements at -10°/s.
This revealed a peak in beta-band oscillatory power decreases over the right hemisphere extra-striate cortex, consistent with MT+, along with a weaker peak voxel identified in left extra-striate cortex. Additionally, there were peaks identified in FEF, SEF, the cerebellum and the PPC.

Figure 32 shows a representative single-subject SAM analysis for the beta response during stimulus tracking at -10°/s, versus the central fixation baseline period. This revealed bilateral 15-25 Hz suppression over extra-striate cortices, consistent with MT+, in addition to peaks over the FEF, SEF, and PPC regions. Similar patterns of activity to this were observed for this subject in the alpha band for all other pursuit velocities in both the left- and rightwards directions. No consistent gamma peaks were identified in any of the participants in the MT+ region. The beta response observed during pursuit, as in previous experiments, was shown to be the most consistent in the SAM source estimation for the majority of subjects for localising MT+. Therefore, it was used to define the ROI for the beamformer reconstruction and subsequent time-frequency analysis.

3.3.3.3 Time-frequency analysis

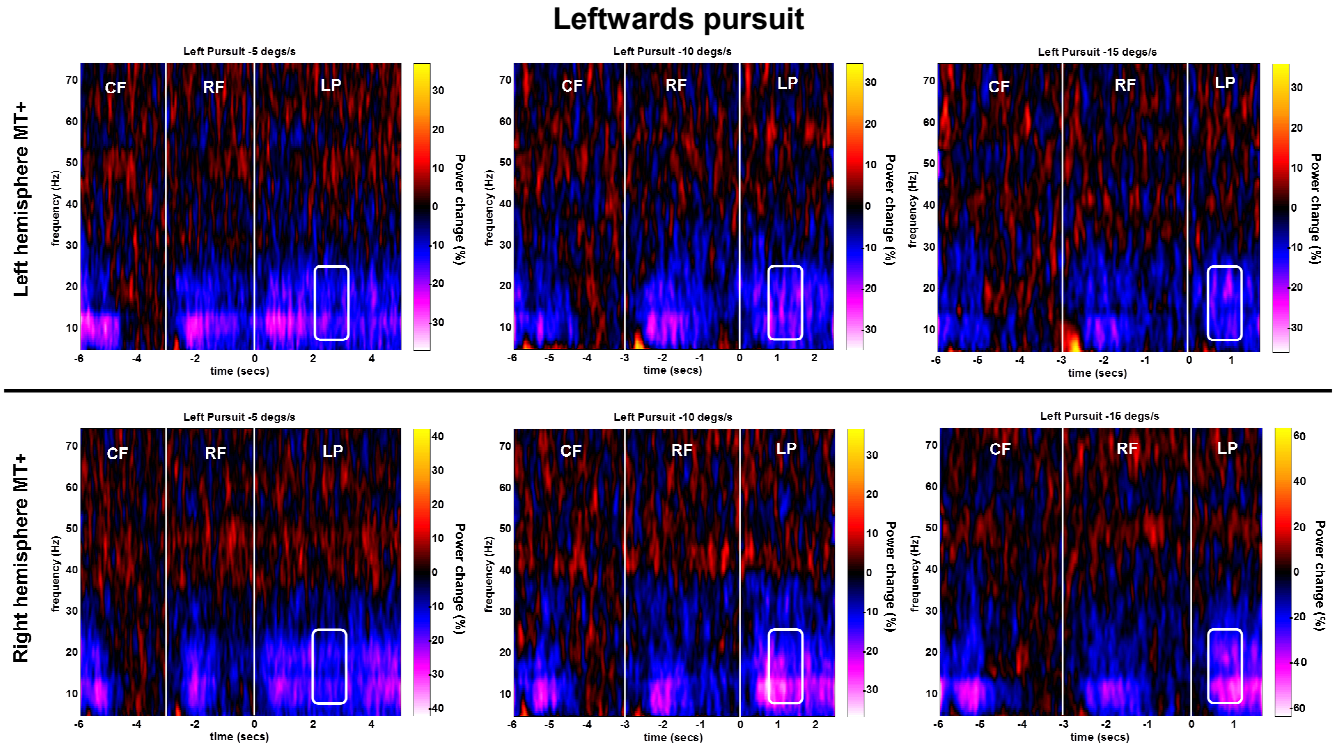

Figure 33. Grand-averaged time-frequency spectrograms from left and right MT+ during leftwards pursuit.
The baseline period (central fixation: CF) was followed by right field fixation (RF) at 12.5º from -3 to 0 secs. Subsequently, there was an active leftwards pursuit (LP) period at either -5, -10, -15 or -20º/s, terminating at -12.5º eccentricity. White box denotes the time-period over which the average oscillatory power change during pursuit was quantified, for both the alpha and beta band. This amplitude envelope change was subsequently used in the correlational analysis when examining eye velocity modulation of the alpha and beta rhythm in MT+.

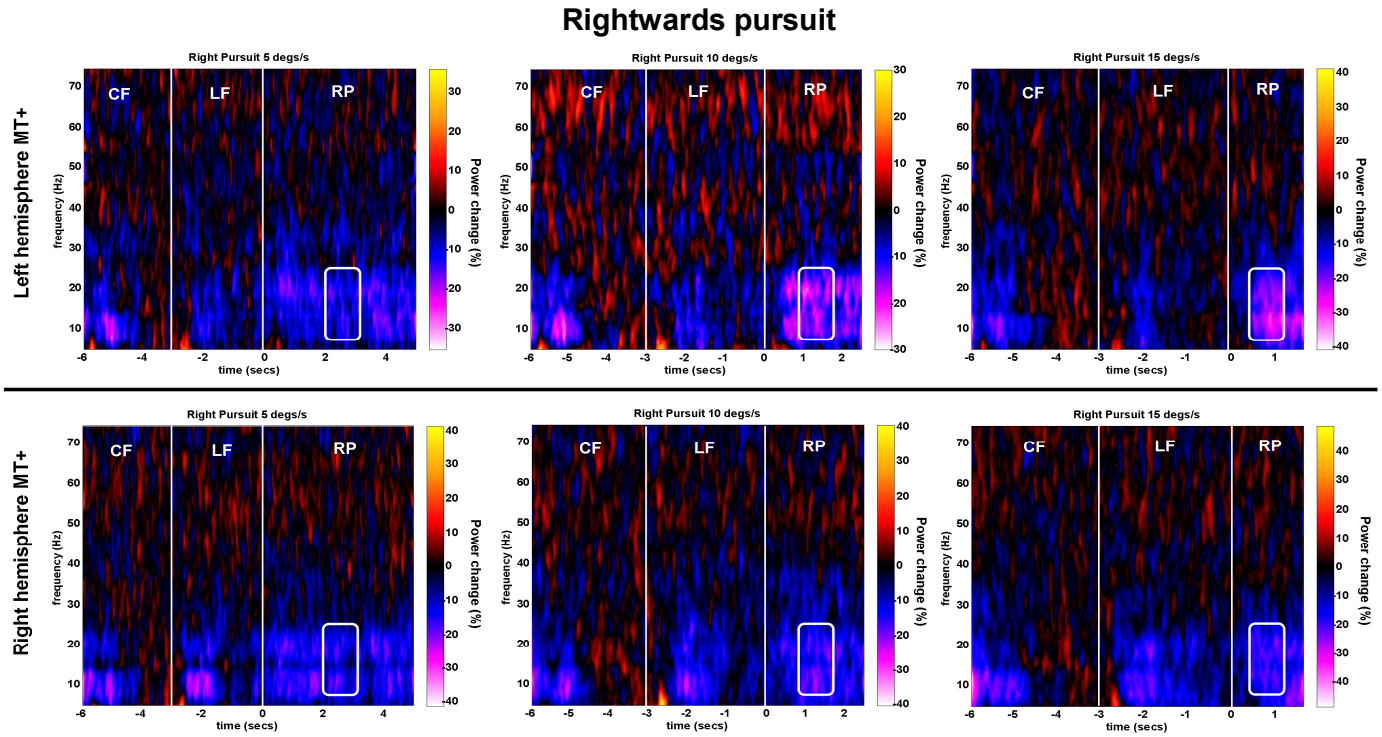

Figure 34. Grand-averaged time-frequency spectrograms from left and right MT+ during rightwards pursuit, for each velocity condition.

As above, except this time fixation was held at -12.5º eccentricity in the left hemifield (denoted by LF) following the central fixation baseline period, and then pursuit tracking was in the opposite direction at 5, 10, 15 and 20º/s (denoted by RP).

Grand-averaged time-frequency plots of the oscillatory changes in MT+ for each condition can be seen in Figure 33 and Figure 34. It is clear that for velocity conditions in both the left- (Figure 33) and rightwards direction (Figure 34) that smooth pursuit eye movements induce sustained low-frequency (5-25 Hz) suppression for the duration of object tracking (in the time window from 0 seconds onwards, and denoted by either LP or RP in the spectrograms) in MT+. This result appears consistent with findings reported in previous experimental chapters. Interestingly, there is also consistent suppression of the 5-25 Hz response in MT+ when the eyes are fixated and stationary in the left or right visual hemifield following saccadic eye movements to the eccentric fixation point (in the time window preceding the actual pursuit phase, denoted by either RF or LF on the spectrograms).

In the central fixation baseline period (the time window -6 to -3 seconds denoted by CF), there is 1-2 seconds of low-frequency suppression following the change in gaze proceeding termination of pursuit and subsequent saccadic eye movement to the central fixation point. This appears especially prominent in the alpha band, with an increased magnitude in the relative power decrease and often sustained for longer than the suppression during this period seen in the beta band. Following this, for approximately the last 1-2 seconds of central fixation (-5 to -3 seconds on the spectrogram), alpha and beta power returns to baseline levels.

Following the time-frequency analysis, the mean alpha (5-15 Hz) and beta (15-25 Hz) amplitude change in the central one second time window of the pursuit phase was extracted from each individual's spectral data and used to examine pursuit velocity modulation of the alpha and beta suppression from this region (denoted by the white box in the spectrograms).

3.3.3.4 Effect of eye velocity on low-frequency suppression

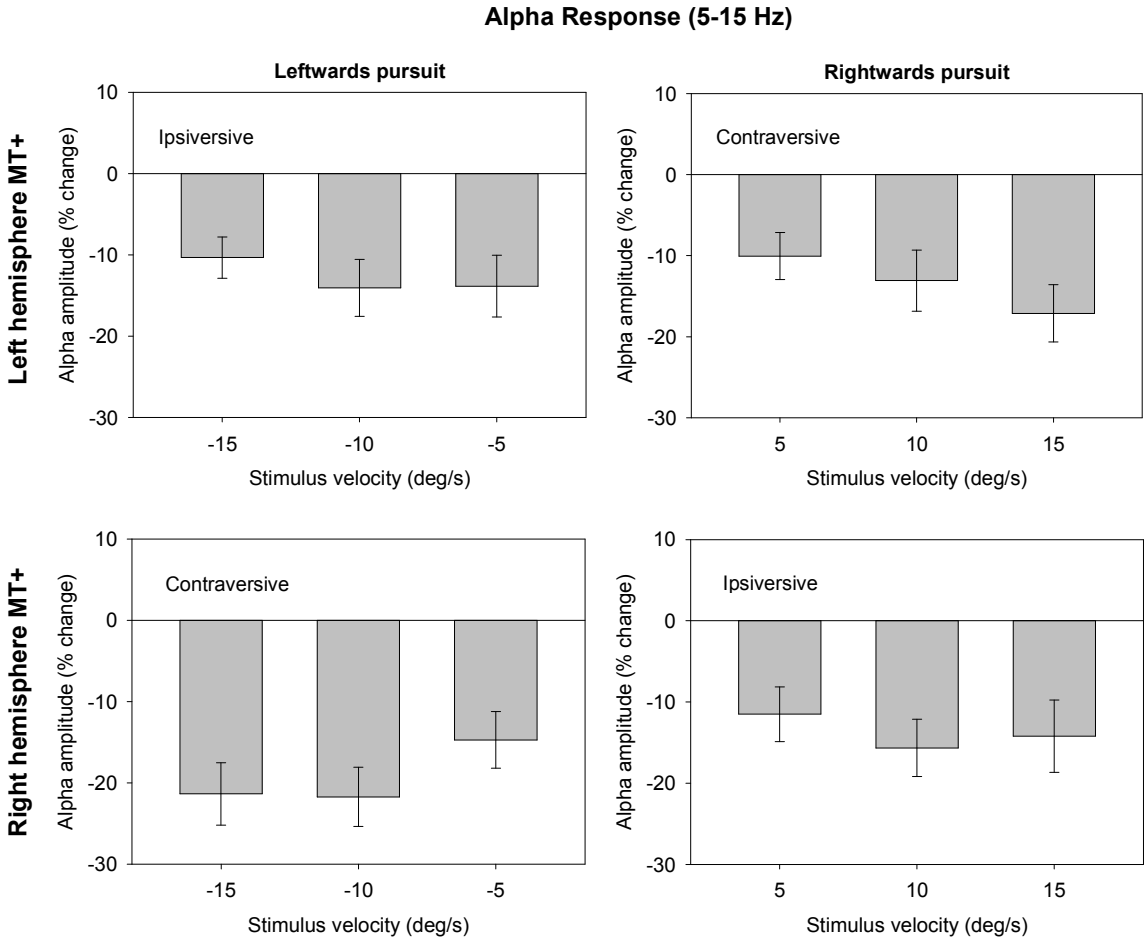

Figure 35. Graphs for the mean alpha response from both left and right MT+ for each of the stimulus velocity conditions in the left- and rightwards pursuit direction.
Negative alpha amplitude values indicate percentage power change during the pursuit condition compared to the baseline fixation condition. There was no main effect of stimulus velocity on the induced alpha response recorded from MT+.

Figure 35 depicts the mean alpha response for each stimulus velocities in left (top row of panels) and right (bottom row) MT+. For the 5-15 Hz response, a one-way Repeated Measures ANOVA was run on each of the hemispheres and pursuit directionality separately (however, it should be noted that this particular analysis technique does not take account of possible random effects; for more information see (Baayen, Davidson, & Bates, 2008)).

Results indicated there was no significant effect of stimulus velocity on the alpha amplitude change (all ANOVA tests $p > 0.05$).

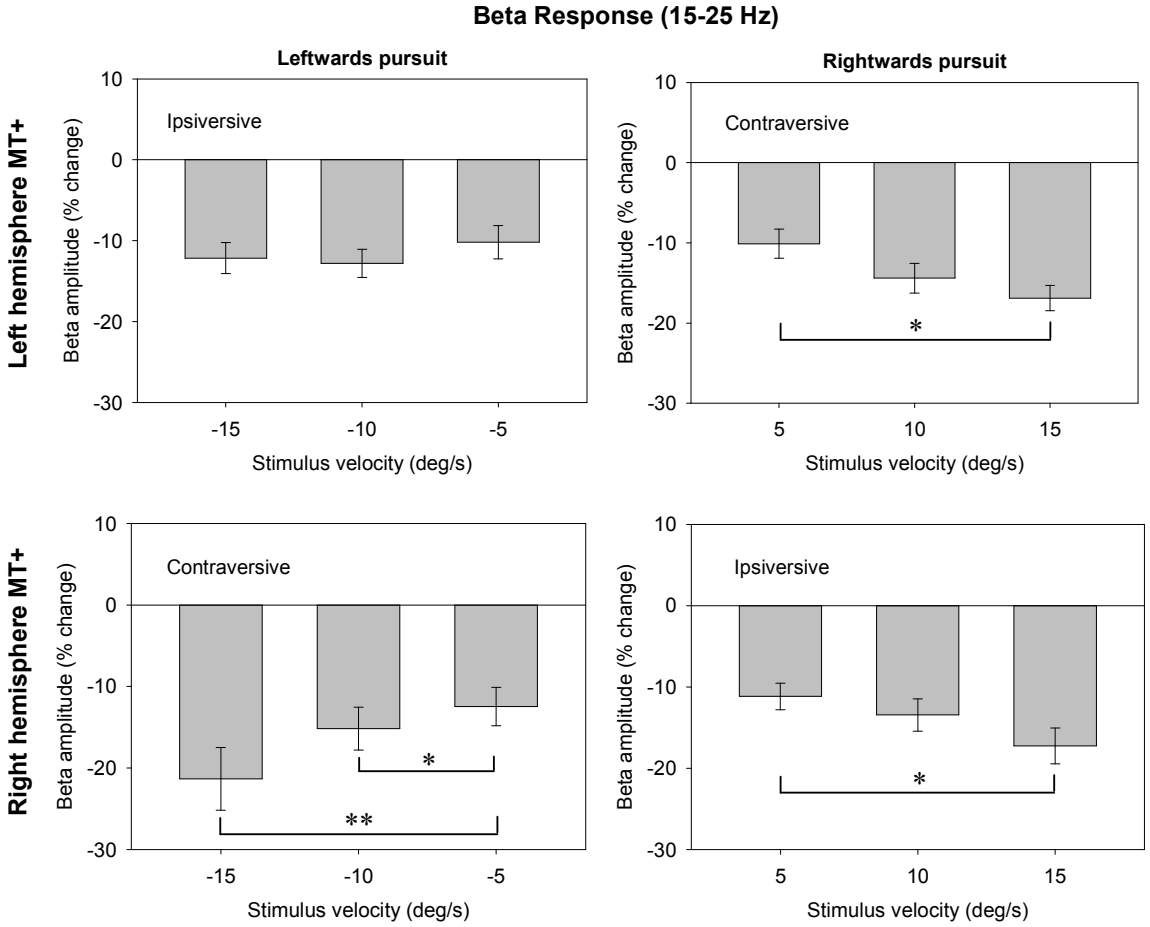

Figure 36. Graphs for the mean beta response from both left and right MT+ for each of the stimulus velocity conditions in the left- and rightwards pursuit direction.
Results from Repeated Measures ANOVA found a significant effect of stimulus velocity on the beta response in 3 of the 4 analyses, with what appears to be a general decrease in beta amplitude with increasing stimulus velocity (* = $p < 0.05$, ** = $p < 0.01$).

Figure 36 shows the mean beta amplitude for each of the stimulus velocity conditions, in both the leftwards and rightwards direction, in left (top row of panels) and right MT+ (bottom row of panels). Four separate one-way Repeated Measures ANOVA's were conducted to compare the mean induced beta amplitude change as a result of pursuit tracking at different stimulus velocities.

For the beta amplitude change from the left hemisphere during leftwards pursuit (top left panel), there was no significant difference in the mean induced beta response as a result of stimulus velocity ($p > 0.05$).

It was found that there was a significant effect of stimulus velocity on the beta amplitude measured from the left hemisphere during rightwards pursuit (top right panel, $F(2,32) = 4.39$, $p < 0.05$). Post-hoc comparisons using the Tukey HSD test indicated a significant difference between the beta response for the 5º/s ($M = -10.12$, $SD = 7.68$) and 15º/s ($M = -16.91$, $SD = 6.68$) conditions ($p < 0.05$). No significant differences were found between either the 5º/s and 10º/s conditions, or the 10º/s and 15º/s conditions, although once again there appeared to be a decrease in the mean beta amplitude with increasing stimulus velocity.

There was a significant effect of stimulus velocity on the induced beta response for leftwards pursuit in the right hemisphere (bottom left panel, $F(2,32) = 6.74$, $p < 0.01$). Post-hoc tests revealed a significant difference in beta amplitude for the -5º/s ($M = -12.46$, $SD = 10.28$) and -15º/s ($M = -21.33$, $SD = 15.83$) conditions ($p < 0.01$), and a significant difference in beta between the -10º/s ($M = -15.15$, $SD = 10.84$) and -15º/s ($M = -21.33$, $SD = 15.83$) conditions ($p < 0.05$). There was no significant difference in the beta response between the -5º/s and -10º/s conditions. Again, there appears to be a general trend towards decreasing amplitude with increasing stimulus velocity.

Finally, for the beta response from the right hemisphere during rightwards pursuit (bottom right panel), there was a significant effect of stimulus velocity on the magnitude of the beta amplitude change in MT+ ($F(2,31) = 3.862$, $p < 0.05$). Post-hoc comparisons using the Tukey HSD test indicated that the mean beta amplitude decrease for the 15º/s velocity condition ($M = -17.24$, $SD = 9.04$) was significantly different ($p < 0.05$) compared to the 5º/s velocity condition ($M = -11.14$, $SD = 6.73$). However, the beta response for 10º/s velocity

condition did not significantly differ from either the 5 or 15 °/s condition, although there appears to be a trend for decreasing beta amplitude changes with increasing stimulus velocity.

Overall, although there doesn't appear to be any velocity-specific changes in the oscillatory response as originally predicted, there does however appear to be a trend for a decrease in the beta power with increasing eye speed, irrespective of the direction of the pursuit eye movement. This would suggest that beta amplitude decreases might be linked to activity in these regions that are related to the processing of oculomotor and/or extraretinal eye movement signals coding for eye speed. A further set of analyses were performed to compare alpha and beta activity with changes in stimulus speed test whether there is a dependence of the oscillatory change stimulus speed. This was performed simply by reversing the sign of the leftwards stimulus velocity and collapsing the left- and rightwards data together, resulting in 4 tests (for both alpha and beta responses, and each hemisphere).

3.3.3.5 Effect of eye speed on low-frequency suppression

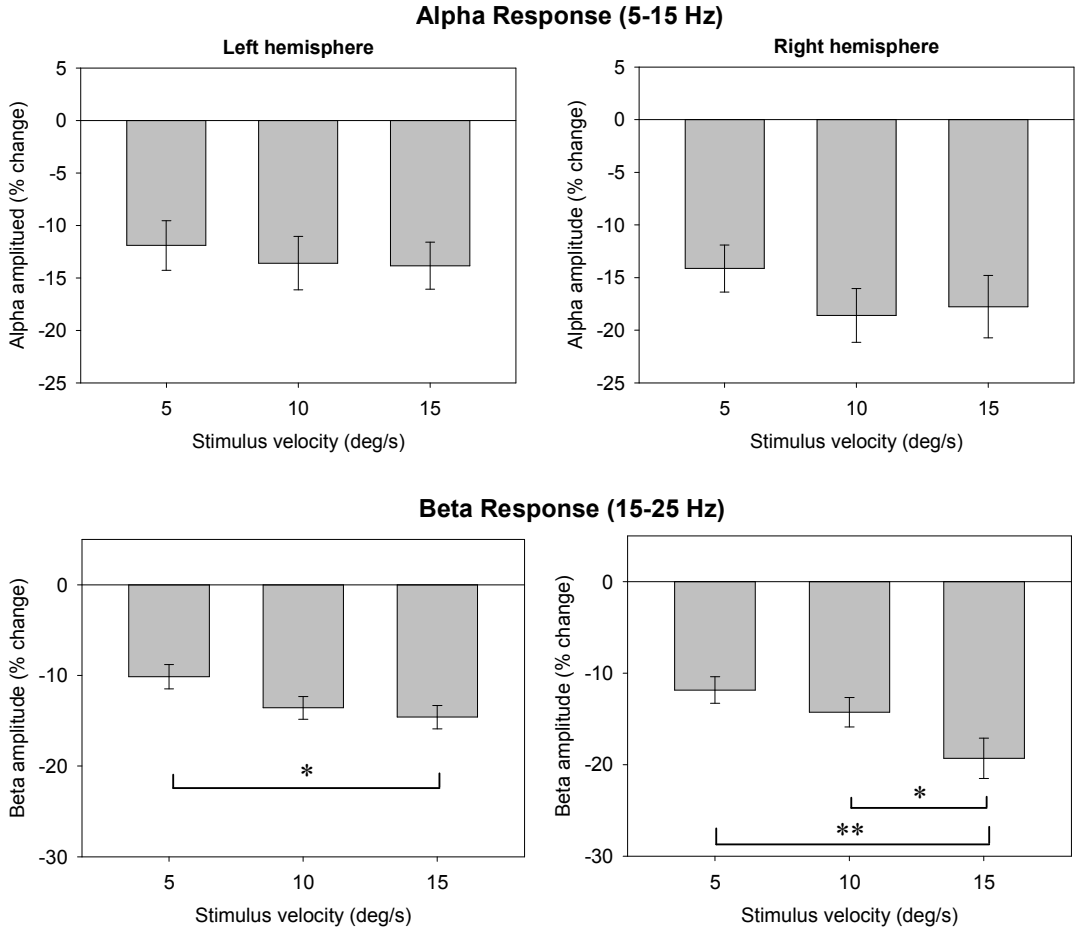

Figure 37. Graphs for the mean magnitude of alpha and beta suppression in both the left and right hemispheres at various pursuit speeds.

Figure 37 shows the mean alpha (top panels) and the beta (bottom panels) amplitudes for each eye speed condition, from both the left and right hemispheres. Repeated-measured ANOVA tests for the alpha response found there was no significant effect of eye speed on oscillatory amplitude in this frequency band in either the left or the right hemispheres (top panels, $p > 0.05$).

Conducting the same analysis on the beta amplitude change revealed a significant effect of eye speed on the beta response in the left hemisphere (bottom left panel, $F(2,65) = 4.73$, $p = 0.01$)). Post-hoc comparisons (Tukey HSD) found beta suppression in the 15º/s (M

= -10.15, SD = 7.95) condition was significantly greater than the 5º/s (M = -14.60, SD = 7.61) condition ($p = 0.015$), whilst there was no significant difference between either the 10º/s and 15 º/s conditions, or the 10º/s and 15º/s conditions.

For the right hemisphere MT+ beta response, there was a significant effect of eye speed on the amplitude change ($F(2,65) = 10.65$, $p < 0.001$), with post-hoc comparisons indicating a significant difference between the 5º/s (M = -11.84, SD = 8.69) and 15º/s (M = -19.29, SD = 12.87) conditions ($p < 0.001$). Additionally, there was also a significant difference between the 10º/s (M = -14.27, SD = 9.57) and 15º/s (M = -19.29, SD = 12.87) conditions ($p = 0.012$), but not the 5º/s (M = -11.84, SD = -8.69) and 10º/s (M = -14.27, SD = 9.57) conditions ($p > 0.05$). Therefore, this might suggest some functional distinction in the role of alpha and beta suppression in MT+ during pursuit.

3.3.3.6 Ipsi- versus contraversive pursuit

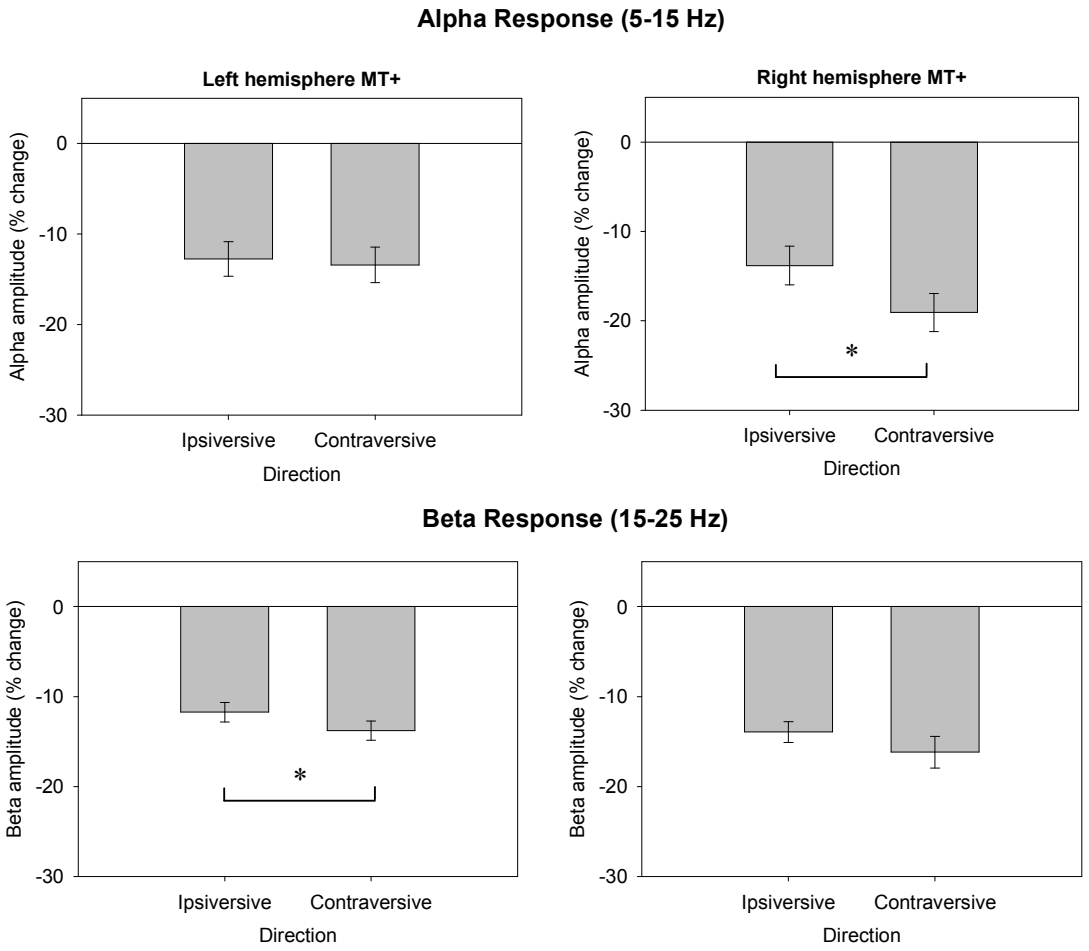

Figure 38. Mean alpha and beta suppression averaged across all velocities for ipsi- versus contraversive pursuit directions from left and right hemisphere MT+, with ±1 standard error bars.

As mentioned in the Overview of Experiment 4, it has been shown in the animal literature that the overwhelming majority of neurons in MST that display a purely pursuit-related response have a preferred directionality for ipsiversive eye movements. In other words, these MST neurons appear to code for the direction of pursuit towards the hemisphere from which the recording was taking place. As previous research suggests the magnitude of the alpha and beta response correlates highly with spike rate function, therefore, the relative

magnitude of the recorded alpha and beta activity decreases from MT+ might show a direction-bias and be greater for pursuit in the ipsiversive direction.

To test this, the alpha and beta amplitude change from each hemisphere induced during all stimulus speeds was quantified based on the relative directionality of the pursuit movement, irrespective of stimulus velocity. Figure 38 shows the mean alpha (top panels) and beta (bottom panels) from left and right MT+ during pursuit for ipsi- and contraversive directions, averaged over all velocities. Alpha suppression from the left hemisphere for pursuit in the ipsiversive (M = -12.76, SD = 13.73) versus contraversive direction (M = -13.42, SD = 14.37) showed no significant effect for relative direction of pursuit (top left panel, $t(49) = 0.375$, $p > 0.05$). From the right hemisphere, (top right panel), there was a significant effect of directionality on the alpha suppression (ipsiversive mean = -13.83, SD = 15.61, contraversive mean = -19.08, SD = 15.38, $t(49) = -2.935$, $p < 0.01$).

For the beta response, there was a significant difference between beta suppression in the left hemisphere for ipsi- (M = -11.73, SD = 7.83) versus contraversive (M = -13.80, SD = 7.73) pursuit directions (bottom left panel, $t(49) = 2.26$, $p < 0.05$). No such effect was found in the right hemisphere (bottom right panel, ipsiversive mean = -13.93, SD = 8.36, contraversive mean = -16.17, SD = 12.8, $t(49) = -1.33$, $p > 0.05$).

3.3.4 Conclusion

In this experiment, the link between alpha and beta suppression in MT+ and pursuit velocity was explored. It was predicted that there would be a link between low-frequency suppression and eye velocity, although the current data suggests no decisive connection between the two (however, there was slightly greater suppression for contraversive pursuit directions, although the lack of significance in all these tests provide no decisive evidence of this). Despite the lack of specific relationship between eye velocity and oscillatory activity, a significant effect of eye speed on beta activity was found, whereas there was no effect of eye speed on alpha amplitude. By way of dissociation, this suggests that suppression of the beta rhythm plays a distinct role in pursuit, reflecting a fundamental aspect of the eye movement, while alpha suppression does not and probably signifies either an 'inhibitory gating' mechanism or general engagement of other superordinate functions such as visuo-spatial attention.

It is possible that beta suppression is the manifestation of underlying microscopic neuronal activity either involved in oculomotor behaviour (perhaps contributing to pursuit maintenance or coordinate transforms), or it could indicate the integration of extraretinal information used in spatial stability during ego-motion. It is not possible to draw a definitive conclusion from this experiment on either of these issues, as this task was performed in the presence of visual feedback to maintain pursuit, and could therefore be the result of retinal stimulation used in closed-loop pursuit. Given this, it is not entirely possible to isolate extraretinal components of a reference signal without looking at the neuronal correlates of pursuit in absence of any visual input (thereby fully isolating nonretinal mechanisms). Additionally, without an objective measure of perceptual stability using psychophysical procedures, it is also not possible to conclude that these signals are used in this process either.

However, this experiment does suggest a fundamental role of beta suppression in MT+ during ongoing pursuit, whether it be in the generation of oculomotor signals and coordinate transforms, or the integration of an internally generated reference signal that codes eye speed estimates.

3.3.4.1 Low frequency suppression during peripheral gaze fixation

During gaze fixation at the farther eccentricities of the visual hemifield following central fixation, there appears to be evidence of a largely sustained low-frequency suppression observed in the grand-averaged spectral response from MT+. This result is interesting because during this time, the eyes are stationary and there is only a transient case of retinal motion as a result of the gaze change. There are a number of possible reasons for this. It could represent an response elicited by the appearance of the dot on the retina; a saccade-related response to do with planning and execution of the movement, and subsequent retinal motion induced by the eye movement; the recruitment of higher-level superordinate processes (such as covert shifts of visuo-spatial attention); activity of spatiotopic neurons that code for eye position; or a combination of all these neuronal processes.

First, the sustained oscillatory response evident in the spectrogram during gaze change and the following period are likely not to reflect a transient evoked response elicited by the appearance of the dot. It is well known that a large portion of neurons in retinotopic MT+ are sensitivity to visual motion, with a preferred speed and direction (Maunsell & Essen, 1983b). Therefore, the appearance of a faint, low-contrast stimulus with low-frequency content is unlikely to evoke a measurable macroscopic response in extra-striate regions.

Second, saccadic eye movements are transient shifts of eye direction, and during this motion, the dot will move across the retina. Visual motion processing occurs in MT+, but the motion of the dot during the saccadic eye movements is not processed by visual motion sensitive neurons, as a result of what is known as saccadic suppression (Thiele, Henning,

Kubischik, & Hoffmanndagger, 2002). Neurons tuned to a particular speed and direction are silenced during this time, and any transient processing that might occur is unlikely to result in sustained suppression for the entire excursive gaze fixation.

Third, it has been shown that alpha and beta amplitude decreases over visual striate and visual association extra-striate cortices might reflect the allocation and engagement of visuo-spatial attention and anticipatory processing of any predictable sensory change and incoming information (Worden, et al., 2000; Yamagishia, et al., 2008). In other words, the alpha and beta oscillatory amplitude decreases occur over the area of cortex known to be active when covert visuo-spatial attention mechanisms are engaged, and this effect is enhanced in this region of the brain by anticipatory signals awaiting an impending sensory change (the onset of the stimulus motion, which was not jittered and therefore predictable in its onset). Therefore, it is entirely possible the sustained alpha and beta suppression witnessed during gaze fixation reflects an "inhibitory filter mechanism" (Jensen & Mazaheri, 2010) that helps focus attention (or perhaps attention itself modulates this change; causality cannot be implied in this case) and prevents distracting stimuli from interfering with task-related processing, given that the onset of the motion stimulus can be anticipated.

Finally, it could be possible that the alpha-beta suppression during this time reflects the macroscopic signature of neuronal activity in MT+ from neurons that code for eye position (Ilg & Thier, 2003). Neurons that show a propensity for eye position sensitivity code for gaze direction in the density of their spike-rates, and this could result in the induced and sustained alpha-beta modulation we see here, given that we know increased spike-rate correlates highly with the magnitude of the 5-25 Hz neuronal suppression (Mukamel, et al., 2005).

Therefore, it seems likely that the oscillatory response observed in MT+ during excursive gaze fixation could represent either the allocation of selective visuo-spatial attention and

anticipatory priming of the brain for stimulus motion onset, the macroscopic signature of neuronal activity reflecting eye position sensitivity, or a combination of both these processes.

3.4 Discussion

In this chapter, two experiments were presented that aimed to establish a more conclusive link between oscillatory suppression in MT+ during pursuit, and whether this modulation reflects eye position or velocity. The position-dependence of this signal was explicitly tested in Experiment 3 using an excursive pursuit cycle paradigm (whereby eye movements remained identical other than the eccentricity at which smooth pursuit was engaged). No difference in the amplitude of the alpha or beta rhythm was found, being otherwise indistinguishable regardless of where in head-centred space pursuit was performed. This suggests oscillatory suppression in MT+ induced by pursuit was not directly related to head-centred eye position. However, activity from neurons sensitive to eye position is also likely to contribute to the MEG signal changes measured here. These results suggest the alpha and beta rhythm was most likely modulated by some other aspect of the eye movement, and based on existing literature and the results of the Experiment 3, it was proposed that this dependence was likely to be on eye velocity.

In Experiment 4, this was examined by utilising a step-ramp paradigm similar to that used in other studies (Ilg & Thier, 2003; Nagel, et al., 2008), and test whether the neuronal response characteristics, defined as oscillatory amplitude changes, reflect a velocity-based signal. Additionally, the data was examined further to see whether a response for a preferred direction could be extracted from the macroscopic signature, given that animal research suggests the majority of neurons in MST that display a pursuit-related response code for ipsiversive pursuit (Ilg & Thier, 2003).

Consistent beta suppression was found over extra-striate cortices for all stimulus conditions and a significant effect of pursuit eye speed on the magnitude of the beta power decrease, with increasing suppression noted with increasing eye speed. Furthermore, no effect of eye speed on alpha magnitude in MT+ was found. By dissociation, this suggests there

might be some functionally distinct role that these frequency bands play in the maintenance of pursuit and the integration of extraretinal eye movement signals. In addition, and although this was not an explicit aim of this experiment, there was evidence of alpha and beta suppression when the eyes were in the left or right hemifield. Finally, any sign of a directional bias in these responses was tested for, irrespective of pursuit velocity, and whilst there appears to a slightly greater increase in oscillatory suppression during contraversive eye movements, no consistent significant differences were found in the magnitude of these changes.

The findings presented here do not conform to our original predictions regarding a velocity-sensitive bias in the alpha and beta suppression for ipsiversive pursuit directionality (relative to the recording site). Given these results, the tentative proposition is made that the relationship between beta activity and eye speed suggests it has some functionally mechanistic role in the smooth pursuit. Specifically, it appears that the brain may engage in active beta band suppression in MT+ during pursuit, which could either reflect the generation of oculomotor signals for pursuit maintenance in the presence of ongoing visual feedback and/or the integration of extraretinal signals, which are used as a mechanism in maintaining perceptual stability and estimating target motion in head-centred coordinates. Conversely and by dissociation, it is also proposed that the lack of any clear relationship between alpha activity and the eye movement suggests its suppression mediates, or is perhaps in turn mediated by, some other sensory or cognitive process taking place in this area associated with deliberate pursuit. For example, it could be due to superordinate processes like engagement in visuo-spatial attention implicated in intentional pursuit eye movements (Lovejoy, et al., 2009; Ono & Mustari, 2006) or has an gating mechanism that facilitates task processing (Jensen & Mazaheri, 2010). Furthermore, the recorded alpha and beta suppression when the eyes were moved to eccentric portions of space could reflect the activity of position-sensitive neurons.

In conclusion, Experiment 3 was designed to examine whether there exists a relationship between eye velocity and alpha and beta activity. Contrary to initial predictions, it was found that there was no specific relationship between eye velocity and the magnitude of the alpha and beta amplitude, or any clear bias in the directionality of the response, but there was an effect of eye speed on the beta amplitude changes in MT+. Furthermore, no such relationship between alpha magnitude and eye speed was found, which taken together suggests two separate and perhaps distinct functional roles for suppression of these cortical rhythms in the integration of extraretinal signals into MT+. On this basis, it is proposed that beta suppression perhaps reflects integration and processing of nonretinal eye movement estimates as one of a number of mechanisms used in perceptual stability, and alpha suppression is perhaps linked to more general attentional mechanisms or 'inhibitory gating' of task irrelevant information.

4 Chapter 4 – The neuronal substrates of the extraretinal and retinal motion aftereffect

4.1 Abstract

The motion aftereffect (MAE) is a visual illusion where a stationary test stimulus is perceived to move in the opposite direction to that of sustained retinal motion following an adaptation period. It has also been shown that oculomotor adaptation induced through repetitive unidirectional smooth pursuit eye movements also gives rise to a motion aftereffect known as the extraretinal motion aftereffect (ERMAE). It has been proposed by Freeman & Sumnall (2005) that the ERMAE results in part from adaptation of pursuit-sensitive neurons in the human homologue of MST. Furthermore, it was observed in Experiment 1, 3 and 4 that there was evidence of oscillatory power decreases in the baseline period upon cessation of repetitive pursuit, which might reflect the cortical substrates of oculomotor adaptation. In Experiment 5, the role of alpha and beta activity underlying the perception of illusory motion as a result of pursuit adaptation was explored. It was predicted that the duration of the sustained oscillatory changes in areas of cortex thought to underlie pursuit would correlate with the subjective percept of the ERMAE, particularly MT+. A complementary experiment was also designed to examine the 'classical' retinal motion aftereffect (RMAE) to further elucidate the role of alpha and beta oscillatory suppression during illusory motion. In the ERMAE experiment, oculomotor adaptation was induced in observers by tracking an upwards moving stimulus in the dark (a repetitive sawtooth pattern at 12º/s for 12 seconds), followed by a 12 second test phase which comprised of a stationary central test stimulus. During this time, participants were required to report the duration and direction of any resultant ERMAE. In the RMAE experiment, observers fixate a stationary central point, whilst a rotating random dot field adapted motion-processing regions for 12 seconds. This

was then followed by a 12 second test phase comprising of a stationary random dot field during which time observers report the direction and duration of the RMAE. Results from the ERMAE experiment show sustained low-frequency suppression in areas FEF, IPS and MT+ during eye movement adaption. The main finding from this experiment was that beta activity in MT+ during the eye movements significantly predicts the duration of the resultant ERMAE. In other words, greater beta suppression during oculomotor adaptation appears to modulate the duration of the subsequent illusory motion when viewing a stationary test stimulus. In the RMAE experiment, no such correlation was found, but it was noted that sustained alpha and beta suppression appears to persist for the duration of the reported motion aftereffect. Given the results from the ERMAE experiment and studies reported in previous chapters of this thesis, it appears that suppression of beta oscillations plays a significant functional role in oculomotor control, the integration of extraretinal eye movement signals and motion processing in MT+.

4.2 Introduction

Adapting to a moving stimulus gives rise to the perception of illusory motion when viewing a subsequent stationary test stimulus, which is known as the motion aftereffect (MAE). Early theoretical models of the motion aftereffect were based on the idea of neuronal 'fatigue'. This model posits that persistent motion adapts neurons coding for a specific speed and direction, which results in a subsequent imbalance in baseline activity for neurons coding opposing directions of motion (Anstis, Verstraten, & Mather, 1998). This imbalance in activity, which is greater for the non-adapted neurons, it thought to result in the perception of illusory motion in the direction opposite to that of the adapter. However, the neuronal fatigue model for the motion aftereffect fails to account for the phenomenon known as 'storage'. Following adaptation, the observer is placed in total darkness for some time, where no MAE is observed; however, when a stationary stimulus then reappears, the illusion is still there. If the neuronal fatigue model held true, then one might expect the neurons that were adapted to have recovered to during the blank storage interval and no MAE to be perceived upon being presented with a stimulus.

This has led some authors to propose a number of alternative theoretical notions to explain the MAE, including that of 'error correction' and 'coding optimization' (Anstis, et al., 1998). In the 'error correction' explanation, the gain of motion-sensitive cells tuned for particular strengths and direction of movement is set by the relative strength of "actual and ideal time-averaged activity" in the motion system. Veridical perception of motion is maintained in normal viewing conditions but sustained input in any one direction of motion would be misinterpreted for a change in the gain of that input channel. This change in relative time-averaged activity would lead to a reduction in this channels output and result in the perception of an MAE in the direction opposing that of the sustained motion (Ullman & Schechtman, 1982).

A second explanation for the MAE is known as 'coding optimization'. In this model, the MAE is thought to result from residual lateral inhibition following sustained large patterns of motion that covered the receptive fields of many neurons. Here, the large patterns of motion will cover a portion of the visual field coded by the receptive fields of numerous neurons that will in turn inhibit activity in neurons with adjacent receptive fields. This sustained motion will ultimately lead to residual bilateral inhibition in these neurons when the sustained motion stops and a stationary field appears, and so a reversed pattern of motion is perceived (Ullman & Schechtman, 1982).

Despite these theoretical explanations of the MAE, there remains little consensus on the meaning of experimental results from the neurophysiological and imaging literature in humans. Regarding neuroimaging studies of the MAE, a number have found correlations between the MT+ BOLD signal and the perception of motion (Culham et al., 1999; He, Cohen, & Hu, 1998), as well as one MEG study reporting a correlation between the magnitude of gamma activity localised to extrastriate regions and the size of the motion aftereffect (Tikhonov, Handel, Haarmeier, Lutzenberger, & Thier, 2007). These results suggest activity in MT+, measured as a function of BOLD and MEG signal changes, reflects neuronal changes implicated in the MAE and that this is the principal site responsible for the motion aftereffect.

Furthermore, it has been found that the motion aftereffect can also been induced through oculomotor adaptation by repetitive pursuit eye movements in the absence of strong retinal motion (Chaudhuri, 1991a; Freeman & Sumnall, 2005; Freeman, Sumnall, & Snowden, 2003). Freeman, Sumnall & Snowden (2003) termed this the extraretinal MAE (which will referred to as ERMAE from this point onwards, to distinguish between a motion aftereffect induced as a result of extraretinal eye movement adaptation, and that of 'classical' retinal motion adaptation, which will be referred to as RMAE). Following eye movement adaptation,

a stationary test stimulus under fixation is perceived to move in the opposite direction to that of the adapting eye movement. Some early researchers proposed that this was due to motion induction following adaptation of motion sensitive neurons in the peripheral visual field (Mack et al., 1987; Morgan, Ward, & Brussell, 1976). In later experiments, however, it was found that the illusion remains intact when eliminating any peripheral background motion processing during pursuit in complete darkness (Chaudhuri, 1990, 1991a). Therefore, it has been proposed by Freeman & Sumnall (2005) that oculomotor adaptation affects neuronal response characteristics in multiple regions of the brain (both higher- and lower level), and that the ERMAE is perceived for a number of reasons. They suggest that this is due in part to afternystagmus suppression and the adaptation of pursuit-sensitive neurons in the human homologue of MST that receives extra-retinal eye movement signals during the eye movement (Freeman & Sumnall, 2005).

Oculomotor adaptation and the resultant ERMAE provides an additional means of examining the integration and processing of extraretinal signals in MT+. On this basis, the main aim of Experiment 5 was to have observers perform repetitive eye movements and explore the neurophysiological and perceptual consequences of oculomotor adaption on visual perception and the subsequent illusory motion given the lack of previous imaging literature on the subject. Additionally, there has only been one known study on the MEG correlates of the motion aftereffect (Tikhonov, et al., 2004), where it was found that the magnitude of the high-frequency gamma response correlated with the magnitude of the motion percept following adaptation. The authors propose that this suggests gamma activity reflects a decrease in response inhibition and a corresponding increase in neuronal synchronisation for groups of neurons coding similar preferred directions of motion (opposite to that of the adapter). Thus, it seems possible that oscillatory changes in MT+ play a key role in the neuronal underpinnings of motion perception. Given the lack of literature on the

subject, it seemed reasonable to expand on the previous psychophysical ERMAE literature and use MEG to probe the neuronal correlates of extraretinal activity in MT+ as a result of pursuit adaptation, as well as the physiological mechanisms that underlie resultant changes in visual perception. In addition to this, a further experiment was designed to explore the retinal motion aftereffect (Experiment 6; RMAE) as to compare the oscillatory correlates associated with a passive perceptual aftereffect with those induced through an active motor task (Experiment 5; ERMAE).

Given that a number of studies show a correlation between BOLD in MT+ and the percept of illusory motion (Culham, et al., 1999; He, et al., 1998), and there is an established link between BOLD and beta activity (Brookes, et al., 2005; Singh, et al., 2002; Stevenson, Brookes, & Morris, 2011), it was hypothesised that there would be a link between the subjective report duration of the motion aftereffect and oscillatory changes in motion processing regions. Specifically, it was predicted that there would be a correlation between the duration of the motion aftereffect and the duration of the amplitude in beta activity in regions thought to underlie pursuit eye movements in Experiment 5, in particular the MT+ region. Furthermore, it was also predicted that a similar relationship would exist for the duration of oscillatory changes in MT+ and perception of illusory motion in Experiment 6. Taken together, this would suggest cortical oscillations in this area reflect adaptation of motion-sensitive neurons and that this activity in turn mediates aspects of the illusory motion.

4.3 Method

4.3.1 Experiment 5 – The extraretinal motion aftereffect

4.3.1.1 Participants

Seventeen healthy participants (ten females, mean age = 23 years) completed Experiment 5 examining the extraretinal motion aftereffect. All participants were naïve as to the purpose of the experiment.

4.3.1.2 Design and Procedure

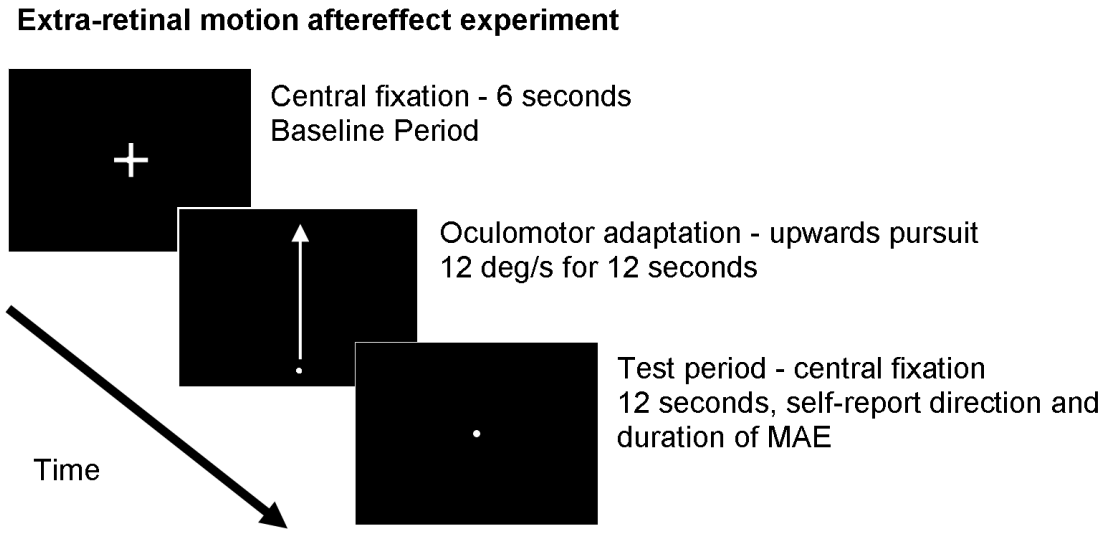

Figure 39. Experimental protocol for Experiment 5, oculomotor adaptation and the extraretinal motion aftereffect.
Participants fixate a central crosshair for six seconds (baseline period), then pursue an upwardly moving dot in sawtooth fashion at 12º/s for 1.8 seconds (22º visual angle), whereby the dot disappears for 0.2 seconds before reappearing at the base of the screen. The pursuit adaptation period is continued for 6 cycles (12 seconds in total). Following eye movement, a stationary central test appears during which time participants report the duration and direction of the subsequent ERMAE illusion.

Figure 39 details the experimental protocol for the extraretinal motion aftereffect study. Following a 6 second baseline period, comprising a stationary central fixation target, the participants adapted the oculomotor system by pursuing an upwardly moving stimulus in

a sawtooth fashion at 12º/s for 1.8 seconds, covering a distance of 22º visual angle. The dot then briefly disappeared (200 msec), during which time the participants were instructed to make an anticipatory saccade to the bottom of the screen in time for the next pursuit phase. The momentary disappearance of the moving target was employed to minimise any retinal motion and subsequent aftereffect resulting from such motion that might have been induced during a saccade downwards to track the reappearing stimulus. The target then reappeared and the cycle was repeated, 6 times in each trial, given 12 seconds of oculomotor adaptation in all, which was continued for 40 trials in total. Upwards pursuit was chosen as it has been shown to elicit the strongest percept of illusory motion following adaptation (Chaudhuri, 1991b; Freeman & Sumnall, 2005). Therefore, it might follow that this produces the greater change in the alpha and beta frequency bands.

Following this, a stationary test stimulus appeared in the centre of the screen, during which time the participants were instructed to report the direction and duration of any perceived ERMAE upon decay and eventual cessation of the illusion using a 5-button MEG-compatible response box using their left hand. Participants were given three options in their response and instructed to respond appropriately when the dot appeared to stop moving, either by reporting no perception of an ERMAE, an upwards illusory motion or a downwards ERMAE. It was decided to use imaging data from the ipsilateral (left) hemisphere relative to the response limb location so as to minimise the influence of any activity directly related to motor commands generated in pushing the button box. Whilst this is no guarantee of success, given that it has been shown unimanual motor tasks generate bilateral suppression in motor areas (Hamandi, Singh, & Muthukumaraswamy, 2011), the greatest activity due to the preparation and execution of a motor command should be predominantly confined to the contralateral side of the limb movement. Therefore, any influence due to the preparation and execution of the unimanual motor command, and not oculomotor adaptation, should be

sufficiently attenuated, at least within the limits of the technique, as the SAM source localisation should separate out these components.

Only trials on which a downwards ERMAE was induced and reported were included in the imaging analysis, with all other trials, either classified as no ERMAE or upwards ERMAE, being omitted from the final analysis. Therefore, we can be confident the imaging data presented reflects the cortical substrates that reflect oculomotor adaptation and subserve the ERMAE illusion, during pursuit adaptation and/or during the subsequent perceptual effect. Additional exclusion criteria included the omission of those participants that reported a downwards ERMAE on <50% of trials, so as to maintain an acceptable SNR in the MEG data and those participants who head motion exceeds that of the 5mm movement threshold during data acquisition. In addition to this, it was found that a number of participants were making eye blinks that were time-locked to the cessation of the MAE, and these participants were also excluded from further examination. This left 10 participants of the 17 in total with satisfactory data for the remaining MEG analysis. Of these 10 participants, an MAE was reported on 85.8% of trials (~34 of 40 trials).

4.3.2 Experiment 6 – The retinal motion aftereffect

4.3.2.1 Participants

Thirteen healthy participants (six females, mean age = 23 years) completed Experiment 6 looking at the retinal motion aftereffect. All participants were naïve as to the purpose of the experiment.

4.3.2.2 Design and Procedure

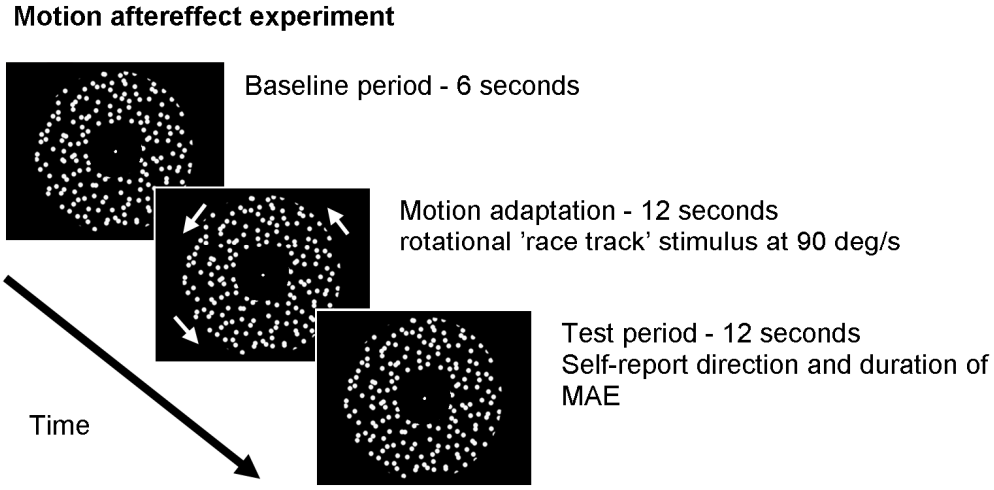

Figure 40. Experimental protocol for Experiment 6, examining retinal motion adaptation and the 'classical' motion aftereffect.
Participants fixate a central fixation point for 6 seconds (baseline period), then adapt to a rotating stimulus comprised of a random-dot field presented in an annulus (adaptation phase). The stimulus rotates in the anti-clockwise direction at an angular velocity of 90º/s for 12 seconds. Following the adaptation phase, participants then view a stationary test comprised of a random-dot field with the same dimensions as that viewed in the adaptation phase, during which time participants report the duration and direction of the subsequent RMAE illusion.

Figure 40 details the experimental protocol for the retinal motion aftereffect study. Participants fixate a central fixation dot for 6 seconds (baseline period), which is surrounded by a stationary random-dot field presented in an annulus. Following this, participants were instructed to maintain fixation of the central target at all times whilst the random-dot field rotates in an anti-clockwise direction at an angular velocity of 90º/s for 12 seconds, completing three rotations, adapting the retinal motion system. There were a total of 40 trials. In Experiment 5, an upwards pursuit eye movement was used to adapt the oculomotor system as this has been found to generate a particularly strong ERMAE (Freeman, et al., 2003).

Given this, it seemed logical to use a stimulus motion for Experiment 6 that also generates a strong retinal MAE, in the likelihood that this would also correspond to a greater change in alpha and beta rhythms in the MEG data. It has been shown that complex motions

comprised of rotation and radial components elicit a stronger MAE (defined by both magnitude and duration) than translations (Bex, Metha, & Makous, 1999). Furthermore, it has been shown using MEG that a region in the MT+ complex (termed by the authors hMSTs, with the *s* denoting 'spiral-space') displays selective responses to complex spiral motion over translational patterns of motion (Holliday & Meese, 2008). Therefore, we can assume that using such a pattern of adapting motion is likely to generate the greatest MAE and elicit responses in the putative MST region of the MT+ complex. Additionally, using complex motions such rotation or radial patterns would also minimise the likelihood of generating any reflexive eye movements when compared to translational patterns of motion, therefore it seemed reasonable to use a rotating stimulus for adaptation.

Following this, the stimulus stopped moving and remained stationary for 12 seconds (known as the test period), the stimulus maintaining the same dimensions as the stimulus in the baseline period. During this time, participants were once again instructed to report the direction and duration of any perceived MAE upon decay and eventual cessation of the illusion. Using their left hand and a 5-button MEG-compatible response box, participants were given three options and were instructed to respond appropriately, either by reporting no percept of a motion aftereffect, a clockwise illusory motion or an anti-clockwise motion aftereffect. As in Experiment 5 (ERMAE), only cortical responses from the left hemisphere were considered.

Only trials on which a clockwise motion aftereffect was induced and reported were included in the imaging analysis, with all other trials omitted from the final results. As before, the same exclusion criteria were enforced with one participant excluded due to reporting a motion aftereffect on less than 50% of trials. This resulted in the exclusion of one participant, leaving 12 datasets for use in the later neuromagnetic analysis. Of those 12 participants, 84.1% of trials contained a MAE and were used in the MEG analysis.

4.3.3 Data analysis

Peak coordinates for activation in the specified frequency band in the SAM images were visualised using mri3dX (Singh, 2009) and chosen on the basis of their locality within each of the three designated regions of cortex in Experiment 5 (ERMAE) and MT+ in extra-striate cortex for Experiment 6 (RMAE). For Experiment 5, the percentage change in oscillatory amplitude during the active period (pursuit adaptation) was baselined against the 0-6 second passive period (central fixation). For Experiment 6, the same criteria were also employed.

4.4 Results

4.4.1 Behavioural data

4.4.1.1 Eye movements

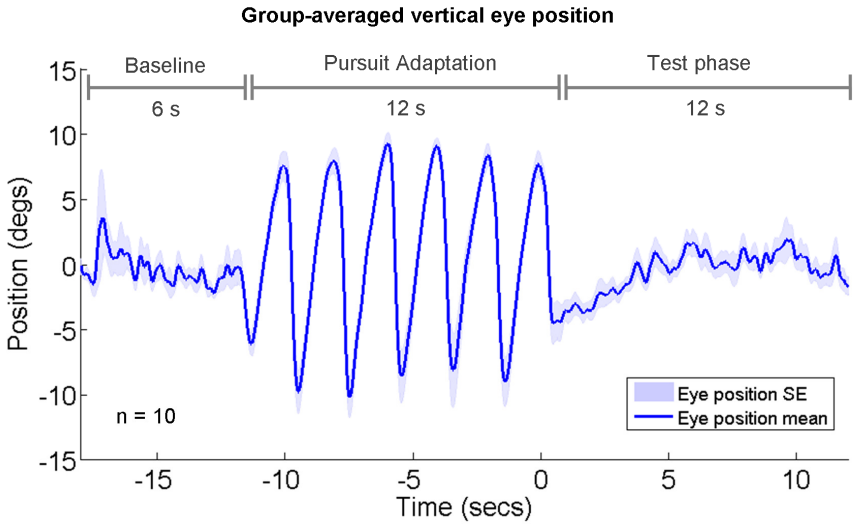

Figure 41. Group-averaged vertical eye position trace for Experiment 5.
Participants fixate the central stimulus in the baseline period, and then track a vertically moving stimulus at 12 degs/s for 12 seconds in a sawtooth fashion. Following this, participants fixate a central test stimulus and report the duration of the ERMAE.

Figure 41 shows the group-averaged vertical eye movement (in blue, with shaded standard error bars) in Experiment 5. This data is for the 10 participants who were included in

the final analysis after the exclusion criteria were enforced. Observers were on average able to accurately track the target dot during the 1.8 seconds of upwards pursuit eye movement in the adaptation period (mean gain = 1.005, SD = 0.149), although there was some variability in their performance (minimum = 0.802, maximum = 1.330, range = 0.528).

This suggests there was some element of retinal motion as a result of non-optimal pursuit during the adaptation period. Additionally, it appeared that there was a consistent overshoot of the target dot when making a downwards saccade to the central stimulus in the test period, with evidence of a slow upwards of the eyes to correct for this.

4.4.1.2 Comparing the extraretinal and retinal MAE duration

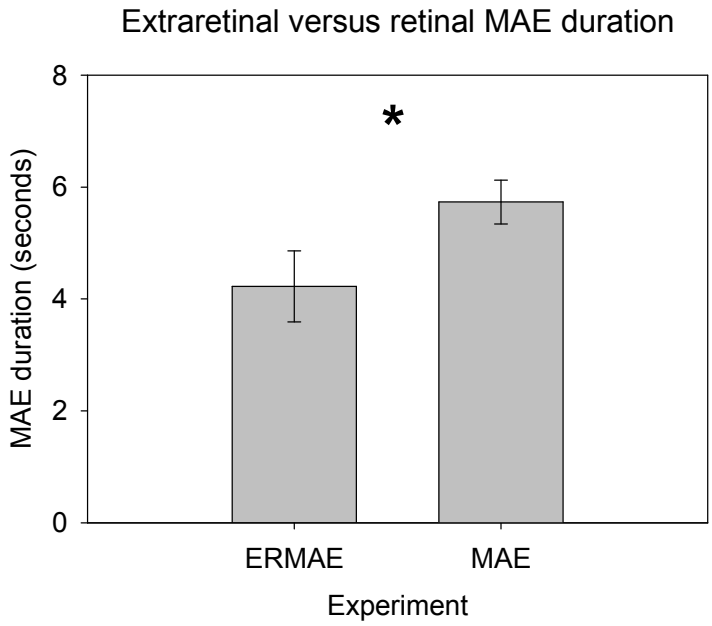

Figure 42. Mean duration judgements for the perceptual motion aftereffect in the extraretinal and retinal motion aftereffect experiments.
Bar graph to show group averaged mean duration reported for the motion aftereffect, with ±1 standard error bars (* $p < 0.05$).

Figure 42 shows the duration judgements for the motion aftereffect in the test phase for both the extraretinal and retinal MAE experiments following adaptation. The ratio of the ERMAE:RMAE duration was 1:1.36 (the illusory motion lasting on average ~36% longer for

retinal versus extraretinal adaptation).Results indicate a significant difference in the duration of the motion aftereffect for the extraretinal MAE versus the retinal MAE ($t(20) = 2.09$, $p < 0.05$).

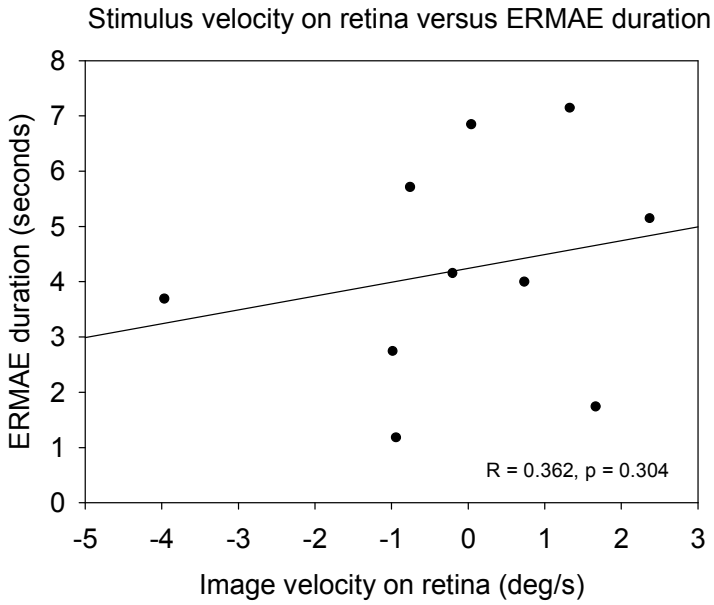

Figure 43. Average stimulus velocity on the retina during pursuit adaptation versus ERMAE duration.
Correlation between the average retinal image velocity of the moving dot during pursuit against the reported duration of the subsequent ERMAE.

Given that the strength of the ERMAE could in part be influenced by retinal motion adaptation because of slip when not pursuing the target accurately, a correlation was performed between the average velocity of the target on the retina during pursuit (difference between stimulus and eye velocity, positive values indicating a pursuit gain of less than one, the eye moving slower than the stimulus) and the duration of the subsequent ERMAE. This is shown in Figure 43. There was a small negative, albeit non-significant, correlation between image velocity and ERMAE duration ($R = 0.362$, $p = 0.304$). As shown in the graph, this correlation appears to be largely driven by one outlier who was tracking the target with a gain of ~1.33. The majority of the retinal image velocity values are clustered around approximately velocity differences of 0°/s. The lack of any correlation between the strength

of the retinal slip and the duration of the subsequent ERMAE reported suggests this effect is not driven by adaptation of retinal motion sensors in this region of the visual field.

4.4.2 MEG data

4.4.2.1 Experiment 5 – The extraretinal motion aftereffect

4.4.2.1.1 Source localisation

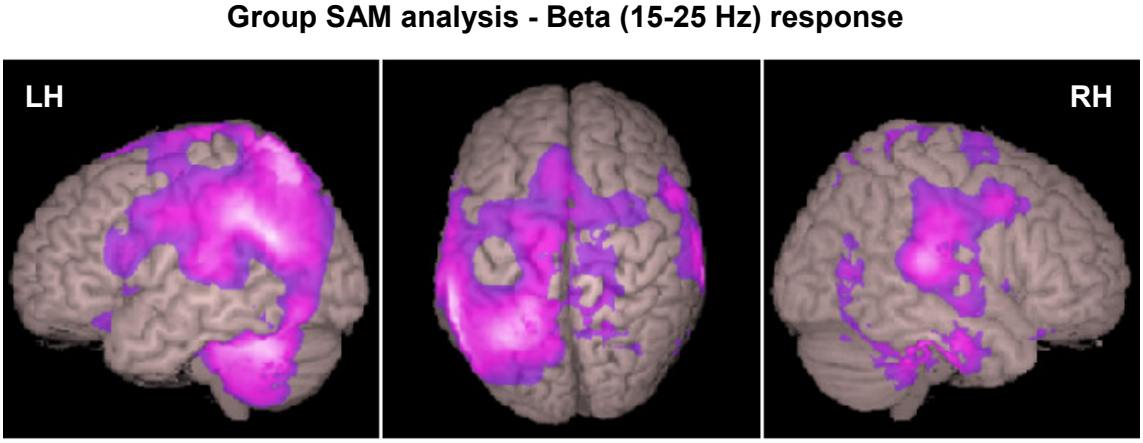

Figure 44. Group averaged SAM source localisation for the beta response during pursuit adaptation versus the baseline central fixation period.
Dominant peaks were identified in left extra-striate and temporoparietal regions of the cortex. Note activity in regions consistent with MT+, the IPS and FEF.

Figure 44 depicts the group-averaged SAM analysis (n=9) for reductions in the beta band during pursuit adaptation versus the central fixation baseline. Consistent peaks were found in MT+, IPS and FEF regions. As in previous experiments, the 15-25 Hz response proved to be the most reliable in localising these areas with the majority of participants (90%) showing peaks in this band in these ROIs, with one participant being omitted from further analysis as there were no identifiable peaks in these regions. Alpha activity was inconsistently shown in these areas and no reliable gamma peaks were found, so therefore the beta response was used as a localiser for these regions in the left hemisphere, on which a subsequent amplitude envelope analysis of the adaptation and MAE periods was conducted.

4.4.2.1.2 Time-frequency analysis for cortical regions subserving pursuit

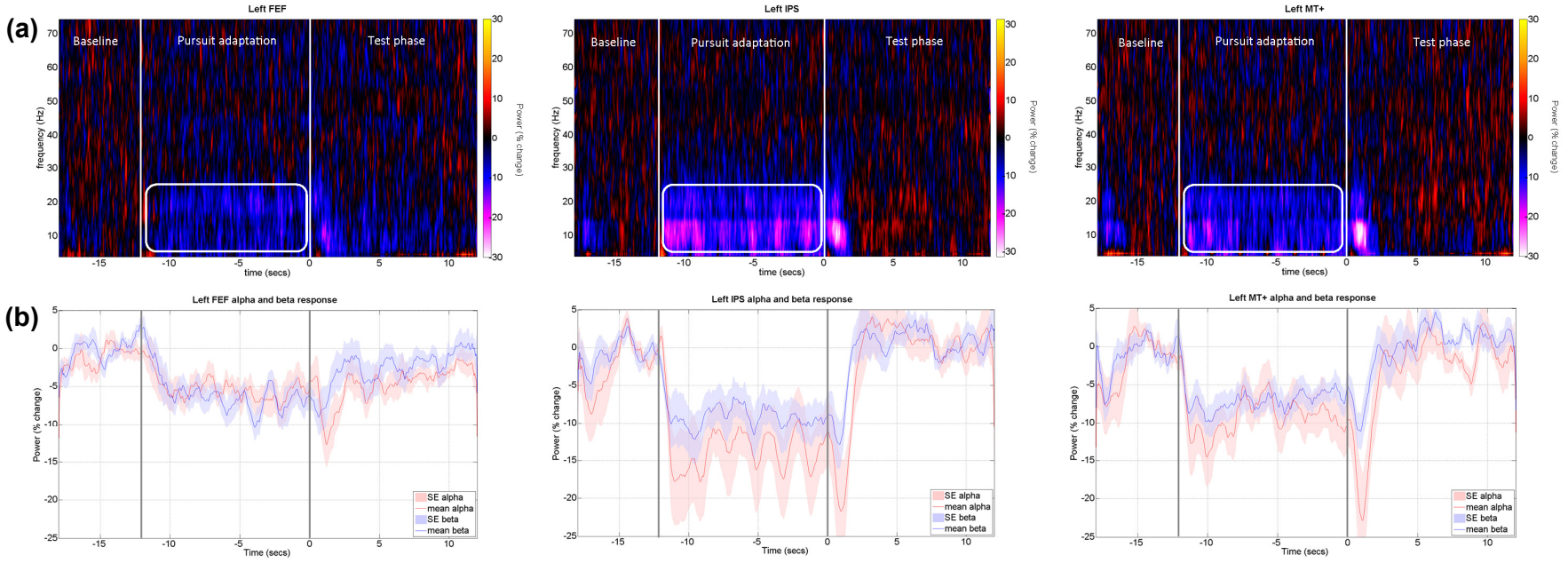

Figure 45. Grand-averaged time-frequency spectrograms and amplitude envelopes for ROIs in Experiment 5.
(a) Spectrograms in the three ROIs, for FEF (top left panel), the IPS (top middle panel) and MT+ (top right panel). The white bounded box in the pursuit adaptation phase indicates the time window over which the mean amplitude envelope was calculated for all further correlational analyses. (b) Group averaged alpha (red traces) and beta (blue traces) amplitude envelope time-series from the three ROIs.

Figure 45a shows the grand-averaged time-frequency spectrogram (n=9, top row of panels) in the three putative ROIs (FEF, top left; IPS, top middle; MT+, top right) derived from the peaks in the initial SAM source estimation. The white bounded boxes depicted in the 'pursuit adaptation' phase indicates the time-window and frequency range over which the mean amplitude of the oscillatory response was quantified for use in further analyses described later on. Below the spectral data are the group-averaged amplitude envelope analyses (Figure 45b, bottom row of panels) for the alpha (5-15 Hz, red trace) and the beta (15-25 Hz, blue trace) frequency bands over the course of an average trial.

For responses in the FEF region (Figure 45a & b, left panels), sustained power changes of the alpha and beta response in the region of approximately -5% were observed for the duration of the pursuit adaptation phase when observers were tracking the moving stimulus. Following cessation of the eye movement in the test phase (during which time participants give duration judgements on the ERMAE), it appears that the beta response returns to baseline levels after ~2-3 seconds, whilst alpha activity appears to be suppressed (in the region of approximately -5%) for the majority of this period.

The IPS region (Figure 45a & b, middle panels) shows sustained power decreases in the beta band for the duration of the pursuit adaptation phase (approximately -10%), whilst the alpha response appears to be modulated in a time-varying fashion. This pattern of activity is particularly striking in the latter half of this pursuit when the phasic changes of power in the alpha band appears to closely match the position of the eyes as they track the moving stimulus.

In the final ROI, the MT+ area (Figure 45a & b, right panels), sustained alpha and beta suppression was once again observed for the duration of pursuit adaptation phase. Subsequently a large power decrease is seen in the alpha response (~22%) in the 1 second following the final eye movement of the pursuit adaptation phase, which then returns to

baseline after ~3 seconds. A more modest beta power reduction is seen in this same time window following the final eye movement, in the region of ~10%.

The original aim of this study was to examine the relationship between the subjective ERMAE duration and an objective neuronal measure defined as the duration of oscillatory power changes during the perception of illusory motion. However, it was found not possible to quantify the duration of the oscillatory change during the ERMAE in each individual as the time-series data proved to be noisy, with transient changes in the envelope amplitude returning to baseline levels almost immediately following adaptation, and then continuing to change in amplitude over the duration of the test period. This made it difficult to reliably estimate signal power changes at the single subject level. Therefore, it seemed most appropriate to explore other aspects of cortical activity that can be more accurately quantified and examine whether those measures mediate characteristics of the ERMAE. With this in mind, it was decided to look at extraretinal activity in regions thought to subserve pursuit eye movements, and whether oscillatory changes during pursuit play some role in the perceptual consequences of oculomotor adaptation.

4.4.2.1.3 Relationship between pursuit-induced oscillatory activity and ERMAE duration

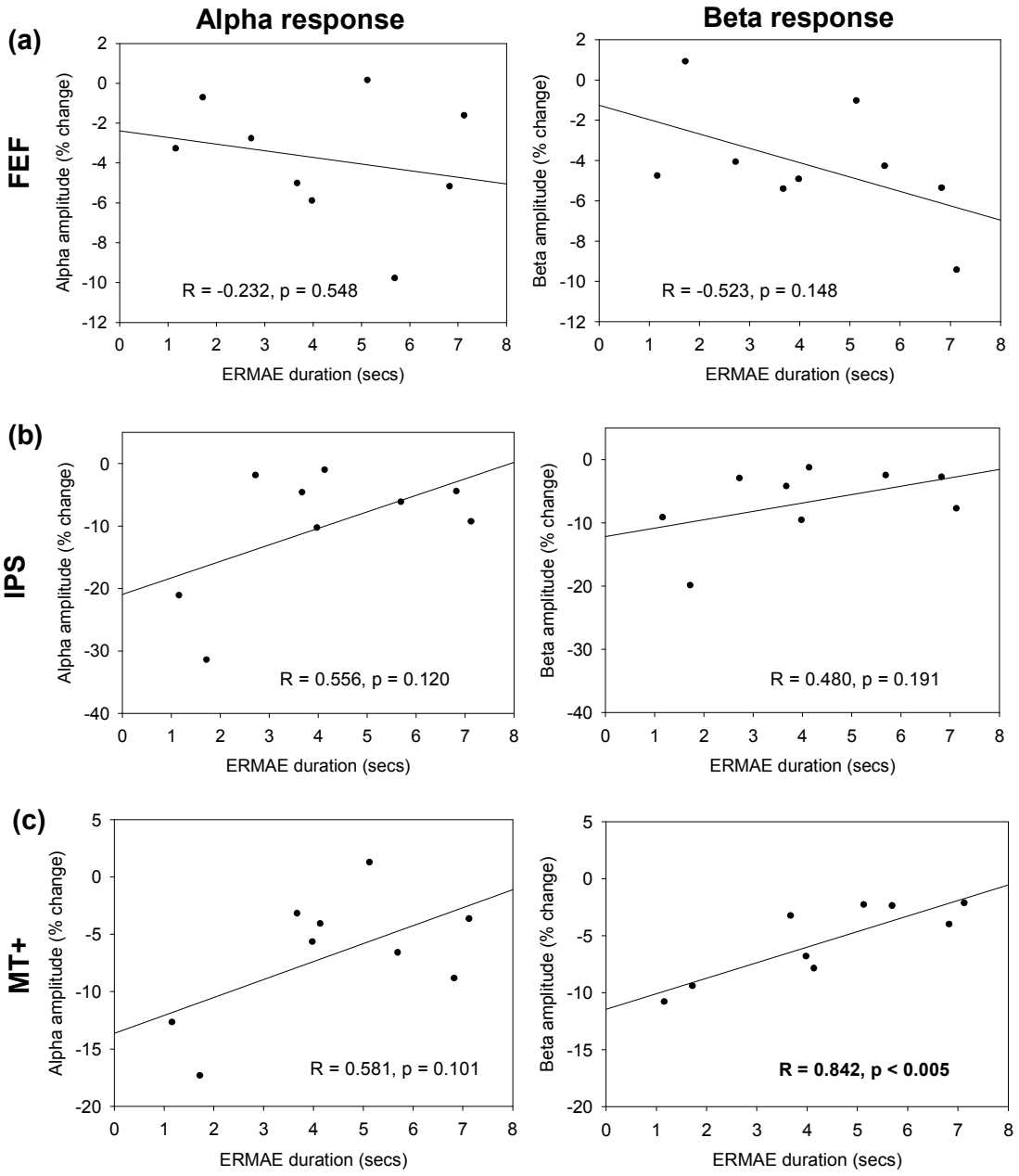

Figure 46. Correlation between the mean alpha (left column panels) and beta (right column panels) activity in the three ROIs and the reported duration of the subsequent ERMAE.

FEF (top row), IPS (middle), and MT+ (bottom) mean oscillatory amplitude during the pursuit adaptation phase (the -12 to 0 second time window denoted by the white box in the spectrograms) versus the subsequent reported duration of the ERMAE.

Figure 46 depicts the correlation between the mean alpha (left column panels) and beta (right column panels) activity during the pursuit adaptation phase in the three ROIs (FEF, top row panels; IPS, middle row panels; MT+, bottom row panels) versus the mean duration judgement of the ERMAE reported in the test phase.

In the FEF region (Figure 46a, top row), there was a small, but non-significant negative correlation between alpha activity and ERMAE duration ($R = -0.232$, $p = 0.548$), and a moderate but still non-significant correlation between beta activity and ERMAE duration ($R = -0.523$, $p = 0.148$). For the IPS region (Figure 46b, middle row), there were moderate but non-significant correlations between alpha ($R = 0.556$, $p = 0.120$) and beta ($R = 0.480$, $p = 0.191$) activity versus ERMAE duration.

For the MT+ region (Figure 46c, bottom row), there was a moderate but non-significant correlation between alpha activity and the duration of the ERMAE ($R = 0.581$, $p = 0.101$). For the beta activity versus ERMAE duration, a large, highly significant correlation was found ($R = 0.842$, $p < 0.005$). Therefore, it was found that pursuit-related beta activity in MT+ during extraretinal adaptation correlates highly with the duration of the ERMAE. In other words, it seems that weaker beta suppression during pursuit eye movements in MT+ corresponds to an increase in the duration of the illusory motion.

To discount any possible effect of retinal slip on the magnitude of the alpha and beta suppression during the adaptation phase, correlations of stimulus speed on the retina versus oscillatory amplitude change were performed. None of these were found to be significant ($p > 0.05$).

4.4.2.2 Experiment 6 – The retinal motion aftereffect

4.4.2.2.1 Source localisation

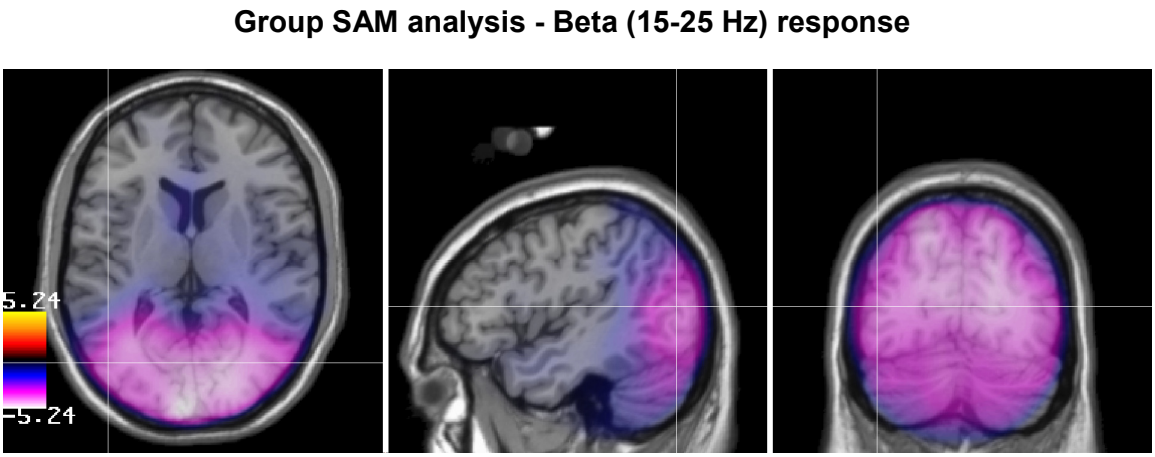

Figure 47. Group-averaged SAM source estimation for the beta response during retinal motion adaptation versus the stationary stimulus baseline period.
Peaks in beta power decreases were predominantly found in occipital regions, including early visual cortex and areas consistent with MT+.

Figure 47 depicts the group-averaged SAM analysis for power reductions in the beta frequency band for the retinal motion adaptation phase versus the stationary stimulus baseline period overlaid on a template brain. Source localisation of beta activity revealed consistent peaks in occipital regions, including early visual cortex and extra-striate regions. As with all previous experiments, including Experiment 5, the 15-25 Hz response proved to be the most reliable in localising the left MT+ ROI with all participants showing peaks in this band in this region. Alpha peaks in MT+ were inconsistent with its putative location and no reliable gamma was found, so therefore the beta rhythm was used as a functional localiser for MT+ in the left hemisphere. The beta peaks were used to construct virtual sensors so as to examine oscillatory changes related to motion adaptation and the subsequent RMAE.

4.4.2.2.2 Time-frequency analysis of retinal motion adaptation in MT+

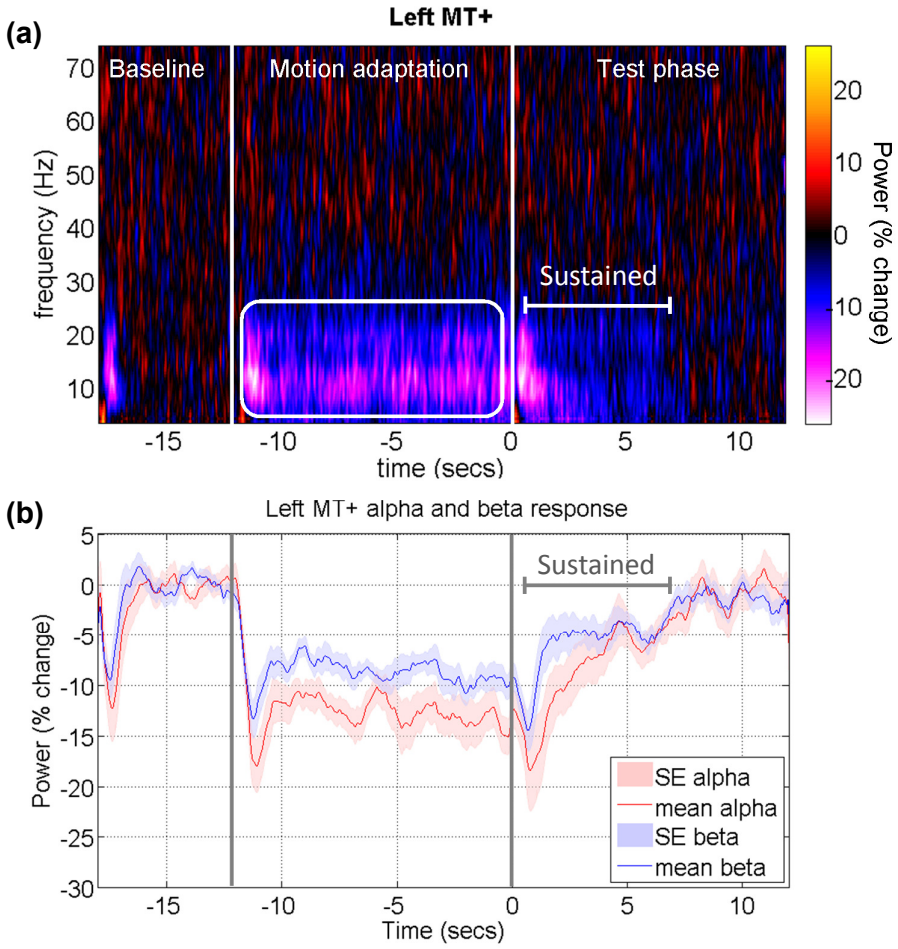

Figure 48. Grand-averaged time-frequency spectrogram and amplitude envelope power changes in left MT+ during retinal motion adaptation and the subsequent RMAE.
(a) Time-frequency analysis of MT+ responses for motion adaptation and the retinal MAE. The white bounded box denotes the time-window and frequency range over which the mean alpha and beta activity during retinal motion was quantified for use in the later correlations with the RMAE duration. In the test phase, sustained alpha and beta suppression was observed for approximately 7 seconds. (b) Amplitude envelope analysis from left MT+ for alpha (red trace) and beta (blue trace) activity extracted from the spectral data.

Figure 48a shows the grand-averaged time-frequency analysis in MT+ derived from the peaks in the initial SAM source estimation. The white bounded box depicted in the 'motion adaptation' phase indicate the time-window and frequency range over which the mean amplitude of the oscillatory response was quantified for use in further analyses

described later on. Below the spectral data are the group-averaged amplitude envelope time-series (Figure 48b, bottom row) for the alpha (5-15 Hz, red trace) and the beta (15-25 Hz, blue trace) frequency bands over the course of an average trial.

During retinal motion adaptation, sustained power decreases of the alpha and beta frequencies were observed for the duration of adaptation. In the test phase following cessation of stimulus motion, there appeared to be transient spike in the alpha and beta amplitude envelope, with a gradual return to baseline levels of power after approximately 7 seconds. As in the previous experiment, it was not possible to quantify the duration of the oscillatory change during the motion aftereffect in each individual as the time-series data was noisy. This made it difficult to estimate the duration of any sustained power changes given the transient changes in amplitude that often returned to baseline levels almost immediately following the adaptation period. Therefore, a similar analysis to that conducted previously was implemented, where the relationship between alpha and beta activity during adaptation to the duration of the RMAE was explored.

4.4.2.2.3 Relationship between the motion-induced oscillatory responses and duration of the perceived RMAE

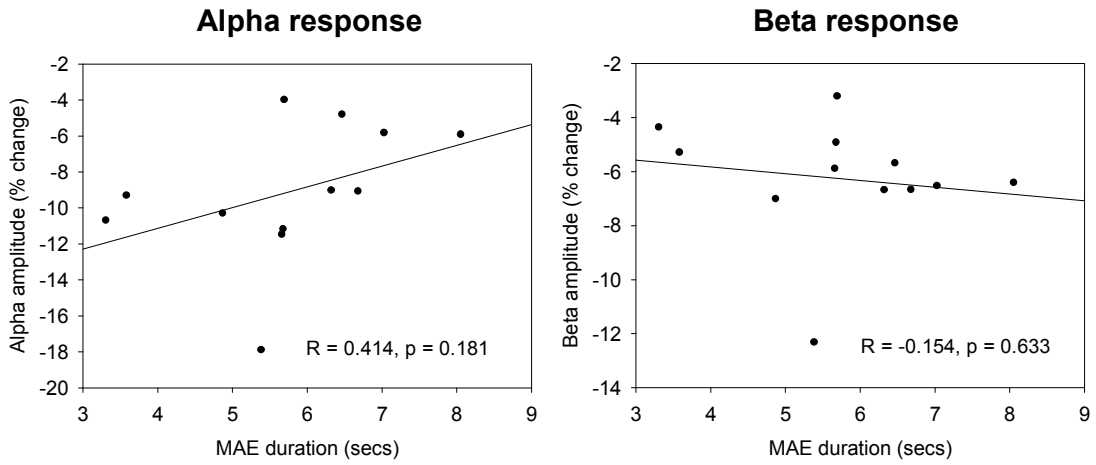

Figure 49. Correlations for alpha (left panel) and beta (right panel) activity in left MT+ during retinal motion adaptation versus the duration of the RMAE.

Figure 49 shows the correlation between the mean alpha (left panel) and beta (right panel) activity during the retinal motion adaptation phase in the MT+ versus the mean reported duration of the RMAE perceived in the test phase. For the alpha response (left panel) there was a moderate, but non-significant correlation with MAE duration ($R = 0.414$, $p = 0.181$), and a small but still non-significant negative correlation between beta activity and MAE duration ($R = -0.154$, $p = 0.633$).

4.4.2.3 Contrasting low-frequency suppression in MT+ during extraretinal and retinal motion adaptation

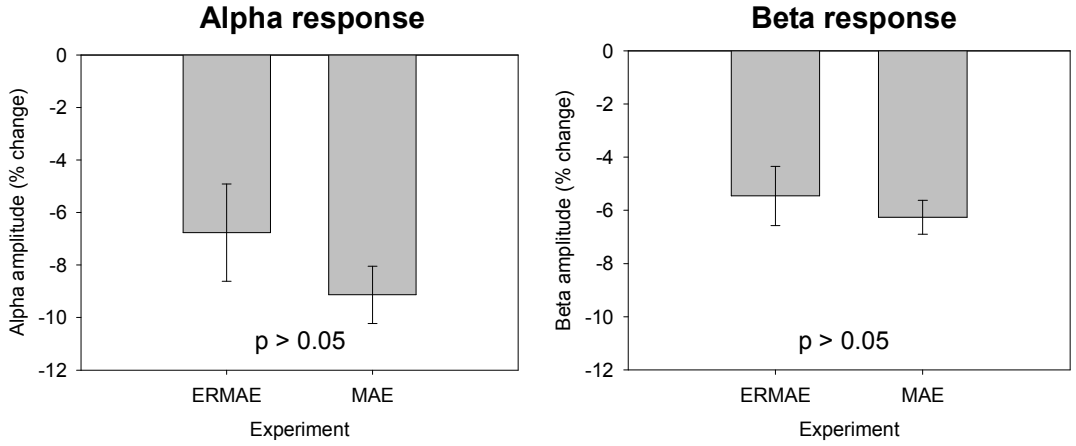

Figure 50. Contrasting alpha (left panel) and beta (right panel) activity in left MT+ during extraretinal adaptation in the ERMAE experiment and retinal motion adaptation in the MAE experiment.

Figure 50 depicts the mean alpha (left panel) and beta (right panel) activity in left MT+ during smooth pursuit adaptation (ERMAE experiment) and retinal motion adaptation (MAE experiment). There was no significant difference between alpha amplitude for extraretinal adaptation (M = -6.768, SD = 5.552) versus retinal motion adaptation (M = -9.136, SD = 3.776), t(19) = 1.165, p = 0.258, and no significant difference between beta amplitude for extraretinal (M = -5.459, SD = 3.343) versus retinal motion adaptation (M = -6.258, SD = 2.212), t(19) = 0.66, p = 0.517. The ratio for alpha activity between ERMAE:RMAE was 1:1.35 (about 35% greater for retinal motion adaptation versus extraretinal adaptation), and for beta activity the ratio was 1:1.15 (about 15% greater for retinal motion adaptation versus extraretinal adaptation). Therefore, the ratio of the ERMAE:RMAE duration (36% difference) and the alpha activity during adaptation for ERMAE:RMAE (35% difference) were approximately equal.

4.5 Discussion

The extraretinal MAE provides an additional means with which to probe the nature of nonretinal signals in motion processing cortex, and how these signals might be integrated as one of the mechanisms that is thought to maintain space constancy. The purpose of the experiments presented here was to explore the neuronal correlates of oculomotor and retinal motion adaptation using MEG. Furthermore, these studies set out to probe the consequences of these actions on the oscillatory dynamics in cortical areas thought to subserve pursuit eye movements and motion perception. More specifically, the aim was to test the prediction that the duration of changes in cortical oscillations proceeding adaptation would correlate with the duration of the motion aftereffect. These experiments put to the test that a correlation between these measures (the duration of low-frequency suppression in cortical sites subserving pursuit and MT+ for retinal motion, and the duration of the illusory motion) would indicate that alpha and/or beta activity in these areas mediate aspects of the perception of motion. This was, to the best of our knowledge, the first neuroimaging study of oculomotor adaptation and the extraretinal MAE.

Unfortunately, the correlation between motion aftereffect duration and oscillatory changes could not be tested due to the quality of the signal extracted from these regions. Therefore, it was decided to examine whether changes in the alpha and beta activity in these areas during eye movement (Experiment 5) and motion (Experiment 6) adaptation play some subsequent role in the extraretinal and retinal MAE. In Experiment 5, whilst the majority of the oscillatory changes in most of the areas implicated in pursuit appeared to have no impact on the post-adaptation ERMAE, one particularly striking result was found; a highly significant correlation was observed between the magnitude of the beta suppression in MT+ during oculomotor adaptation and the duration of the following extraretinal MAE. In other words, the greater the suppression of the beta rhythm in MT+ during smooth pursuit eye

movements, the shorter the duration of the perceived ERMAE was when observing a stationary test stimulus.

This result was surprising, as other studies have found a close correlation between the magnitude of illusory motion and increases in BOLD following retinal adaptation (He, et al., 1998; Tootell, Reppas, Dale, & Look, 1995). Moreover, both beta suppression and BOLD increases are thought to reflect a rise in cortical activity (Brookes, et al., 2005; Dunkley, Freeman, Muthukumaraswamy, & Singh, 2011; Mukamel, et al., 2005; Singh, et al., 2002; Stevenson, et al., 2011), not the decline found here.

Results from Watamaniuk & Heinen (2007) might go some way to explain the findings presented here. They found that following retinal motion adaptation, observers biased their eye movements in a direction opposing that of the direction of retinal adaptation when presented with a subsequent stimulus (Watamaniuk & Heinen, 2007) They termed this the oculomotor motion aftereffect (OMAE). Crucially, they found that this effect was as pronounced following a blank storage period, but that the oculomotor effect/eye movement bias was absent in the storage period, with the OMAE only being expressed in the presence of a visual stimulus. They conclude that the OMAE exhibits the phenomenon of storage, much like the perceptual motion aftereffect induced by passive retinal adaptation. Along with other studies of the storage of an MAE, this suggests that the neuronal fatigue model usually invoked to explain the perceptual MAE cannot be the whole story. Watamniuk & Heinen (2007) propose an alternative model, in which visual "adaptation recalibrates the motion processing network by adjusting the weights of the inputs to neurons…in MT", and that subsequent visual stimulation to be used as a reference is necessary for the system to recalibrate itself following changes in network weights as a result of adaptation (Watamaniuk & Heinen, 2007).

It has been suggested that active low-frequency oscillations in the cortex reflects the ability of the system to maintain an ongoing network state (Engel & Fries, 2010), and inhibit the processing of task-irrelevant information (Jensen & Mazaheri, 2010). Conversely, decreases in low frequency power might be envisaged as the ability of the brain to suppress ongoing rhythmic activity to facilitate cortical processing, which in the studies presented in this thesis are the processing of oculomotor signals in MT+. Therefore, linking this back to the recalibration idea of Watamniuk & Heinen, the beta suppression witnessed during adaptation might be a reliable macroscopic biomarker of the efficacy of the motion processing system to recalibrate itself for motion in the presence of a stationary stimulus. This might explain why greater beta suppression during eye movement adaptation corresponds with a shorter ERMAE duration.

The results of Experiments 5 and 6 show that the motion aftereffect was greater following adaptation to retinal motion than pursuit eye movements. This is opposite to Freeman, et al. (2003), who found oculomotor adaptation induced through optokinetic nystagmus produced a greater motion aftereffect than adapting to translating retinal motion. One possible explanation for this discrepancy could be in the finding that stronger MAEs are elicited for complex patterns of motions, such as rotation and expansion (Bex, et al., 1999). Bex, et al. (1999) propose that this reflects the adaptation of motion sensors at increasing levels of the motion processing hierarchy, which are tuned for different patterns of motion, with cells having a greater receptive field size, pattern specialization, and increasing selectivity for complex motions at increasing spatial scales. This 'functional hierarchy' integrates local motion signals to mediate perception of motion of real objects in the world, with more complex motion systems existing further up the hierarchy. This might explain why such a difference was found between the duration of ERMAE and RMAE reported here.

The interpretation of the beta activity being related to the ability of the motion system to recalibrate following adaptation should be interpreted with some caution. Primarily, it is difficult to reconcile the results from the ERMAE study with those found in Experiment 6, the RMAE experiment. The fact that the beta activity during retinal motion adaptation did not correlate with the duration of the RMAE suggests the interpretation given here does not hold for adaptation of retinal motion. Speculatively, it seems possible that the beta suppression plays a specific functional role in the integration of extraretinal signals in areas further up the motion processing hierarchy in MST, and perhaps reflects a more general inhibitory gating mechanism during the perception of motion in the absence of eye movements at lower levels of the hierarchy in MT.

There are a number of behavioural and perceptual considerations to take into account concerning the experiments presented here. Regarding oculomotor adaptation and the ERMAE in Experiment 5, the reported motion aftereffect might be induced by retinal slip when tracking the stimulus non-optimally during the pursuit adaptation phase. This artefactual retinal motion stimulation could adapt motion sensors that code the retinotopic position of the stimulus. Given that the subsequent stimulus was presented in approximately the same retinotopic position as the adapter, the apparent illusory motion of the test stimulus could be due to retinal slip that adapts motion sensors in this portion of visual space. Ideally, the retinotopic position of any stimulus to be tracked during oculomotor adaptation should appear in a different retinotopic position to that of the test stimulus to disambiguate any retinal MAE from a true ERMAE. In the paradigm used by Freeman, & Sumnall (2005), intentional tracking smooth eye movements were induced by a translating dot field presented in the periphery of the visual field (known as optokinetic 'stare' nystagmus). To test the ERMAE, a test stimulus was presented in the unadapted central region of visual space, and the MAE was still found. Whilst this would be a more suitable way to test oculomotor

adaptation and the ERMAE, a large amount of retinal motion stimulation would be introduced to the MEG signature if a similar paradigm were used, which would impossible to disambiguate from the extraretinal signals in MT+.

A potential future experiment could use a modified version of the adaptation paradigm used in Experiment 5. Observers would adapt the pursuit system by tracking a single moving target and then be presented with a stationary test stimulus in disparate retinotopic coordinates (perhaps presented in a relatively peripheral part of the visual field). Doing so would mitigate any potential confounds introduced by adaptation of retinal motion sensors that are stimulated in the same portion of the visual field as the subsequent test stimulus when pursuit gain is non-optimal and there is slip of the target on the retina. If this were to happen, it could result in a retinal MAE that is misinterpreted as illusory motion resulting from oculomotor adaptation. By modifying the experiment and presenting a stationary test in another region of space, this potential confound would be largely abolished. However, without a central fixation dot with which to foveate, this could prove difficult. Nevertheless, in Experiment 5, results suggest the ERMAE does not appear to be driven by the relative velocity of the target on the retina when the pursuit gain is non-optimal, which points to the effect being induced by extraretinal signal adaptation of motion areas, rather than by retinal adaptation.

Moreover, there does appear to be evidence of a small, but consistent, overshoot of the eyes when fixating the stationary test stimulus following adaptation in the group EOG data. This is then followed by an upwards eye drift to fixate the target. Given this, the ERMAE reported by the observers could actually be resultant retinal motion from the corrective eye movements when fixating the test target. This potential misinterpretation of eye movement induced retinal motion for a genuine ERMAE means the explanation given here for the role of beta activity should be treated with caution.

In light of the apparent limitations of the ERMAE experiment, future studies could use a blank storage interval between adaptation and test to overcome these problems, as has been readily used in a number of previous studies exploring the MAE. The advantage of this would be twofold; first, it would eliminate any overshoot of the eyes when fixating the stationary, eliminating any potential misinterpretation of an ERMAE for eye-movement induced retinal motion. Second, if a relationship were found to exist between beta activity during pursuit adaptation and duration of the MAE following a blank storage period, this would support the view that beta suppression during the integration of oculomotor signals into MT+ reflects the ability of the brain to recalibrate the visual motion and perceptual stability system after oculomotor adaptation.

5 Chapter 5 – General Discussion

5.1 Overview

The experiments in this thesis were designed to contribute to the understanding of the neurophysiological mechanisms underlying smooth pursuit eye movements. In particular, it aimed to investigate the role of neuronal oscillatory changes in human motion processing cortex during pursuit. Furthermore, it sought to examine how these changes might reflect the processes underlying oculomotor control, coordinate transformations, head-centred motion perception and the integration of nonretinal eye movement estimates thought to be a primary mechanism in the maintenance of space constancy. Four experiments were designed to explore how eye kinematics and motion processing were encoded in this region of cortex. A further two experiments investigated the consequences of pursuit and retinal motion adaptation on visual perception, how this adaptation induces the percept of illusory motion in a static stimulus and whether these illusions might be mediated by cortical oscillatory dynamics.

Together these experiments aimed to explore the relationship between pursuit eye movements and the modulation of neuronal oscillations in the middle temporal cortex, and infer from this their role in head-centred motion perception. In the following section, a description of the key experimental findings is given and the rationale for the progressions between experiments is provided. In the penultimate section of this chapter, the limitations of these studies and recommendations for future work are given, with the final section given over to concluding remarks.

5.2 Main Findings

Smooth pursuit eye movements are of major adaptive importance. They allow animals with a fovea (such as humans and non-human primates) to track a moving object and stabilise

that object on a part of the retina where visual acuity is greatest. However, pursuit introduces a tricky perceptual problem the brain must resolve; the movement of the eyes induces motion of the background on peripheral parts of the retina when following a target. This self-induced retinal motion of the environment must be disambiguated from real motion in the world, which is, for the most part, stationary on the fovea when an object is being tracked. A number of compensatory mechanisms are implemented to achieve the goal of perceptual stability, one being the use of extraretinal signals to delineate real motion from image motion. Numerous models have been proposed for how the brain accomplishes this, which broadly posit that world motion is derived by the summation of retinal motion estimates and nonretinal information regarding the eye movement.

Whilst the exact nature of this 'extraretinal' information is debated, and often interchangeably referred to as 'corollary discharge', 'efference copy' or 'reference signals' (for the sake of brevity in this thesis at least), these signals primarily originate from internal sources, most often thought to be efferent oculomotor commands. In terms of the brain regions thought to be principally involved in the generation of coordinate transforms and extraretinal signal integration required for space constancy, MST in monkeys (Churchland & Lisberger, 2005; Ilg & Thier, 2003; Komatsu & Wurtz, 1988; Newsome, et al., 1988; Ono & Mustari, 2006), and the human homologue MT+ (Dukelow, et al., 2001; Kimmig, et al., 2008; Konen, et al., 2005), has received the most attention in recent years. In particular, this area of the cortex plays a principal role in motion perception, both in retinotopic and spatiotopic reference frames, deriving world motion by integrating non-retinal eye movement signals with those from retinal sources produced by the eye movement.

The aim of this thesis was to use non-invasive multimodal neuroimaging in humans to study the cortical correlates of smooth pursuit eye movements. In particular, this work focused on using magnetoencephalography to probe induced oscillations in the MT+ region

during activation of the visual pursuit and retinal motion systems. Of special importance was how aspects of the eye movement were encoded in the magnitude of neuronal synchronisation, and whether there existed any functional distinction in changes within the 'classical' brain rhythms, which have been studied extensively in recent years but for which still lack a unifying hypothesis (Andino, et al., 2005; Engel & Fries, 2010; Fries, 2005; Fries, et al., 2001; Hadjipapas, et al., 2007; Jensen & Mazaheri, 2010; Muthukumaraswamy, et al., 2009; Tallon-Baudry, et al., 1996; Wilke, et al., 2006; Womelsdorf, et al., 2005; Zhang, et al., 2009). It was hoped that using MEG to study these changes would provide insight into some of the neurophysiological mechanisms the brain might use during sensorimotor processing, such as how oculomotor commands required for pursuit might be generated and how the brain might integrate extraretinal eye movement signals in MT+ as a means of achieving perceptual stability.

Experiment 1 probed the cortical representation of smooth pursuit and retinal motion processing using fMRI and MEG. Using fMRI, the regions implicated in the processing of visual motion stimuli and oculomotor control of pursuit were resolved. This activity was then compared with the MEG correlates of activity using identical paradigms. Of special focus was the comparative spatial localisation revealed in both neuroimaging modalities of the induced activity in extra-striate cortex, thought to be the putative MT+ complex, and how oscillatory changes in this region during pursuit, retinal motion and a combination of the two compared. It was predicted that pursuit and retinal motion stimulation in the absence of eye movements and a combination of the two would reveal BOLD activity increases in regions spatially coincident with alpha and beta rhythm changes in extrastriate cortex. Consistent activity was found in MT+ associated with retinal motion processing and pursuit eye movements in the dark in both imaging modalities, which provides a cross-validation of the task. The putative MT+ region activated by these tasks were consistent with previously

reported coordinates of this area (Dukelow, et al., 2001; Kimmig, et al., 2008; Konen, et al., 2005; Nagel, et al., 2008; Nagel, et al., 2006; Petit & Haxby, 1999; Tikhonov, et al., 2004). Furthermore, these results confirm the findings of other studies that report a link between BOLD activity and low-frequency suppression in the cortex (Brookes, et al., 2005; Singh, et al., 2002; Stevenson, et al., 2011).

An additional result suggested that changes in alpha-beta activity in this area reflect an eye position-dependent signal during pursuit, which in conjunction with the results from the other conditions suggested this area carries retinal as well as extraretinal eye movement signals. These signals are most likely used in the maintenance of perceptual stability during head-centred motion perception (Champion & Freeman, 2010; Freeman, et al., 2010; Haarmeier, et al., 2001; Naji & Freeman, 2004; Schutz, et al., 2008; Souman, et al., 2006; Spering & Gegenfurtner, 2006; Turano & Massof, 2001).

Experiment 2 was a control study for the eye-position signal observed in Experiment 1. it has been shown previously that MT+ responds to direction changes in a moving stimulus (Martinez-Trujillo, et al., 2007). Therefore, it seemed possible that the hemifield-dependent eye position response could have been an artefactual result, driven by retinal slip of the target dot. This is evident in the eye movement data when the eyes were at the maximum contralateral position during pursuit and the stimulus was changing direction. Thus, the modulation of the alpha and beta responses in Experiment 1 that showed eye position-dependency were compared with those induced by retinal slip of a target during fixation. Results revealed alpha and beta activity in regions consistent with MT+ as found previously. Whilst certain characteristics of the response were similar for both eye position and transient retinal motion processing, retinal motion induced alpha and beta activity with a significant latency in the maximal response. The latency was beyond that which might have been observed if the apparent eye position-dependency effect in the ‘pursuit’ condition observed in

Experiment 1 was due to retinal slip. The timing differences found in these responses between Experiment 1 and Experiment 2 suggest that the pattern of activity observed in the 'pursuit' condition of Experiment 1 was due to either eye position or some other fundamental aspect of the eye movement, and not retinal error caused by an ineffective tracking response.

Experiment 3 was designed to test the interpretation of the hemifield-dependent eye position signal found in Experiment 1. In Experiment 3, the excursive pursuit paradigm, observers pursued a moving sinusoid at various head-centred eccentricities. Alpha and beta amplitude envelopes when performing pursuit were compared, and from this it was possible infer whether modulation of similar activity observed in Experiment 1 was due to the processing of eye position signals in MT+, or some other aspect of the eye movement. The results showed that the pattern of activity for both alpha and beta did not vary significantly during smooth pursuit at various head-centred positions. This suggests that the modulation of the alpha and beta rhythm during sinusoidal pursuit was due to some other aspect of the eye movement, with no evidence of a specific head-centred eye position signal in the magnitude of the alpha or beta activity in MT+.

Given the results from Experiment 3, it seemed plausible that the alpha and beta activity modulation seen during sinusoidal pursuit could actually reflect a velocity-encoding signal that lags the movement of the eyes. This would be in agreement with some previous invasive electrophysiological studies in the monkey, which have shown that the majority of neurons in MST that carry an extraretinal signal related to pursuit appear to code for eye velocity (Ilg & Thier, 2003; Ono & Mustari, 2006). However, it has also been shown by others that pooled MST responses only predict eye velocity 50% of the time and they therefore conclude that activity in this area from pursuit-related neurons regulates some other aspect of the eye movement (Churchland & Lisberger, 2005), rather than driving the velocity of the eyes. Additionally, although a number of neuroimaging studies in humans have shown that BOLD

activity increases with increasing eye speed (scalar, a magnitude measure without reference to a coordinate change), but there was no specific test of BOLD-related changes to velocity (vector, taking consideration of both magnitude and direction) (Nagel, et al., 2008; Nagel, et al., 2006).

Therefore, the objective of Experiment 4 was to expand on the previous neuroimaging literature and examine the modulation of the alpha and beta activity as a function of eye velocity (movement in both the leftwards and rightwards direction). This was done to see whether there was any functional distinction in the role of either alpha or beta activity in encoding this behaviour. In addition, it was examined whether there is any eye movement direction-bias in the response properties of those neurons in MT+ that display pursuit-related activity, and any direction-specific effects related to ipsi- versus contraversive pursuit, which would be predicted from the animal literature. Whilst there appeared to be no clear specific dependency of this response on eye velocity as hypothesised, there was an effect of eye speed on the magnitude of the beta suppression, with increasing eye speed inducing greater suppression of this rhythm. There seemed to be a slightly greater suppression in both the alpha and beta rhythm when pursuing in the contraversive direction compared to ipsiversive pursuit, but inferential tests failed to clarify whether there was a clear or consistent bias in these responses. Furthermore, there was no clear relationship between alpha amplitude changes and eye speed. The dissociation suggests some functional distinction in the role of the alpha and beta rhythm in oculomotor control and the processing of extraretinal signals in MT+, whilst complementing other neuroimaging research which found eye speed encoding in this region of cortex (Nagel, et al., 2008; Nagel, et al., 2006).

It is proposed that beta suppression in MT+ during pursuit reflects the integration of extraretinal movement signals for use in perceptual stability during eye movements, whilst the alpha suppression reflects the disengagement of some general inhibitory gating

mechanism required for the processing of task-relevant information (Jensen & Mazaheri, 2010).

Experiment 5 (ERMAE) and 6 (RMAE) examined the neuronal substrates of oculomotor and retinal motion adaptation (respectively), and the consequences of both types of adaptation on visual perception. Adaptation to retinal motion is known to induce an illusion known as the motion aftereffect where a subsequent stationary test stimulus appears to move in the opposite direction to that of the motion of the adapter, with the magnitude of the illusion correlating with activity in MT+ (Culham, et al., 1999; He, et al., 1998; Tikhonov, et al., 2007; Tootell, et al., 1995). The motion aftereffect can also be induced by repetitive unidirectional smooth pursuit eye movements, even in the absence of any retinal motion, known as the extraretinal motion aftereffect. There are multiple reasons why this illusion occurs, but one of the reasons behind this is thought to be because extraretinal eye movement signals are integrated into spatiotopic MT+ and adapt motion-sensitive neurons in this area (Chaudhuri, 1991a; Freeman & Sumnall, 2005; Freeman, et al., 2003). Therefore, this effect provides an additional means with which to study extraretinal processing in MT+.

Experiment 5 was designed to elucidate whether changes in cortical oscillations in some of the principal cortical regions that subserve pursuit mediate aspects of the extraretinal MAE. In particular, this study aimed to see whether objective neuronal measures, such as the duration of alpha and beta suppression, correlate with the subjective percept of illusory motion. Whilst it was not possible to conduct this analysis due to noisy estimates of signal changes, it was however found that beta activity in motion-processing cortex during adaptation was a significant predictor of the subsequent ERMAE duration. It was concluded that beta suppression during the pursuit adaptation phase is an indicator as the efficacy of the visual motion system to subsequently recalibrate itself in the presence of a stationary visual stimulus following adaptation (Watamaniuk & Heinen, 2007).

However, in Experiment 6, results appeared to contradict this finding because there appeared to be no clear relationship between the low-frequency suppression in MT+ induced during retinal motion adaptation and the duration of the RMAE. It is not clear why the beta activity should be such a strong predictor of the ERMAE but not RMAE. There was some weak evidence that alpha and beta suppression persists during the perception of illusory motion in the stationary test phase, when there is no real motion, which perhaps suggests this activity mediates aspects of the RMAE and is in agreement with results from other studies on MT+ activity during illusory motion (Culham, et al., 1999; He, et al., 1998).

In summary, these experimental results suggest that beta frequency suppression in human MT+ is an active process during smooth pursuit eye movements that reflects the generation of oculomotor signals in the presence of visual feedback for the maintenance of pursuit. Additionally, these beta rhythm changes may also signify the integration of internally generated nonretinal signals related to the eye movement required for the maintenance of perceptual stability. In particular, changes in the macroscopic beta rhythm measured using MEG probably reflects a combination of underlying processes in the putative MST region. Pursuit of a target in the absence of any background motion will give rise to activity in pursuit-related neurons in this region that are most likely to preferentially code for multiple aspects of the eye movement, including eye velocity, speed and position. However, it seems clear that aspects of the beta activity encode certain metrics of the eye movement and there does seem to be some distinction in the role of beta and alpha. As suggested by Engel & Fries (2010), beta oscillations appear to play a putative functional role in the integration of motor commands with sensory signals in polysensory regions (in this case, the integration of oculomotor commands with visual motion signals in association cortex). Additionally, the findings here that suggest no specific role of alpha oscillations in the pursuit eye movements are in good agreement with the role of alpha activity proposed by Jensen & Mazaheri (2010),

which they suggests is likely to play a more generic role in the inhibitory gating of information during task processing.

The remainder of the General Discussion considers the limitations of the present studies and potential future directions to answer questions generated by the findings of this thesis.

5.3 Limitations and Future Directions

Despite the claim that beta suppression in area MT+ during smooth pursuit reflects underlying extraretinal activity related to the maintenance of space constancy and the estimation of target motion in a head-centred coordinate system, this interpretation should be treated with caution. This section of the thesis considers a number of the limitations of the current experiments, potential future modifications to remedy such inadequacies, and unanswered questions from the observations made here.

Firstly, the presence of ongoing visual feedback during object tracking poses a problem for the interpretation of the nonretinal nature of the signals found here. Extra care was taken to eliminate any retinal motion stimulation during pursuit through the use of occluding goggles and only data when pursuit was close to unity was considered in the final results. This means that any activity predominantly related to strong retinal motion, either because of target slip or background motion during the eye movement, was omitted from the final results. However, the design of the experiments meant that pursuit behaviour was conducted in the presence of ongoing visual feedback (albeit when pursuit gain when close to unity and retinal slip was negligible). Therefore, the isolation of *purely* extraretinal signals related to eye movements can only be achieved through the complete absence of any visual feedback (in motion or not) whilst the eyes are still moving smoothly. Given this, it would be hasty to conclude that beta oscillatory suppression observed here is the result of solely extraretinal components, although Experiment 2, the control for the result found in the 'pursuit' condition

of Experiment 1, suggests that retinal slip on its own produces substantially different alpha and beta profiles which can be disambiguated from a pursuit-related response. Hence, one of the most appropriate modifications to the present study would be to incorporate an occluder condition, where the target momentarily disappears and MT+ activity is examined during this period (when the eyes are moving but there is no visual component to drive activity).

It is known that the pursuit system has a limited ability to maintain smooth pursuit during transient disappearance of a target in anticipation of its return (Barnes & Asselman, 1991; Becker & Fuchs, 1985; Bennett & Barnes, 2003). Furthermore, such limitations as those of the present studies in this thesis (such as the stimulus providing ongoing visual feedback) have been controlled for in similar imaging experiments investigating MT+ responses during pursuit by comparing activity when the eyes were followed a target with that when the target momentarily disappears but pursuit is maintained (Lencer et al., 2004; Nagel, et al., 2008; Nagel, et al., 2006). A study by Nagel, et al. (2008) reported extraretinal activity in MT+ when the eyes moved in the absence of a pursuit target, which is evidence that motion cortex processes oculomotor signals even in the complete absence of visual stimulation. Therefore, future studies might expand on the research presented here and compare MEG signal changes during object tracking with that during target blanking to see whether the relationship between beta activity and eye speed remains.

Whilst it is proposed that this beta suppression is an active neurophysiological process in the maintenance of pursuit and the estimation of target motion, it would be speculative to claim this signal is an integral compensatory mechanism used by the brain in the maintenance of perceptual stability without directly measuring motion invariance psychophysically. Given that the task only involved tracking an isolated dot in the absence of any other motion stimulation, it can only be inferred from these correlative measures that oscillatory changes in this brain region are part of a process that mediates perceptual stability during ego motion.

Interestingly, a MEG study that directly measured estimates of pursuit-induced retinal motion suggests perceptual motion invariance may not be primarily localised to MT+, but rather further up the visual processing hierarchy in the parietooccipital cortex (Tikhonov, et al., 2004). The authors remark that "early stages of cortical motion processing up to cortical area MT/V5…seem to be unable to distinguish whether visual motion is external or self-induced".

A later study utilising TMS to study causal effects found that stimulation to the MT+ region during pursuit over a background failed to impair motion invariance but compromised oculomotor behaviour with an evident decrease in pursuit gain (Haarmeier & Kammer, 2010). This led them to conclude that the neuronal substrates of space constancy actually reside in a number of distributed but interconnected cortical sites, rather than primarily within MT+. As a follow up to the experiments presented here then, future studies investigating pursuit utilising MEG might therefore measure perceptual stability during the eye movement. Additionally, it would be interesting to see whether eye movement metrics are encoded within additional areas of the cortex not explicitly researched here.

5.4 Conclusion

In concluding this thesis, the results presented here from a number of magnetoencephalographic studies suggest a functional role for the suppression of low-frequency neuronal oscillations in the middle temporal region of the human cortex during smooth pursuit eye movements. In particular, it appears that decreases in the amplitude of the ongoing beta rhythm during pursuit eye movements show that neurons in motion processing cortex carry extraretinal signals required for oculomotor control and head-centred motion perception. Whilst perceptual stability was not explicitly measured here, it is proposed that these macroscopic oscillatory changes are evidence that this region is at least one of a number of sites that is integral in oculomotor control, the perception of a stable environment during eye movements and the estimation of target motion.

6 References

Andersen, R. A., Essick, G. K., & Siegel, R. M. (1985). Encoding of spatial location by posterior parietal neurons. *Science, 230*, 456-458.

Andino, S. L., Michel, C. M., Thut, G., Landis, T., & Peralta, R. G. (2005). Prediction of response speed by anticipatory high-frequency (gamma band) oscillations in the human brain. *Human Brain Mapping, 24*, 50-58.

Anstis, S., Verstraten, F. A., & Mather, G. (1998). The motion aftereffect. *Trends Cogn Sci, 2*(3), 111-117.

Azzopardi, P., Fallah, M., Gross, C. G., & Rodman, H. R. (2003). Response latencies of neurons in visual areas MT and MST of monkeys with striate cortex lesions. *Neuropsychologia, 41*, 1738-1756.

Baayen, R. H., Davidson, D. J., & Bates, D. M. (2008). Mixed-effects modeling with crossed random effects for subjects and items. *Journal of Memory and Language, 59*(4), 390-412.

Baillet, S., Mosher, J. C., & Leahy, R. M. (2001). Electromagnetic brain mapping. *Ieee Signal Processing Magazine, 18*(6), 14-30.

Bandettini, P. A., Wong, E. C., Hinks, R. S., Tikofsky, R. S., & Hyde, J. S. (1992). Time course EPI of human brain function during task activation. *Magn Reson Med, 25*(2), 390-397.

Barnes, G. R., & Asselman, P. T. (1991). The mechanism of prediction in human smooth pursuit eye movements. *Journal of Physiology, 439*, 439-461.

Barnes, G. R., & Hillebrand, A. (2003). Statistical flattening of MEG beamformer images. *Human Brain Mapping, 18*, 1-12.

Barton, J. J., Simpson, T., Kiriakopoulos, E., Stewart, C., Crawley, A., Guthrie, B., et al. (1996). Functional MRI of lateral occipitotemporal cortex during pursuit and motion perception. *Annals of Neurology, 40*(3), 387-398.

Becker, W., & Fuchs, A. F. (1985). Prediction in the Oculomotor System - Smooth Pursuit during Transient Disappearance of a Visual Target. *Experimental Brain Research, 57*(3), 562-575.

Bennett, S. J., & Barnes, G. R. (2003). Human ocular pursuit during the transient disappearance of a visual target. *Journal of Neurophysiology, 90*, 2504-2520.

Berger, H. (1929). Electroencephalogram in humans. *Archiv Fur Psychiatrie Und Nervenkrankheiten, 87*, 527-570.

Berman, R. A., Colby, C. L., Genovese, C. R., Voyvodic, J. T., Luna, B., Thulborn, K. R., et al. (1999). Cortical networks subserving pursuit and saccadic eye movements in humans: an fMRI study. *Human Brain Mapping, 8*, 209-225.

Berryhill, M. E., Chiu, T., & Hughes, H. C. (2006). Smooth pursuit of nonvisual motion. *Journal of Neurophysiology, 96*, 461-464.

Bex, P. J., Metha, A. B., & Makous, W. (1999). Enhanced motion aftereffect for complex motions. *Vision Research, 39*(13), 2229-2238.

Blohm, G., Missal, M., & Lefevre, P. (2005). Direct evidence for a position input to the smooth pursuit system. *Journal of Neurophysiology, 94*, 712-721.

Brookes, M. J., Gibson, A. M., Hall, S. D., Furlong, P. L., Barnes, G. R., Hillebrand, A., et al. (2005). GLM-beamformer method demonstrates stationary field, alpha ERD and gamma ERS co-localisation with fMRI BOLD response in visual cortex. *NeuroImage, 26*(1), 302-308.

Busch, N. A., Dubois, J., & VanRullen, R. (2009). The Phase of Ongoing EEG Oscillations Predicts Visual Perception. *Journal of Neuroscience, 29*(24), 7869-7876.

Carl, J. R., & Gellman, R. S. (1987). Human smooth pursuit: stimulus-dependent responses. *Journal of Neurophysiology, 57*, 1446-1463.

Carpenter, R. (1988). *Movements of the eyes* (2nd ed.). London: Pion Ltd.

Champion, R. A., & Freeman, T. C. A. (2010). Discrimination contours for the perception of head-centered velocity. *Journal of Vision, 10*(6), 1-9.

Chaudhuri, A. (1990). A Motion Illusion Generated by Afternystagmus Suppression. *Neuroscience Letters, 118*(1), 91-95.

Chaudhuri, A. (1991a). Eye movements and the motion aftereffect: Alternatives to the induced motion hypothesis. *Vision Research, 31*(9), 1639-1645.

Chaudhuri, A. (1991b). Pursuit Afternystagmus Asymmetry in Humans. *Experimental Brain Research, 83*(3), 471-476.

Churchland, A. K., & Lisberger, S. G. (2005). Relationship between extraretinal component of firing rate and eye speed in area MST of macaque monkeys. *Journal of Neurophysiology, 94*, 2416-2426.

Collins, C. J. S., & Barnes, G. R. (1999). Independent control of head and gaze movements during head-free pursuit in humans. *Journal of Physiology-London, 515*(1), 299-314.

Coltz, J. D., Johnson, M. T., & Ebner, T. J. (2000). Population code for tracking velocity based on cerebellar Purkinje cell simple spike firing in monkeys. *Neurosci Lett, 296*(1), 1-4.

Culham, J. C., Dukelow, S. P., Vilis, T., Hassard, F. A., Gati, J. S., Menon, R. S., et al. (1999). Recovery of fMRI activation in motion area MT following storage of the motion afteraffect. *Journal of Neurophysiology, 81*, 388-393.

Dukelow, S. P., DeSouza, J. F. X., Culham, J. C., Berg, A. V. v. d., Menon, R. S., & Villis, T. (2001). Distinguishing subregions of the human MT+ complex using visual fields and pursuit eye movements. *Journal of Neurophysiology, 86*, 1991-2000.

Dumoulin, S. O., Bittar, R. G., Kabani, N. J., Baker, C. L., Le Goualher, G., Pike, G. B., et al. (2000). A new anatomical landmark for reliable identification of human area V5/MT: a quantitative analysis of sulcal patterning. *Cerebral Cortex, 10*(5), 454-463.

Dunkley, B. T., Freeman, T. C. A., Muthukumaraswamy, S. D., & Singh, K. D. (2011). Cortical Oscillatory Changes in Human Middle Temporal Cortex Underlying Smooth Pursuit Eye Movements. *Human Brain Mapping*.

Edden, R. A. E., Muthukumaraswamy, S. D., Freeman, T. C. A., & Singh, K. D. (2009). Orientation Discrimination Performance Is Predicted by GABA Concentration and Gamma Oscillation Frequency in Human Primary Visual Cortex. *The Journal of Neuroscience, 29*(50), 15721-15726.

Engel, A. K., & Fries, P. (2010). Beta-band oscillations - signalling the status quo? *Current Opinion in Neurobiology, 20*(2), 156-165.

Freeman, T. C. A. (1999). Path perception and Filehne illusion compared: model and data. *Vision Res, 39*(16), 2659-2667.

Freeman, T. C. A., & Banks, M. S. (1998). Perceived head-centric speed is affected by both extra-retinal and retinal errors. *Vision Res, 38*(7), 941-945.

Freeman, T. C. A., Champion, R. A., & Warren, P. A. (2010). A Bayesian Model of Perceived Head-Centered Velocity during Smooth Pursuit Eye Movement. *Current Biology, 20*, 757-762.

Freeman, T. C. A., & Sumnall, J. H. (2005). Extra-retinal adaptation of cortical motion-processing areas during pursuit eye movments. *Proceedings of the Royal Society B, 272*, 2127-2132.

Freeman, T. C. A., Sumnall, J. H., & Snowden, R. J. (2003). The extra-retinal motion aftereffect. *Journal of Vision, 3*, 771-779.

Fries, P. (2005). A mechanism for cognitive dynamics: neuronal communication through neuronal coherence. *Trends in Cognitive Sciences, 9*(10), 474-480.

Fries, P., Nikolic, D., & Singer, W. (2007). The gamma cycle. *Trends in Neurosciences, 30*(7), 309-316.

Fries, P., Reynolds, J. H., Rorie, A. E., & Desimone, R. (2001). Modulation of oscillatory neuronal synchronisation by selective visual attention. *Science, 291*, 1560-1563.

Fuchs, M., Wagner, M., & Kastner, J. (2007). From ECoG near fields to EEG and MEG far fields. *Internation Congress Systems 1300*, 125-128.

Gauthier, G. M., & Hofferer, J. M. (1976). Eye tracking of self-moved targets in the absence of vision. *Experimental Brain Research, 26*, 121-139.

Gilbertson, T., Lalo, E., Doyle, L., Di Lazzaro, V., Cioni, B., & Brown, P. (2005). Existing motor state is favored at the expense of new movement during 13-35 Hz oscillatory synchrony in the human corticospinal system. *Journal of Neuroscience, 25*(34), 7771-7779.

Haarmeier, T., Bunjes, F., Lindner, A., Berret, E., & Thier, P. (2001). Optimizing Visual Motion Perception during Eye Movements. *Neuron, 32*, 527–535.

Haarmeier, T., & Kammer, T. (2010). Effect of TMS on oculomotor behavior but not perceptual stability during smooth pursuit eye movements. *Cerebral Cortex Advance Access*.

Haarmeier, T., Thier, P., Repnow, M., & Petersen, D. (1997). False perception of motion in a patient who cannot compensate for eye movements. *Nature, 389*, 849-852.

Hadjipapas, A., Adjamian, P., Swettenham, J. B., Holliday, I. E., & Barnes, G. R. (2007). Stimuli of varying spatial scale induced gamma activity with distinct temporal characteristics in human visual cortex. *NeuroImage, 35*, 518-530.

Hamandi, K., Singh, K. D., & Muthukumaraswamy, S. (2011). Reduced movement-related beta desynchronisation in juvenile myoclonic epilepsy: A MEG study of task specific cortical modulation. *Clinical Neurophysiology, 122*(11), 2128-2138.

Handel, B., & Jensen, O. (2009). Human Alpha Band Activity Reflects Resource Allocation by Disengaging Task-Irrelevant Areas. *Psychophysiology, 46*, S7-S7.

He, S., Cohen, E. R., & Hu, X. (1998). Close correlation between activity in brain MT/V5 and the perception of a visual motion aftereffect. *Current Biology, 8*(22), 1215-1218.

Heydt, R. v. d., Peterhans, E., & Duersteler, M. R. (1992). Periodic-pattern-selective cells in monkey visual cortex. *Journal of Neuroscience, 12*, 1416-1434.

Hillebrand, A., Singh, K. D., Holliday, I. E., Furlong, P. L., & Barnes, G. R. (2005). A new approach to neuroimaging with magnetoencephalography. *Human Brain Mapping, 25*, 199-211.

Holliday, I. E., & Meese, T. S. (2008). Optic flow in human vision: MEG reveals a foveo-fugal bias in V1, specialization for spiral space in hMSTs, and global motion sensitivity in the IPS. *Journal of Vision, 8*(10).

Hubel, D. H., & Wiesel, T. N. (1977). Functional architecture of macaque visual cortex. *Proceedings of the Royal Society of London, 198*, 1-59.

Ilg, U. J., Schumann, S., & Thier, P. (2004). Posterior parietal cortex neurons encode target motion in world-centred coordinates. *Neuron, 43*, 145-151.

Ilg, U. J., & Thier, P. (2003). Visual tracking neurons in primate area MST are activated by smooth-pursuit eye movements of an "imaginary" target. *Journal of Neurophysiology, 90*, 1489-1102.

Jenkinson, M., Bannister, P., Brady, M., & Smith, M. (2002). Improved optimisation for the robust and accurate linear registration and motion correction of brain images. *NeuroImage, 17*, 825-841.

Jensen, O., & Mazaheri, A. (2010). Shaping functional architecture by oscillatory alpha activity: gating by inhibition. *Frontiers in Human Neuroscience, 4*, 1-8.

Joiner, W. M., & Shelhamer, M. (2006). Pursuit and saccadic tracking exhibit a similar dependence on movement preparation time. *Experimental Brain Research, 173*, 572-586.

Kao, G. W., & Morrow, M. J. (1994). The relationship of anticipatory smooth eye movements to smooth pursuit initiation. *Vision Research, 34*, 3027-3036.

Kimmig, H., Biscaldi, M., Mutter, J., Doerr, J. P., & Fischer, B. (2002). The initiation of smooth pursuit eye movements and saccades in normal subjects and in "express-saccade makers". *Experimental Brain Research, 144*, 373-384.

Kimmig, H., Ohlendorf, S., Speck, O., Sprenger, A., Rutschmann, R. M., Haller, S., et al. (2008). fMRI evidence for sensorimotor transformations in human cortex during smooth pursuit eye movements. *Neuropsychologia, 46*, 2203-2213.

Komatsu, H., & Wurtz, R. H. (1988). Relation of cortical areas MT and MST to pursuit eye movements. I. Localization and visual properties of neurons. *Journal of Neurophysiology, 60*(2), 580-603.

Konen, C. S., Kleiser, R., Seitz, R. J., & Bremmer, F. (2005). An fMRI study of optokinetic nystagmus and smooth-pursuit eye movements in humans. *Experimental Brain Research, 165*, 203-216.

Krauzlis, R. J. (2003). Neuronal activity in the rostral superior colliculus related to the initiation of pursuit and saccadic eye movements. *J Neurosci, 23*(10), 4333-4344.

Krauzlis, R. J. (2004). Recasting the smooth pursuit eye movement system. *Journal of Neurophysiology, 91*, 591-603.

Krauzlis, R. J. (2005). The Control of Voluntary Eye Movements: New Perspectives. *The Neuroscientist, 11*(2), 124–137.

Krauzlis, R. J., & Lisberger, S. G. (1994a). A model of visually-guided smooth pursuit eye movements based on behavioral observations. *Journal of Computational Neuroscience, 1*, 265-283.

Krauzlis, R. J., & Lisberger, S. G. (1994b). Temporal properties of visual motion signals for the initiation of smooth pursuit eye movements in monkeys. *Journal of Neurophysiology, 72*(1), 150-162.

Kuh, A. A., Kempf, F., Brucke, C., Doyle, L. G., Martinez-Torres, I., Pogosyan, A., et al. (2008). High-Frequency Stimulation of the Subthalamic Nucleus Suppresses Oscillatory Activity in Patients with Parkinson's Disease in Parallel with Improvement in Motor Performance. *The Journal of Neuroscience, 28*(24), 6165–6173.

Kwong, K. K., Belliveau, J. W., Chesler, D. A., Goldberg, I. E., Weisskoff, R. M., Poncelet, B. P., et al. (1992). Dynamic magnetic resonance imaging of human brain activity during primary sensory stimulation. *Proc Natl Acad Sci U S A, 89*(12), 5675-5679.

Leigh, R. J., & Zee, D. S. (2006). *The Neurology of Eye Movements* (4th ed.). Oxford: Oxford University Press.

Lencer, R., Nagel, M., Sprenger, A., Zapf, S., Erdmann, C., Heide, W., et al. (2004). Cortical mechanisms of smooth pursuit eye movements with target blanking. An fMRI study. *European Journal of Neuroscience, 19*(5), 1430-1436.

Lencer, R., & Trillenberg, P. (2008). Neurophysiology and neuroanatomy of smooth pursuit in humans. *Brain and Cognition, 68*, 219-228.

Livingstone, M. S., & Hubel, D. (1984). Anatomy and physiology of a colour system in the primate visual cortex. *Journal of Neuroscience, 7*, 3416-3468.

Lopes da Silva, F. H., Vanliero, T. H., Schrijer, C. F., & Vanleeuw, W. S. (1973). Organization of Thalamic and Cortical Alpha Rhythms - Spectra and Coherences. *Electroencephalography and Clinical Neurophysiology, 35*(6), 627-639.

Lovejoy, L. P., Fowler, G. A., & Krauzlis, R. J. (2009). Spatial allocation of attention during smooth pursuit eye movements. *Vision Research, 49*, 1275-1285.

Macavoy, M. G., Gottlieb, J. P., & Bruce, C. J. (1991). Smooth-pursuit eye movement representation in primate frontal eye field. *Cerebral Cortex, 1*, 95-102.

Mack, A., Goodwin, J., Thordarsen, H., Benjamin, D., Palumbo, D., & Hill, J. (1987). Motion Aftereffects Associated with Pursuit Eye-Movements. *Vision Research, 27*(4), 529-536.

Martinez-Trujillo, J. C., Cheyne, D., Gaetz, W., Simine, E., & Tsotsos, J. K. (2007). Activation of area MT/V5 and the right inferior parietal cortex during the discrimination of transient direction changes in translational motion. *Cerebral Cortex, 17*(7), 1733-1739.

Maunsell, J., & Essen, D. v. (1983a). The connections of the middle temporal visual area (MT) and their relationship to a cortical hierachy in the macaque monkey. *Journal of Neuroscience, 3*, 2563-2586.

Maunsell, J., & Essen, D. V. (1983b). Functional properties of neurons in middle temporal visual area of the macaque monkey. I. Selectivity for stimulus direction, speed, and orientation. *Journal of Neurophysiology, 49*(5), 1127–1147.

Maunsell, J., & Newsome, W. T. (1987). Visual processing in monkey extra-striate cortex. *Annual Review of Neuroscience, 10*, 363-401.

Mazaheri, A., & Jensen, O. (2010). Rhythmic pulsing: linking ongoing brain activity with evoked responses. *Frontiers in Human Neuroscience, 4*.

Meyer, C. H., Lasker, A. G., & Robinson, D. A. (1985). The upper limit of human smooth pursuit velocity. *Vision Research, 25*, 561-563.

Missal, M., & Heinen, S. J. (2001). Facilitation of smooth pursuit initiation by electrical stimulation in the supplementary eye fields. *Journal of Neurophysiology, 86*, 2413-2425.

Morgan, M. J., Ward, R. M., & Brussell, E. M. (1976). Aftereffect of Tracking Eye-Movements. *Perception, 5*(3), 309-317.

Mukamel, R., Gelbard, H., Arieli, A., Hasson, U., Fried, I., & Malach, R. (2005). Coupling Between Neuronal Firing, Field Potentials, and fMRI in Human Auditory Cortex. *Science, 309*, 951-954.

Muthukumaraswamy, S. D., Edden, R. A. E., Jones, D. K., Swettenham, J. B., & Singh, K. D. (2009). Resting GABA concentration predicts peak gamma frequency and fMRI amplitude in response to visual stimulation in humans. *Proceedings of the National Academy of Science, 106*(20), 8356–8361.

Muthukumaraswamy, S. D., & Singh, K. D. (2008). Spatiotemporal frequency tuning of BOLD and gamma band MEG responses compared in primary visual cortex. *NeuroImage, 40*, 1552-1560.

Nagel, M., Sprenger, A., Hohagen, F., Binkofski, F., & Lencer, R. (2008). Cortical mechanisms of retinal and extraretinal smooth pursuit eye movements to different target velocities. *NeuroImage, 41*, 483-492.

Nagel, M., Sprenger, A., Zapf, S., Erdmann, C., Kompf, D., Heide, W., et al. (2006). Parametric modulation of cortical activation during smooth pursuit with and without target blanking. An fMRI study. *NeuroImage, 29*, 1319-1325.

Naji, J. J., & Freeman, T. C. A. (2004). Perceiving depth order during pursuit eye movement. *Vision Research, 44*, 3025–3034.

Newsome, W. T., Wurtz, R. H., & Komatsu, H. (1988). Relation of Cortical Areas MT and MST to Pursuit Eye Movements. II. Differentiation of Retinal From Extraretinal Inputs. *Journal of Neurophysiology, 60*(2), 604-620.

Ogawa, S., Lee, T. M., Kay, A. R., & Tank, D. W. (1990). Brain magnetic resonance imaging with contrast dependent on blood oxygenation. *Proc Natl Acad Sci U S A, 87*(24), 9868-9872.

Ogawa, S., Lee, T. M., Nayak, A. S., & Glynn, P. (1990). Oxygenation-sensitive contrast in magnetic resonance image of rodent brain at high magnetic fields. *Magn Reson Med, 14*(1), 68-78.

Ogawa, S., Tank, D. W., Menon, R., Ellermann, J. M., Kim, S. G., Merkle, H., et al. (1992). Intrinsic signal changes accompanying sensory stimulation: functional brain mapping with magnetic resonance imaging. *Proc Natl Acad Sci U S A, 89*(13), 5951-5955.

Ono, S., & Mustari, M. J. (2006). Extraretinal signals in MSTd neurons related to volitional smooth pursuit. *Journal of Neurophysiology, 96*, 2819-2825.

Parkes, L. M., Bastiaansen, M. C. M., & Norris, D. G. (2006). Combining EEG and fMRI to investigate the post-movement beta rebound. *NeuroImage, 29*(3), 685-696.

Petit, L., & Haxby, J. V. (1999). Functional anatomy of pursuit eye movements in humans as revealed by fMRI. *Journal of Neurophysiology, 82*, 463-471.

Pfurtscheller, G., Stancak, A., & Neuper, C. (1996). Event-related synchronization (ERS) in the alpha band - An electrophysiological correlate of cortical idling: A review. *International Journal of Psychophysiology, 24*(1-2), 39-46.

Pogosyan, A., Gaynor, L. D., Eusebio, A., & Brown, P. (2009). Boosting cortical activity at beta-band frequencies slows movement in humans. *Current Biology, 19*, 1637-1641.

Pola, J., & Wyatt, H. J. (1980). Target position and velocity: the stimuli for smooth pursuit eye movements. *Vision Research, 20*, 523-534.

Rashbass, C. (1961). The relationship between saccadic and smooth tracking eye movements. *Journal of Physiology, 159*, 326-338.

Rihs, T. A., Michel, C. M., & Thut, G. (2007). Mechanisms of selective inhibition in visual spatial attention are indexed by alpha-band EEG synchronization. *European Journal of Neuroscience, 25*(2), 603-610.

Ritter, P., Moosmann, M., & Villringer, A. (2009). Rolandic Alpha and Beta EEG Rhythms' Strengths Are Inversely Related to fMRI-BOLD Signal in Primary Somatosensory and Motor Cortex. *Human Brain Mapping, 30*(4), 1168-1187.

Schutz, A. C., Braun, D. I., Kerzel, D., & Gegenfurtner, K. R. (2008). Improved visual sensitivity during smooth pursuit eye movements. *Nature Neuroscience, 11*(10), 1211-1216.

Sharpe, J. A. (2008). Neurophysiology and neuroanatomy of smooth pursuit: Lesion studies. *Brain and Cognition, 68*, 241-254.

Singer, W. (1999). Neuronal synchrony: A versatile code for the definition of relations? *Neuron, 24*(1), 49-65.

Singh, K. D. (2006). Magnetoencephalography. In C. Senior, T. Russell & M. S. Gazzaniga (Eds.), *Methods in mind* (pp. 291-326). London: The MIT Press.

Singh, K. D. (2009). mri3dX - http://cubric.psych.cf.ac.uk/Documentation/mri3dX/features.

Singh, K. D., Barnes, G. R., Hillebrand, A., Forde, E. M., & Williams, A. L. (2002). Task-related changes in cortical synchronisation are spatially coincident with the hemodynamic response. *NeuroImage, 16*, 103-114.

Smith, S. M. (2002). Fast robust automated brain extraction. *Human Brain Mapping, 17*(3), 143-155.

Souman, J. L., Hooge, I. T. C., & Wertheim, A. H. (2006). Frame of reference transformations in motion perception during smooth pursuit eye movements. *Journal of Computational Neuroscience, 20*(1), 61-67.

Spering, M., & Gegenfurtner, K. R. (2006). Contextual effects on smooth-pursuit eye movements. *Journal of Neurophysiology, 97*, 1353-1367.

Stancak, A., & Pfurtscheller, G. (1995). Desynchronization and Recovery of Beta-Rhythms during Brisk and Slow Self-Paced Finger Movements in Man. *Neuroscience Letters, 196*(1-2), 21-24.

Stevenson, C. M., Brookes, M. J., & Morris, P. G. (2011). b-Band Correlates of the fMRI BOLD Response. *Human Brain Mapping, 32*, 182-197.

Stoerig, P., & Cowey, A. (1997). Blindsight in man and monkey. *Brain, 120 (Part 3)*, 535-559.

Tallon-Baudry, C., Bertrand, O., Delpuech, C., & Pernier, J. (1996). Stimulus specificity of phase-locked and non-phase-locked 40 Hz visual responses in humans. *Journal of Neuroscience, 16*, 4240-4249.

Thiele, A., Henning, P., Kubischik, M., & Hoffmanndagger, K. P. (2002). Neural Mechanisms of Saccadic Suppression. *Science, 295*(5564), 2460 - 2462.

Thier, P., & Ilg, U. J. (2005). The neural basis of smooth pursuit eye movements. *Current Opinions on Neurobiology, 15*, 645-652.

Thut, G., & Miniussi, C. (2009). New insights into rhythmic brain activity from TMS–EEG studies. *Trends in Cognitive Sciences, 13*(4), 182-189.

Tian, J. R., & Lynch, J. C. (1996). Functionally defined smooth and saccadic eye movement subregions in the frontal eye field of Cebus monkeys. *Journal of Neurophysiology, 76*, 2740-2753.

Tikhonov, A., Haarmeier, T., Thier, P., Braun, C., & Lutzenberger, W. (2004). Neuromagnetic activity in medial parietooccipital cortex reflects the perception of visual motion during eye movements. *NeuroImage, 21*, 593-600.

Tikhonov, A., Handel, B., Haarmeier, T., Lutzenberger, W., & Thier, P. (2007). Gamma oscillations underlying the visual motion aftereffect. *NeuroImage, 38*(4), 708-719.

Toma, K., Nagamine, T., Yazawa, S., Terada, K., Ikeda, A., Honda, M., et al. (2000). Desynchronization and synchronization of central 20-Hz rhythms associated with voluntary muscle relaxation: a magnetoencephalographic study. *Experimental Brain Research, 134*(4), 417-425.

Tootell, R. B. H., Reppas, J. B., Dale, A. M., & Look, R. B. (1995). Visual motion aftereffect in human cortical area MT revealed by functional magnetic resonance imaging. *Nature, 375*.

Turano, K. A., & Massof, R. W. (2001). Nonlinear contribution of eye velocity to motion perception. *Vision Research, 41*, 385-395.

Ullman, S., & Schechtman, G. (1982). Adaptation and gain normalization. *Proc R Soc Lond B Biol Sci, 216*(1204), 299-313.

Ungerleider, L. G., & Desimone, R. (1986). Cortical connections of visual area MT in the macaque. *Journal of Comparative Neurology, 248*, 190-222.

Valois, R. L. d., Thorell, L. G., & Albrecht, D. G. (1985). Periodicity of striate-cortex-cell receptive fields. *Journal of the Optical Society of America, 2*, 1115-1123.

VanRullen, R., & Koch, C. (2003). Is perception discrete or continuous? *Trends Cogn Sci, 7*(5), 207-213.

von Holst, E., & Mittelstaedt, H. (1950). The principle of reafference. *Naturwisenschaften, 37*, 464-476.

Vrba, J., & Robinson, S. E. (2001). Signal processing in magnetoencephalography. *Methods, 25*, 249-271.

Watamaniuk, S. N. J., & Heinen, S. J. (2007). Storage of an oculomotor motion aftereffect. *Vision Research, 47*(466-473).

Wertheim, A. (1981). On the relativity of perceived motion. *Acta Psychol (Amst), 48*(1-3), 97-110.

Wertheim, A. (1994). Motion perception during selfmotion: the direct versus inferential controversy revisited. *Behavioral and Brain Sciences, 17*, 293-311.

Wilke, M., Logothetis, N. K., & Leopold, D. A. (2006). Local field potential reflects perceptual suppression in monkey visual cortex. *Proc Natl Acad Sci U S A, 103*(46), 17507-17512.

Womelsdorf, T., Fries, P., Mitra, P. P., & Desimone, R. (2005). Gamma-band synchronization in visual cortex predicts speed of change detection. *Nature, 439*, 733-736.

Worden, M. S., Foxe, J. J., Wang, N., & Simpson, G. V. (2000). Anticipatory Biasing of Visuospatial Attention Indexed by Retinotopically Specific a-Band Electroencephalography Increases over Occipital Cortex. *The Journal of Neuroscience, 20*, RC63.

Xing, J., Li, C. S., & Andersen, R. A. (1995). The temporal-spatial properties of LIP neurons for sequential eye movements simulated in a neural network model. *Society of Neuroscience: Abstracts, 21*, 120.

Yamagishia, N., Callana, D. E., Anderson, S. J., & Kawatob, M. (2008). Attentional changes in pre-stimulus oscillatory activity within early visual cortex are predictive of human visual performance. *Brain Research, 1197*, 115-122

Yang, Q., Bucci, M. P., & Kapoula, Z. (2002). The Latency of Saccades, Vergence, and Combined Eye Movements in Children and in Adults *Investigative Ophthalmology and Visual Science, 43*, 2939-2949.

Zhang, H., Logothetis, N. K., & Liang, H. (2009). Predicting perceptual suppression from local field potential in visual cortex. *Conf Proc IEEE Eng Med Biol Soc, 2009*, 6802-6805.